Charles University in Prague

Faculty of Medicine in Hradec Králové

Doctoral degree program

Medical chemistry and biochemistry

WOUND REPAIR AND DIABETIC WOUND DEFECTS.

HOJENÍ RAN SE ZAMĚŘENÍM NA DIABETICKÉ DEFEKTY.

Rastislav Slavkovský, MSc.

Supervisor: Assoc. Prof. RNDr. Jiří Kanta, CSc.

Hradec Králové, 2013   Defense on: ....

Declaration:

I declare hereby that this dissertation thesis is my own original work and that I indicated by references all used information sources. I also agree with depositing my dissertation in the Medical Library of the Charles University in Prague, Faculty of Medicine in Hradec Králové and with making use of it for study and educational purpose provided that anyone who will use it for his/her publication or lectures is obliged to refer to or cite my work properly.

I give my consent to availability of my dissertation´s electronic version in the information system of the Charles University in Prague.

Hradec Králové

Table of contents

1 Introduction

Diabetes mellitus is the most common metabolic disorder characterized by the hyperglycemia and general metabolic disruption of regulatory and signaling pathways in the body. Pathophysiological changes may include neuropathy, vasculopathy, micro- and macroangiopathy, especially in the legs. These disorders cause tissue hypoxia and ischemia of peripheral tissues. The condition may result in poorly healing chronic wounds, venous ulcers, bedsores, diabetic foot syndrome, and eventually in tissue necrosis. As a result of impaired wound repair, patients' quality of life and prognosis is reduced. Recently, new procedures have been developed for treating complicated wounds. One possibility is to use hyaluronic acid. This glycosaminoglycan has a clinically beneficial effect on wound healing and is a component of various products used for wound treatment. Hyaluronic acid supports tissue hydration, interacts with several receptors, and affects the cells, extracellular matrix and factors regulating wound healing.

2 Aims

The aim of this work was to study mechanism of the action of hyaluronic acid-iodine complex in the models of experimental rat wounds and also to study molecular changes associated with wound repair occurring in the model of rat diabetes.

3 Actual status of knowledge

3.1 Description of wound healing process

Wound healing is a process that occurs after the damage to body tissues. This work deals with the healing of skin wounds, which heal by tissue repair and not by regeneration (Li et al. 2007). Healing of skin wounds takes place in stages, which normally follow each other and overlap each other (Clark 1996; Li et al. 2007), Fig. 1.
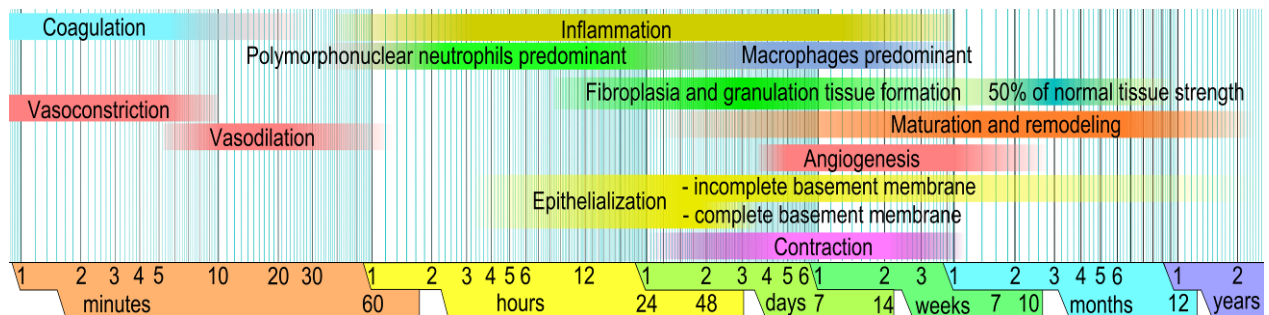
Fig. 1: Phases of normal wound healing. Limits vary within faded intervals, mainly by wound size and healing conditions. Author - Mikael Häggström, picture is in public domain via Wikimedia Commons. http://commons.wikimedia.org/wiki/File:Wound_healing_phases.svg

3.1.1 Coagulation and provisional matrix formation

After the breach of the tissue, the contact activation of Hageman factor (factor XII) by platelet derived polyanionic polyphosphates occurs. The subsequent launch of the intrinsic coagulation pathway takes place involving factors such as kininogen (source of bradykinin), prekalikrein, factor XI and factor X (Muller et al. 2009). Furthermore, there occurs so-called extrinsic coagulation pathway, which has a significant role in the repair. Factors IX and X are activated by the complex of tissue factor (TF) and factor VII (Nemerson 1988). TF is located on the surface of extravascular stromatic cells such as fibroblasts.

Degranulated activated platelets release molecules that are constituents of a provisional matrix. The provisional matrix is a mixture of fibrin fibers, fibronectin, vitronectin, thrombospondin, tenascin and other glycoproteins. They all serve as adhesion molecules for the attachment and migration into the wound (Yamada et al. 1996). The platelets are also releasing platelet derived growth factor (PDGF), transforming growth factor (TGF) alpha and beta (Nečas 2005), and other pro-inflammatory factors such as serotonin, bradykinin, prostaglandins, prostacyclins, thromboxane and histamine (Stadelmann et al. 1998).

The tissue-type and urokinase-type plasminogen activators (PA) are released from endothelial cells after the completion of coagulation factors release. PAs initiate the conversion of plasminogen to plasmin (Loskutoff et al. 1986).

3.1.2 Vasoconstriction

Immediately after a blood vessel is breached, ruptured cell membranes release inflammatory factors like thromboxanes and prostaglandins that cause the vessel to spasm to prevent blood loss and to collect inflammatory cells and factors in the area (Stadelmann et al. 1998). Vasoconstriction lasts five to ten minutes.

3.1.3 Vasodilatation

Vasodilatation is a widening of blood vessels that occurs about 20 minutes post-wounding (Stadelmann et al. 1998). The main factor involved in causing vasodilatation is histamine. Histamine also causes blood vessels to become porous, allowing the proteins from the bloodstream to leak into the wound space. Increased porosity of blood vessels also facilitates the entry of inflammatory cells, such as leukocytes, into the wound site.

3.1.4 Inflammation

Polymorphonuclear neutrophils (PMNs) followed by monocytes are the first cells that migrate into the wound. Neutrophils appear in the wound because of their high number in peripheral blood. Chemoattractants, which attract leukocytes to the site of injury, are: fibrinopeptides, degradation products resulting from fibrin cleavage by plasmin, C5 component of complement, leukotriene B4 released by activated neutrophils, platelet activating factor (PAF) released by endothelium or neutrophils and platelet factor 4 (CXCL-4) released from platelets (Clark 1996).

Neutrophils at the wound site destroy contaminating bacteria by phagocytosis and subsequent enzymatic mechanism and by the formation of reactive oxygen species. The main part of neutrophils remains closed in the precipitate and dried tissue, which is in the form of crust separated from the wound eventually (Clark 1996). Senescent neutrophils are phagocytosed by macrophages (Newman et al. 1982). Wound monocytes and macrophages are also important for the regulation of repair progression. This was shown in animals, where the limited accumulation of macrophages caused delayed wound healing (Leibovich et al. 1975). Macrophages also express the mRNA of TGF-α, TGF-β, PDGF, insulin like growth factor 1 (IGF-1) and these proteins play an important role in regulating wound healing

(Rappolee et al. 1988). In contrast, wound healing can take place normally without the presence of PMNs (de la Torre et al. 2008).

3.1.5 Epithelization

The epithelization of wound surface begins several hours after injury. Epithelial cells from non-damaged area of the skin and hair follicles are continuously covering wound. In addition to the migration and proliferation of keratinocytes also a phenotypic change occurs in the keratinocytes. Metamorphosis involves the withdrawal of intracellular filaments and cleavage of intercellular desmosomes (structures that connect the epithelial cells) and hemidesmosomes (connection between basement membrane and epidermis). The migrating epithelium does not terminally differentiate to cutaneous stratifying keratinocytes that contain keratins and filaggrin (Clark 1996). Mitogenic growth factors for epithelial cells include TGF-α, epidermal growth factor (EGF), tumor necrosis factor alpha (TNF-α), fibroblast growth factor-2 (FGF-2) also known as basic fibroblast growth factor (bFGF) and keratinocyte growth factor (KGF) also known as FGF-7. Keratinocytes produce collagenase-1 (MMP-1) and plasmin during the migration and dissects fibrin eschar from the wound. Fibrin and fibrinogen, as a matter of fact, are anti-adhesive molecules for keratinocytes, because keratinocytes do not express the receptor for fibrin (αV-β3 integrin). Migrating epithelium expresses urokinase type plasminogen activator (uPA) . uPA receptor have a role in the activation of plasminogen. The process of plasmin production is regulated by plasminogen activator inhibitor (PAI) (Hebda et al. 2004). After the completion of migration, the contact inhibition of proliferation occurs, the laminin is synthesized and the basement membrane is reconstructed. Laminin inhibits keratinocyte migration (Clark et al. 1985), whereas fibronectin and type I and type IV collagens promote keratinocyte migration (Woodley et al. 1988).

3.1.6 Formation of granulation tissue, fibroplasia and angiogenesis

New granulation tissue begins to occur about 2 to 4 days after the injury. In addition to fibroblasts it contains also new capillaries, macrophages and loose connective tissue. Growth factors, cytokines with significant mitogenic activity, are needed to support the formation of the granulation tissue (Midwood et al. 2004). The source of growth factors are activated platelets, monocytes, but also activated parenchymal cells.

3.1.6.1 Fibroplasia

The process of formation of wound connective tissue, which serves as a scaffold for the cells, is called fibroplasia. The sources of connective tissue in the wound are fibroblasts. Fibroblasts begin to deposit fibronectin, type III collagen, type I collagen (Grinnell et al. 1981), glycosaminoglycans and proteoglycans due to presence of factors produced by macrophages (de la Torre et al. 2008). Type III collagen and type I collagen synthesis is induced by TGF-β (Roberts et al. 1986). In addition to macrophages also fibroblasts are a source of TGF-β, PDGF, bFGF, KGF and IGF-1 (Clark et al. 1995; de la Torre et al. 2008). Also interleukin-4 was described as another inducer of type III collagen and type I collagen synthesis (Postlethwaite et al. 1992). *In vitro*, the formation of collagen is suppressed by collagen matrix in fibroblasts, but fibrin has little effect on suppression of collagen formation (Clark, Nielsen et al. 1995).

Fibroblasts also assemble collagen molecules into fibers, which are cross-linked and organized into bundles. Collagen is gradually becoming a major component of acute wound connective tissue, with net production continuing for the next 6 weeks. The increasing content of wound collagen correlates with increasing tensile strength (de la Torre et al. 2008).

3.1.6.2 Angiogenesis

Angiogenesis during the wound repair is a formation of new blood vessels as a response to injury. Angiogenesis is required to establish an adequate flow of nutrients and oxygen to the growing tissues. Angiogenesis involves a series of sequential steps controlled by growth factors, cytokines and also by the extracellular matrix (ECM) components. The principal cells that are involved in this process are microvascular endothelial cells. After the enzymatic degradation of the basement membrane, chemotactic and mitogenic factors trigger migration, extension, arrangement and proliferation of endothelial cells. Thus new capillary sprouts are formed (Tomanek et al. 2000; Martin et al. 2003). According to the recent discoveries also the endothelial progenitor cells are essential in the vasculogenesis and wound healing, but their circulating and wound level numbers are decreased in diabetes (Gallagher et al. 2007).

3.1.7 Contraction

A large part of the wound fibroblasts are transforming into myofibroblasts containing alpha smooth muscle actin and are capable of contraction. Myofibroblasts contract due

to influence of TGF-β and PDGF after they form links between themselves and the ECM (Clark 1996). The contraction of myofibroblasts is also mediated by prostaglandin F1 (PGF-1), 5-hydroxytryptamine, angiotensin, vasopressin, bradykinins, epinephrine, and norepinephrine (Li et al. 2007). The subject of the wound contraction is thoroughly reviewed in the article by Grinnel, 1994.

3.1.8 Wound tissue remodeling

The tissue remodeling means temporary or permanent changes in tissue architecture, which includes cleavage of barriers such as basement membrane, basal lamina and interstitial stroma. The remodeling is important during the inflammatory and granulation phase, as well as after the closure of the wound. A typical manifestation of tissue remodeling involves a high production of extracellular proteinases by cells. ECM is organized into complex structures, each composed of various types of collagen, glycoproteins such as fibronectin, laminin, elastin, glycosaminoglycans (GAGs) and proteoglycans. Since these ECM components have different requirements for the enzymatic cleavage, remodeling involves interplay between several enzymes. Proteinases that degrade ECM are divided into three main groups: 1. serine proteinases, 2. matrix metalloproteinases (also metalloproteases, metallopeptidases) and 3. cysteine proteinases (cathepsins) (Li et al. 2007).

Furthermore, endoglycosidases and exoglycosidases selectively degrade GAG component of proteoglycans. Previous reports have shown that serine proteinases and metalloproteinases are the most important during the tissue remodeling (Mignatti et al. 1996). Healthy human skin contains approximately 80% of type I collagen and 10% of type III within the total collagen. However, in early phases of repair, type III collagen is synthesized in higher quantities into the granulation tissue. The maximal secretion is reached at 5-7 days after trauma. Only during later stages of healing and during scar maturation the proportion of type III is lowered and the proportion of type I is increased. The character of scars gradually resembles that of the original skin. The tensile strength increases as the proportion of type I collagen increases and reaches finally approximately 70% of the original value in intact skin. The number of capillaries and fibroblasts decrease over time in the scar (Li et al. 2007).

3.2 Diabetes mellitus

Diabetes mellitus is a chronic disease that manifests as a disturbance of glucose metabolism. There are two basic types according to the causes – type 1 diabetes mellitus (DM1) and type 2 diabetes mellitus (DM2) (Holeček 2006).

3.2.1 Type 1 diabetes mellitus

Type 1 diabetes mellitus is a disease characterized by the damage of pancreatic β-cells, which leads to lack of insulin. Today, DM1 is divided into two subgroups. Type A DM1 – the antibodies against pancreatic islets are present, which leads to the destruction of β-cells. It is an autoimmune mediated form. Type B DM1 is a severe insulin deficiency in the absence of autoimmune response. The autoimmune form may be caused by several factors: environmental factors, viral infections, genetic factors, low immunity of β-cells to the destruction (Rybka 2007).

3.2.2 Type 2 diabetes mellitus

Type 2 diabetes mellitus is the most common metabolic disease characterized by a relative insulin deficiency (absolute insulin levels are often increased). DM2 is characterized by a combination of tissue insulin resistance and impaired thus and insufficient insulin secretion. This leads to an insufficient body glucose utilization resulting in hyperglycemia. The quantitative contribution of both disturbances may be different. It is not clear, which deviation plays a primary role in disease development, but a prerequisite for the DM2 is the presence of both disturbances (Holeček 2006; Rybka 2007). Unfortunately, DM is a medical problem with increasing importance: 246 million adults worldwide were suffering from DM in 2007 and this number is expected to increase to 380 million in 2025 (Gan 2007).

3.2.2.1 Etiology, progress and clinical symptoms of DM2

The emergence of DM2 is connected to both genetic factors and exogenous factors. The most common exogenous factors include lack of physical activity, obesity, poor diet and smoking. One of the main causes of insulin action failure in target tissues is the insulin resistance. It is a condition where the organs and tissues are not able to respond adequately to insulin. The cause lies in the failure of insulin receptors and post-receptor processes. Due to insulin resistance, the demand for insulin secretion is increased. However, the β-cells are unable to produce insulin in the necessary extent. Failure of glucose homeostasis follows and the development of DM2 progresses (Rybka 2007). The most common manifestation

of diabetes occurs at the age of 40 to 50 years, but it may progress hidden for a long time. The main symptom is hyperglycemia. Other clinical signs also include polyuria (frequent urination), polydipsia (excessive thirst), weight loss, weakness, severe fatigue, pain, cramps, blurred vision (Rybka 2007) or dyslipidemia (Holeček 2006).

3.2.2.2   Obesity and type II diabetes mellitus

Obesity is a disease characterized by increased accumulation of adipose tissue. It brings many complications in diabetic patients. The main reason for the development of obesity is an excessive intake and insufficient energy expenditure. Genetic factors also play an important role. The number of obese diabetic patients is increasing every year. Up to 80 - 90% of patients with DM2 also suffer from overweight or obesity. Every kilogram of overweight increases the possibility of diabetes development by 9% on average (Rybka 2007). The presence of obesity affects insulin resistance, which leads to an increase in insulin secretion.

Adipose tissue serves as a reservoir of energy with thermoregulatory function, but it produces a number of proteins. These proteins, called adipokines, have effect on insulin sensitivity. Adipokines include interleukin-6 (IL-6), tumor necrosis factor alpha (TNFα), leptin and others (Škrha 2005).

3.2.2.3   Complications of diabetes

Diabetes is a serious disease especially due to complications it causes. Changes occur in metabolic pathways of carbohydrates, lipids and proteins in the course of diabetes progression. The most common complications include cardiovascular disease, atherosclerosis, impaired vision, diabetic nephropathy, liver disease, diabetic neuropathy, diabetic coma, hypoglycemia and impaired wound healing (e.g. diabetic foot ulcerations). At the molecular level, non-enzymatic glycation of proteins, increased synthesis of polyols and increased synthesis of amino sugars is taking place (Holeček 2006; Rybka 2007).

3.2.3   Wound healing in diabetic patients

The diabetic defects are difficult to treat and often lead to significant patient discomfort or even to limb amputation. The pathogenesis of a diabetic wound is complicated. The formation of wounds is connected with peripheral artery disease (PAD), where blood flow is decreased (Brem et al. 2007), chronic venous insufficiency (CVI), where the return of blood to heart is impaired, neuropathies with the loss of sensibility (Piaggesi 2004),

microangiopathies, macroangiopathies and impaired ability to fight infection. According to recent research, impaired repair is also due to the presence of advanced glycosylation end products (Ahmed 2005) or abundant matrix metalloproteinase expression (Armstrong et al. 2002; Rayment et al. 2008). Approximately 4 - 10% of patients with diabetes suffer from diabetic foot ulcers and diabetic patients often require surgery that may cause the formation of chronic wounds. Impaired wound repair is connected to increased morbidity and mortality (Bakker 1999).

3.2.4 Local factors

So far, several molecular factors were shown to contribute to wound healing deficiencies. They include impaired growth factors production (Brem et al. 2007) or their premature degradation by proteinases. The presence of diabetes can also cause unfavorable proteolytic wound environment due to increased production of several matrix metalloproteinases (MMP) (Burrow et al. 2007) along with lowered levels of tissue inhibitors of MMPs (TIMP) (Lobmann et al. 2002). The expression of IGF-1 is lowered in diabetic wounds (Blakytny et al. 2000).

3.2.5 Cellular factors

Cellular factors of impaired repair include impaired keratinocyte, fibroblast and macrophage function, as well as aberrant angiogenic response and endothelial dysfunction (Laing et al. 2007).

Nonetheless, the exact cellular and molecular mechanisms underlying the pathogenesis of this complication are not fully understood. One way to understand impaired wound healing during DM is to study wound repair in animals. Investigators need a variety of well described models to choose from in order to closely mimic the issue they are planning to study.

3.3 Models of wound repair on experimental animals

From an ethical and humane point of view it is very difficult or even impossible in standardized conditions to study experimental wound healing and to compare different treatments in humans. Therefore, scientists use experimental animals. The advantage of using rodents is the possibility to monitor the healing process during a shorter time than in humans (Cross et al. 1995) and to quantify healing in a reproducible way and in a controlled environment (Davidson 2001). Although using animal models is below the perfect picture of wound healing in humans, animal models remain an important element in developing new strategies for rational wound therapy (Davidson 2001).

Practical issues such as price, availability and the possibility of feeding affect the choice of model. The most commonly used animal is the rat and mouse. Dozens of work are published each year describing the wounds studied in these organisms. Only a small number of scientists study the problem using large animals such as pigs even though they physiologically better mimic human healing (Davidson 2001).

3.3.1 Basic types of experimental wounds

The scheme in Fig. 2 illustrates the basic cutaneous wound models and relative proportions of various components of the wound site. In the incisional, excisional and burn models the epidermis and the basement membrane are disrupted, and all wounds except burns fill with a provisional matrix composed of fibrin, fibronectin, and other plasma-derived components. The dead space model segregates the wound space from surrounding tissue with a barrier that becomes encapsulated. As healing progresses, the wound dimensions may be reduced, epithelialization proceeds from the margins and residual epidermal appendages and the provisional matrix is replaced by granulation tissue that eventually transforms into scar (Davidson 2001).
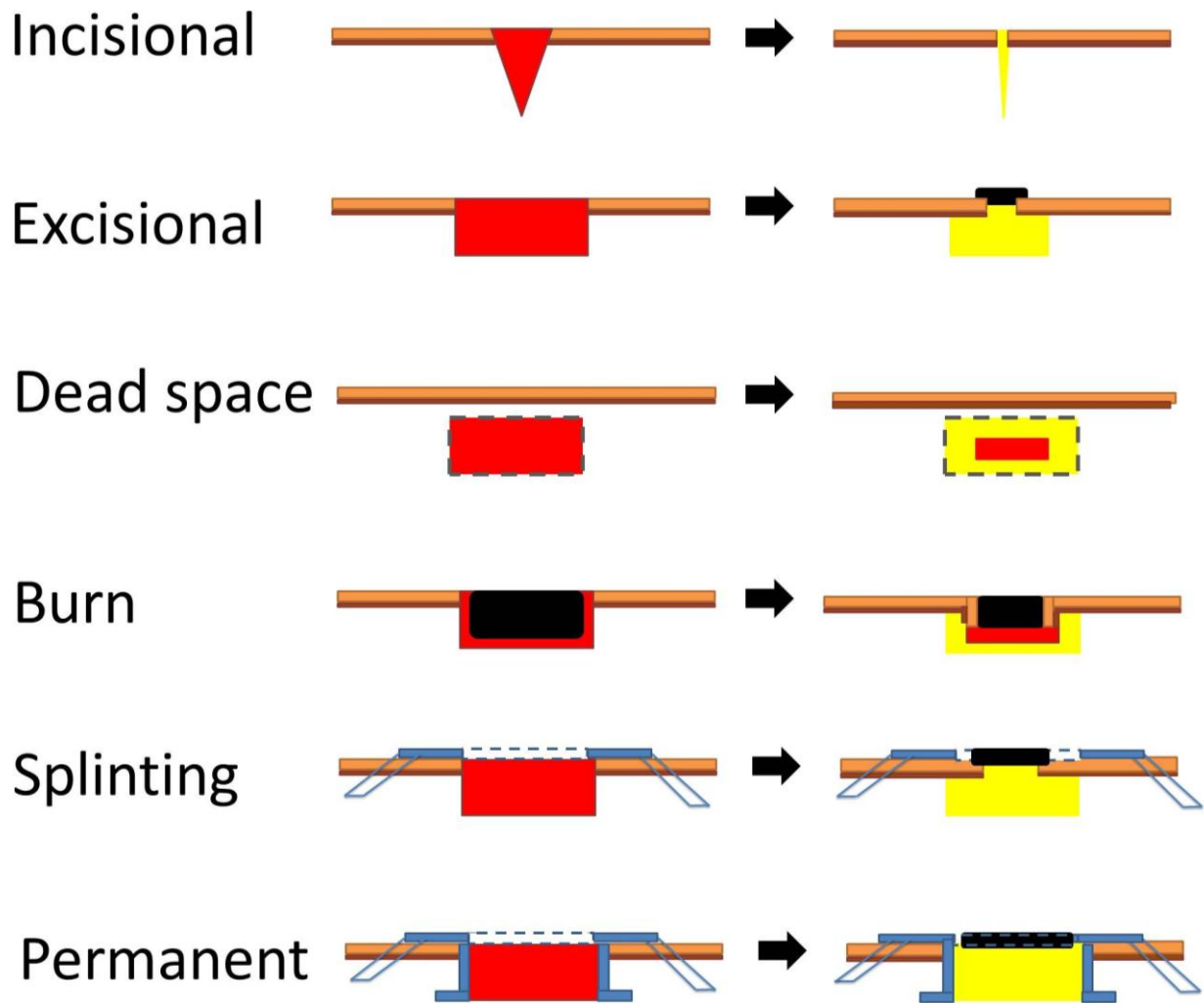
Fig. 2 : Basic types of cutaneous experimental wounds according to Davidson, 2001, Rudas 1960, Galiano 2004 and their mode of healing. Red – provisional matrix, orange – epidermis, brown – basal membrane, yellow – granulation tissue, black – crust/necrotic tissue, grey – the walls of dead space model, blue – the ring being attached with a suture threads over or in the wound.

3.3.1.1 Incisional wounds

Cutting of the skin with a sharp blade results in rapid disruption of tissue integrity with minimal collateral damage (Fig. 2). The size of the gap in the incision will depend on a number of factors, including the amount of subcutaneous fat, the tensional forces on the wound site, the orientation of the incision and the species. The skin of loose-skinned animals, such as rodents, can slide and retract over subcutaneous fascia to produce initially a large gap, while the skin of the pig or man is firmly attached to underlying structures and opens little (Davidson 2001).

Primarily closed wounds are closed by mechanical means and heal rapidly with minimal scar tissue formation. Whether bandaged, sutured, stapled or clipped, the principle is always to reduce the tissue gap to a minimum to allow rapid and efficient bridging of the wounded edges by granulation tissue and new epithelium. This type of wound is suitable for biomechanical analysis of wound strength. It is less adequate for histological assessment, tissue biochemistry or epithelialization analysis because of the limited volume/area of wound repair activity. Wound healed by secondary closure are the incisions that are left open and are also said to heal by secondary intention. In this process, a much more extensive fibrin clot in the wound void eventually gives way to ample granulation tissue and a gap that is eventually bridged by epithelialization. In loose-skinned animals, wound closure is facilitated by the contraction of the margins to approximate the edges. Nevertheless, these wounds begin with several millimeters of gap and usually resolve with several tens of microns of scar tissue (Davidson 2001).

3.3.1.2 Excisional wounds

Excisional wounds involve the removal of a significant volume of the target tissue and the filling of the void created allows more material to be collected for determining biochemical and histological parameters in comparison to incisional wounds (Fig. 2). The excision site can be biopsied to obtain cells, tissue, RNA, exudates and histological specimens that have much more ample cross-sectional area and volume in comparison to incisions. Excisional wounds can be covered with occlusive dressings, which retain the exudate (wound fluid) that may be used to assess the content of various soluble factors in the wound environment, such as nutrients, proteinases, cytokines and tissue degradation products (Davidson 2001).

3.3.1.3 Dead space models

Dead space models are artificial, porous implants, which are used to study tissue formation and the effects of substances on the wound (Fig. 2). Some of the commonly used materials include polyvinyl alcohol (PVA) sponges, steel wire mesh cylinders, expanded polytetrafluoroethylene (ePTFE) and the cellulose sponge. Each dead space model has its own limitations based on its material's composition and implantation methods. The steel wire mesh cylinder model has a lag phase of infiltration after implantation and requires a long amount of time before granulation tissue formation begins. Later stages of wound healing are best analyzed using the ePTFE model. A cellulose sponge inside a silicon tube model is typically

used for studying human surgery wounds and wound fluid. The PVA sponge is limited to acute studies because with time it induces foreign body response, which causes a giant cell reaction in the animal. Unlike other materials, PVA sponges are easy to insert and remove, made of inert and non-biodegradable materials and yet are soft enough to be sectioned for histological analysis. In wound healing, the PVA sponge is very useful for analyzing granulation tissue formation, collagen deposition, wound fluid composition, and the effects of substances on the healing process (Deskins et al. 2012).

3.3.1.4 Partial-thickness (split-thickness) excisional wounds

The partial-thickness (split-thickness) injury involves the use of a sharp bladed device that is designed to cut parallel to the skin surface at a defined depth. In practice, a dermatome is usually used to shave off a 100 to 1500 µm thick layer of the epidermis and upper dermis in one or more passes. The term "split" refers to the fact that a substantial amount of dermis, mostly reticular, is left behind and, more importantly, the bases of most epidermal appendages (sebaceous and sweat glands, hair follicles) remain intact. Thus epithelialization is rapid and occurs not only from the wound margin but from epidermal appendages as well. Regeneration of hair follicles is dependent on the depth of excision, since progenitor cells reside in the shaft, not in the bulb at the base of the follicle. This type of lesion is difficult to generate in the mouse, because its skin is quite thin. The epidermis is only about 50 µm thick and the dermis is less than 1 mm. Many domestic animals are unsuitable for the model because of the extremely high hair density, which increases the rate of epithelialization. Hairless strains offer an advantage. This model is useful for determining rates of epithelialization and at least in the pig is a good approximation of the behavior of human graft donor sites. The rapid healing rate in healthy animals may make it more difficult to determine clear differences among treatment groups. In either case the epithelialization is not continuous. Extravasation of lymph and blood occurs in this type of lesion, and a typical eschar composed of fibrin clot and granulocytes will accumulate over the site (Davidson 2001).

3.3.1.5 Full-thickness wound excisional wounds

This model involves the complete removal of the epidermis and dermis to the depth of fascial planes or subcutaneous fat. In the loose-skinned species, the thin musculature of the panniculus carnosus, which firmly adheres to the base of the dermis, is usually excised as well. Healing occurs from the margins and the base of the wound by the formation

of a fibrin clot that is invaded by granulation tissue and by the migration of an epidermal tongue along the interface between granulation tissue and clot (eschar). Biopsy punch, scalpel, scissors and dermatome (set to cut very deeply or making several successive passes) are used to generate this type of lesion in a standardized fashion. The laser, if controlled precisely, can produce a type of excision with little bleeding and the wound margins will still contain a zone of coagulation necrosis. The actual wound depth is very dependent on species; the mouse has the thinnest skin, while the pig and other large domestic animals have a dermis that is as thick as or thicker than humans. Bleeding and fluid loss are more extensive in the excisional model and there is greater susceptibility to infection. Wound dressings may be required to obtain predictable healing. This model offers the advantages of significant wound volume, involvement of all dermal components, epithelialization only from the wound margins and the ability to analyze chemistry, histology and cell populations in the wound site. Healing rates are often monitored on the basis of total excisional volume or area filled with granulation tissue (neodermis), extent of epithelialization, histological organization of connective tissue, angiogenesis and biochemical content of collagen or proteoglycans (Davidson 2001).

3.3.1.6   Splinting – permanent wound

In full-thickness excision, the mechanical structure of the dermis is completely disrupted and various forces in the surrounding dermis and the wound site can reduce the dimensions of the wound without actually filling the site with new tissue. Wound closure can be counteracted by physical splinting of the wound with retaining rings (Rudas 1960), biopolymer (e.g. collagen) plugs or other mechanical devices (Davidson 2001), thus creating permanent granulating wound (Fig. 2).

3.3.1.7   Splinting – wound with limited contraction.

Rodent and other loose skinned animals are known to contract their wound rapidly. Thus retaining rings attached on surface were introduced to limit the contraction and thus to replicate partially human physiology of wound repair (Fig. 2). Splinted wounds have an increased amount of granulation but the rate of epithelization is not affected (Galiano et al. 2004). The ring is usually made of silicone (Michaels et al. 2007).

3.3.2   The most frequently used models

In a review article by Dorset-Martin it can be found that 38% of studies used the incision wound model and 38% used the excision wound model. The most common location

of wound was on the back of animals due to practical reasons (78%) (Dorsett-Martin 2004). Other parameters, that may influence the course of the experiment, are animal strain, age, sex, wound size, wound bandages, use of anesthesia and analgesia (Dorsett-Martin 2004). Further information about different wound models can be found in the reviews by (Davidson 1998; Davidson 2001; Birch et al. 2005).

3.4   Models of animal diabetes

In the beginning it must be acknowledged that diabetes mellitus is a complex illness and no animal model is fully descriptive. Animal diabetes models can be divided principally into three groups: surgically induced diabetes, chemically induced diabetes and genetically induced diabetes (Grinnell 1984; Greenhalgh et al. 1990; Greenway et al. 1999).

3.4.1   Surgically induced diabetes mellitus

Surgical removal of the pancreas induces diabetes in dogs and this model has been intensively used in early 20th century. The experiments have led to the discovery of insulin (Engerman et al. 1982). At present, this model is no longer used (Greenhalgh 2003).

3.4.2   Chemically induced diabetes mellitus

Alloxan and streptozotocine attack beta cells in the islets of Langerhans and induce insulin-dependent diabetes mellitus (type I). The treated rats rapidly achieve the high hypoinsulinemia and hyperglycemia (Rerup 1970). It is possible to induce diabetes in rats, mice, hamsters, dogs and monkeys in this way. Although streptozotocine and alloxan are specific for beta cells, the moderate damage of other organs such as kidneys, liver and pancreas can occur. After the administration, the animals gain weight significantly less than control animals (Greenhalgh 2003). The induction of diabetes by this method is simple. Streptozotocine can be administered in one dose (240 mg/kg in mice or 45 mg/kg in rats) or the treatment can be distributed at lower doses for several days (Grodsky et al. 1982).

3.4.3   Genetically dependent diabetes mellitus

Like in humans also in certain animal species some individuals have genetic predispositions to develop diabetes. Genetic models can be divided into two subgroups: insulin-dependent models and insulin-resistant models. Furthermore, these models can be distinguished by the presence of the obesity. In most cases the insulin resistance is associated with the obesity (Greenhalgh 2003).

3.4.3.1   Models of spontaneous insulin dependent diabetes mellitus

There are several species of animals that spontaneously develop insulin-dependent diabetes mellitus (IDDM). Diabetes develops as a result of the auto-destruction of beta cells and consequent decrease in insulin production. NOD mice, BB Wistar rats, Chinese or South African hamsters, Yucatan mini-pigs, and some strains of guinea pigs, dogs and primates

are examples of genetically dependent IDDM. Only limited numbers of wound healing studies have been conducted on these animals. This was possibly due to better availability of chemically induced models of diabetes, and also due to the fact that the majority of patients, who have problems with wound healing have an insulin resistant DM. Studies on these models discovered abnormalities in tissue repair (Greenhalgh 2003).

3.4.3.2 Models of spontaneous non-insulin dependent diabetes mellitus

There exist several animal models with NIDDM. Models are summarized in Tab. 1. The majority of models are based on the mutation of leptin or leptin receptor and posses obese phenotype.

Name of strain/species	Gene symbol	Mutation	heredity	obesity
Mouse				
Obese ob/ob mouse	Ob	leptin	autos. recessive	obese
Diabetic db /db mouse	Db	leptin receptor	autos. recessive	obese
Yellow (Agouti) mouse	A	agouti sig.peptide	autos. dominant	obese
Fat mouse	Fat/cpe	Carboxypeptidase E	autos. recessive	obese
Tubby mouse	Tub	Tubby protein	autos. recessive	obese
Adipose mouse	Ad	?	autos. dominant	obese
New Zealand mouse (NZO)	-	-	polygenic	obese
Japanese KK mouse	-	-	polygenic	obese
TallyHO/JnJ mouse (male)	-	-	polygenic	obese
Rats				
Fatty (Zucker, ZDF)	Fa	leptin	autos. recessive	obese
Goto-Kakizaki	-	-	polygenic	non-obese
JCR:LA-cp	Fa	leptin receptor	autos. recessive	obese
SHROB(Koletsky)	Fa	leptin receptor	autos. recessive	obese
Cohen diabetic	-	-	-	non-obese
Djungar hamser	-	-	polygenic	obese
Rhesus monkey (Macaca mulatta)	-	-	polygenic	obese
Ossabaw pigs	-	-	polygenic	obese

Tab. 1: Animal models with NIDDM. The table is based on information in (Coleman et al. 1990; Naggert et al. 1995; Greenhalgh 2003; Shafrir 2007; Buck et al. 2011).

Further detailed information about various models of diabetes were described in the book: *Animal Models of Diabetes: Frontiers in Research* (Shafrir 2007).

3.5 Advantage and disadvantages of using streptozotocine and ZDF rat models

Streptozotocine induced DM is the easily accessible model of DM1. Our previous research on wound healing showed that at higher doses it is difficult to distinguish which is the effect of DM (elevated blood sugar) and what is the "added" toxic effects of streptozotocine (unpublished data). Epidemiologically the DM2 is the greater issue (90% of the total number of diabetic patients) than DM1. It is therefore preferable to use the ZDF model compared with streptozotocine model. However, the disadvantage of ZDF model is poorer availability (price, a limited number of animals). Laboratory mice have a disadvantage compared to rats that mice are smaller and it is not possible to create larger wounds, which are easier to observe and provide more material for analysis of repaired tissue.

3.6 Zucker Diabetic Fatty rat

The obese male ZDF rat has been an important model for studying the mechanism of onset and treatment of type 2 diabetes (Finegood et al. 2001; Leonard et al. 2005; Peterson 2007), thus we have anticipated that obese ZDF rat could be a suitable model to mimic certain aspects that are present-in diabetic patients suffering from complicated wounds. The ZDF rat is an inbred strain and rats with fa/fa genotype develop a genetically dependent obesity and subsequently diabetes due to a point missense mutation in the extracellular domain of the leptin receptor (Peterson 2007). Lean ZDF animals, with fa/+ or +/+ genotype do not develop obesity or diabetes, and serve as controls. Leptin is an adipokine and regulator of satiety. Leptin system also influences the metabolism of fatty acids. Although in ZDF rats the monogenic genetic defect causes obesity, it is not a common cause of human obesity (Peterson 2007). Nonetheless the mutation causes the polyphagia in ZDF rats and similarly in humans, overeating is also one of the most important causalities of obesity. ZDF rats are characterized by non-insulin dependent DM accompanied by hyperglycemia, neuropathies, nephropathies, insulin resistance, mild hypertension, hypertriglyceridemia, hypercholesterolemia (Lee et al. 2000), polyuria, polydipsia (Peterson et al. 1990) and microvascular damage (Danis et al. 1993). Hyperglycemia starts to develop between the seventh and twelfth week of age, and is preceded by obesity and insulin resistance (Finegood et al. 2001). Animals gradually evolve from hyperinsulin-euglycemic state to

hyperglycemic state with relative insulin deficiency (Finegood et al. 2001; Leonard et al. 2005) and the development of DM is connected with pancreatic beta cells dysfunction (Finegood et al. 2001). Whereas in ZDF rats DM starts to develop at an early age, in humans, the manifestation of type II diabetes is observed usually after the age of 40 or later. The main contributory factors to the development of hyperglycemia in people with type 2 diabetes are insulin resistance and beta cells dysfunction including defects in insulin secretion, proinsulin conversion and amyloid deposition in the islets of Langerhans (Kahn 2000; Finegood et al. 2001). Pathogenesis in ZDF rats is mediated through free fatty acid-induced suppression of insulin that is mediated through NO induction (Shimabukuro et al. 1997). Hyperglycemia can be prevented by NO inhibitors (Shimabukuro et al. 1997). The progression of diabetes is influenced by animal feeding, mainly in females. The high content of saturated fatty acids supports the progression of hyperglycemia (Corsetti et al. 2000). In healthy animals, when the diet with high content of fats is indigested, the de-novo lipogenesis is suppressed, however this mechanism is impaired in obese ZDF rats (Lee et al. 2000; Bassilian et al. 2002).

The influence of DM on the repair of tympanic perforation in ZDF rats was studied. It was found that the healing of this type of defect is impaired in diabetic animals (Vrabec 1998). In spite of the usefulness of obese ZDF rats as a model for studying experimental type II DM and metabolic syndrome, an extensive characterization of skin wound repair has not yet been published.

3.7 Hyaluronan

Hyaluronan (HA), also called hyaluronic acid or hyaluronate in salt form, has been purified in 1934 and its chemical structure was resolved in 1954. Biochemically, HA is a linear polymer of glucuronic acid and N-acetylglucosamine and it is associated with many aspects of biology. HA plays an important role in maintaining the shape and form of the body, fills the space by organizing and modifying the extracellular matrix (ECM). HA has the ability to regulate proliferation and migration responses of cells, to interact with different surface receptors, and has the ability to penetrate the intracellular space of cells and thus affect cell function. It is generally accepted that HA is linked to the process of tissue repair (Chen et al. 1999; Jiang et al. 2007). The role of hyaluronan in wound healing is not yet fully explained, it appears problematic that some work has been investigating hyaluronan *per se*, but has not specified its molecular weight and other properties such as its purity and the source.

3.7.1 Role of hyaluronan in biological processes of cutaneous wound repair

HA plays an important role in tissue regeneration and healing process of skin wounds. As early as in the coagulation stage, during the development of blood clots, HA is integrated into a provisional fibrin matrix and the level of HA in the matrix gradually increases (Weigel et al. 1986). Synthesis of HA increases immediately after injury in place of injury of tissue and remains elevated in inflammatory and early granulation/epithelization phase (Brown 2004). HA synthesis slows down in later granulation phase and accumulated HA is depolymerised by hyaluronidase into smaller fragments (Weigel et al. 1988; Chen et al. 1999). Hyaluronan level gradually decreases and is being replaced by sulphated proteoglycans, presumably by decorin, biglycan and versican (Gallo et al. 1996).

3.7.2 Role and biological properties of high-molecular weight hyaluronan

HA in the ECM controls the retention of water – it maintains the hydrophilic environment, controls ion and molecular diffusion, and provides three-dimensional network (Chen et al. 1999). The function of HA is also associated with the cell adhesion (Miyake et al. 1990). The high molecular hyaluronan reduces fibrotic healing, reduces collagen deposition and fibrilogenesis (Tolg et al. 2004). It has antioxidant properties to PMN-ROS (reactive oxygen species) type radicals ($O_2^{\circ-}$, $OH^{\circ-}$). By the effect of radicals, HA is cleaved into smaller fragments (Moseley et al. 2003). It facilitates the migration of keratinocytes and

fibroblasts into the wound by receptor RHAMM (receptor for hyaluronan-mediated motility) and CD44 (Brown 2004; Tolg et al. 2004). Hyaluronan can inhibit capillary formation (Feinberg et al. 1983).

Weigel and co-authors proposed a model for the role of HA in the early stages of wound healing. This model is based on the formation of fibrin-HA complex, which attracts immune cells into the wound. This matrix is further modified – degraded by entering cells that produce hyaluronidase and plasminogen activator. Degradation products of HA and fibrin are considered to be important regulatory molecules that control cellular functions such as inflammatory response and induction of angiogenesis (Weigel et al. 1986; Weigel et al. 1988). High molecular hyaluronan has been associated with cell proliferation. Several studies have shown that hyaluronan synthesis is linked with the proliferative state of cells. It is proposed that hyaluronan is not directly responsible for mitogenic activity, but creates a hydrated environment in the extracellular space and thereby facilitates separation of cells (Brown 2004). Under certain conditions, it prevents cell growth, while low molecular weight hyaluronan fragments are associated with cell growth and metastasis (Day et al. 2004). It can suppress neutrophil functions such as the reduction adherence and reduce the chemotactic response and thus to control and moderate inflammatory response (Gallo et al. 1996). It can stabilize the granulation tissue (Brown 2004).

3.7.3 Role of low molecular weight hyaluronan and oligosaccharides in wound repair

After the injury, low molecular weight hyaluronan fragments accumulate in the wound (Noble 2002). They play an important role in the inflammation by affecting macrophage functions (McKee et al. 1996; Noble et al. 1996). HA fragments activate inflammatory genes in macrophages and dendritic cells (Noble 2002). They play an important role in angiogenesis: angiogenesis is induced by low molecular weight hyaluronan (LMWHA) (West et al. 1985) and collagen I and VIII is induced in bovine aortic endothelial cells (Rooney et al. 1993). LMWHA acts by preventing drug-induced apoptosis; it induces proliferation of various transformed and untransformed cells (Day et al. 2004).

3.7.4 Accumulation and synthesis of hyaluronan in the skin

Hyaluronan in the skin is synthesized and secreted continuously by fibroblasts and keratinocytes. Normal concentration in the dermis is 0.2 to 0.5 g/kg (0.02 - 0.05%) within 2 – 5 MDa, 0.1 g/kg in the epidermis and 2.5 g/kg (0.25%) in epidermal extracellular matrix

31

(Lepperdinger et al. 2004). During aging, its concentration in the skin decreases. At the age of 60 years there is a 50% decrease of HA and at the age of 75 years up to 77% decrease. In addition, there is an increasing proportion of de-acetylated HA with the age (Longas 2004). The reduced content and reduced synthesis may also partially participate in the fact that healing is impaired in the elderly. Hyaluronan is synthesized by the enzymes hyaluronan synthase 1 and hyaluronan synthase 3 (HAS-1 and HAS-3) with molecular weights ranging from 0.2 to 2 MDa, and also by HAS-2 with molecular weight > 2 MDa (Weigel 2004). After an injury to the epidermidis HAS-2 and HAS-3 are strongly induced and thus HA probably plays an important role in the proper course of epidermal wound repair (Tammi et al. 2005).

3.7.5 Role of hyaluronan receptors during wound repair

There are many receptors and binding proteins (hyaladherins) for HA. These are CD44, RHAMM (receptor for hyaluronan-mediated motility, CD168), TLR-4 (Toll-like receptor-4), Layilin, LYVE-1 (Lymphatic vessel endothelial hyaluronan receptor-1), HARE (Hyaluronan Receptor for Endocytosis), TSG-6 (tumor necrosis factor stimulated gene-6) (Longas 2004). The function of CD44 is the most clarified, the function of others is largely unknown. RHAMM and CD44 are induced during wound repair (Balazs et al. 2000; Tolg et al. 2004). CD44 is expressed on the surface of fibroblasts, smooth muscle cells, epithelial cells, neutrophils, macrophages, lymphocytes (Lepperdinger et al. 2004). HA signaling pathways through CD44 run through the activation of Rho-Rac1 GTPase complex leading to actin cytoskeleton reorganization (Fig. 3) (Lee et al. 2000). Another signal pathway is via activation of ErbB2-CD44, leading to proliferation signal through the MAPK (mitogen activated protein kinase), and activation of TK-src (src-tyrosine kinase) and transcription factor NF-κB (nuclear factor kappa B), see Fig. 3. It was found that 20 kDa HA activates NF-κB, whereas HA > 1MDa inactivates NF-κB (Lee et al. 2000).
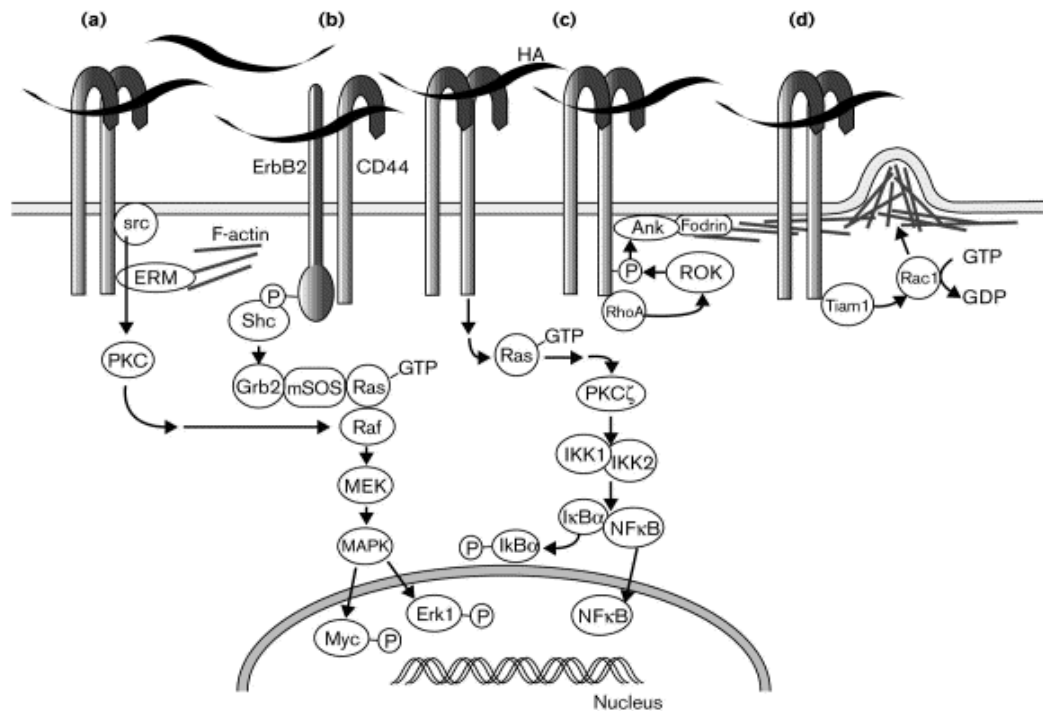
Fig. 3: Hyaluronan–CD44 signaling pathways. HA–CD44 binding may activate several signaling cascades, leading to changes in cell proliferation and cell movement. (a) Activation of the src-family non-receptor tyrosine kinases may be dependent upon colocalization of CD44 and src kinases to lipid microdomains within the plasma membrane, src activation may result in activation of a protein kinase C (PKC) cascade. (b) CD44–erbB2 dimers may activate a MAP kinase cascade or alternate cascades. (c) NF-κB may be activated through a Ras, PKCζ-dependent cascade. (d) Alternatively, HA–CD44 interaction may modify local cytoskeletal assembly through activation of the small GTPases such as RhoA and Rac1. Taken from (Lee et al. 2000). Figure reuse in present thesis was licensed by the Elsevier Copyright Clearance Center.

3.7.6 Interaction of hyaluronan with other ECM molecules and chemokines

Hyaluronan interacts with fibrin (Weigel et al. 1986; Weigel et al. 1988). HA interacts with hyalectins, for example with versican (chondroitin sulfate proteoglycan) that is induced during reparative processes (Carthy et al. 2011). HA organizes collagens and extracellular matrix (Chen et al. 1999; Brown 2004). HA binds to the complex TSG6 IAI-(TNF-stimulated gene, Inter-alpha-inhibitor, proteinase inhibitor) and this complex prevents inflammatory damage to tissue proteinases and stabilizes the granulation tissue (Brown 2004).

3.7.7 Hyaluronan and fetal wound healing

Hyaluronan level is high in fetal wound and HA may play an important role in fetal scar-free healing. Fetal scar-free healing is characterized by faster epithelization, sterile environment, a reduced inflammatory response and reduced angiogenesis (Balazs et al. 2000). Applied HA reduced the expression of TGF–β which is known to occur in wounds that heal

in scar-like manner and TGF-β is reduced to a scar-free fetal wounds (Torregrossa et al. 1983).

3.7.8 Clinical studies with applications of hyaluronan for supporting wound repair

In a multicenter controlled study 50 patients with venous ulcers were treated with daily HA gauze pad compared with dextranomer paste for 3 weeks. In both groups the appearance and the size of ulcers was significantly improved. Faster and larger reduction of ulceration was observed in the HA treated group (Ortonne 1996). In a study of etiologically different ulcers of lower extremities, in which conventional therapy was compared with HA treatment, a significantly greater number of healed wounds was found in the HA group (Torregrossa et al. 1983). Improved healing was observed in a study, where HA was applied with glycerin to patients suffering from venous ulcers (Passarini et al. 1982). In a similar study (Galasso et al. 1978), there was no positive effect of HA compared to control ZnO paste. In clinical trials of Hyalofill (contains benzyl ester modified HA), 36 neuropathic diabetic patients were treated until the wound was fully covered with granulation tissue. Therapy was then replaced by keeping the moisture lining. 75% wounds were healed at an average of 10 weeks (Vazquez et al. 2003).

3.7.9 Observation of effect of HA on wound healing in animals.

Hyaluronan at the concentration of 2% had a positive effect on wound healing in alloxan-induced diabetic rats. It modified and facilitated the migration of the epithelial cells and their differentiation (Abatangelo et al. 1983). Closing of the wound in rats by the action of HA on three-dimensional matrix seeded with keratinocytes and also without keratinocytes is substantially improved (Hu et al. 2003). Further experiments with HA film in rats showed reduced inflammatory activity, accelerated epidermal healing. The HA film may have a strong activity on supporting infiltration in the early stages of healing, can accelerate the healing of the epidermis, and slow the formation of keratinized layer (Ren et al. 2004). The effect of ultrapure HA of different molecular size has been studied in comparison to the effect of saline solution on deep skin wounds in Chinese pigs. The tensile resistance of the wound was reduced by the high and medium molecular weight (MW) HA. Using laser Doppler scan 3 days after injury, the blood perfusion in the wound was decreased in high MW HA and intermediate MW HA groups, but in seven days in the blood perfusion was increased in all of HA groups (Jia et al. 1998). In a study where collagen-HA sponge implant was engineered and implanted into the wounds of guinea pigs, it was found that hyaluronan caused increased

chemoattraction, replication of fibroblasts and collagen deposition (Doillon et al. 1986). HA in the collagen sponge had positive effects on wound healing in guinea pigs. Improved healing from the 16 days to 9 days by the action of HA was observed. Furthermore, in this work doubled vascularization was observed by HA treatment on day 2 to day 4 days after the injury, but these differences settled during the complete closure (King et al. 1991). Artificial skin substitute (collagen matrix without cells) soaked in 0.3% hyaluronan induced the ingrowth of granulation tissue and capillaries on the model of deep wounds in rats, and thus potentially facilitated the use of skin grafts (Murashita et al. 1996). HA modulates acute and chronic inflammation in rat model of arthritis and edema (Ialenti et al. 1994). HA stimulated B cells, which infiltrates into wounds to produce interleukin-6 and transforming growth factor-beta (TGF-β) through TLR-4 in a CD19-dependent manner (Iwata et al. 2009).

3.7.10 Products for wound care based on hyaluronan

Several wound care products contain hyaluronic acid or its salts. Ialugen plus (IBSA, Switzerland) contains the combination of silver sulfadiazine (1%) and sodium hyaluronate (0.2%) in form of cream. Company Fidia, Italy, fabricates several products for wound repair: Hyalosilver (sodium hyaluronate 0.2% + colloidal silver 2%), Jaloplast (Hyaluronic acid sodium salt 0.2%, cream), Jaloplast Plus (Hyaluronic acid sodium salt 0.2% + Silver sulfadiazine 1%, cream). Hyalofill (Convatec, USA) is a dry wound dressing composed of a HYAFF (benzyl ester of hyaluronan). Hyalofill forms a thick HA-rich gel, liberating HA into the wound for up to 2 to 3 days. Traumacell Biodress H-gel (Bioster, Czech Republic) contains 1% of sodium hyaluronate and 1% of hydrogen calcium salt of oxidized cellulose. Hyaluricht/Curiosin (Chemical Works of Gedeon Richter, Hungary) is marketed in the form of gel or solution and it contains 0.102% or 0.205% of zinc hyaluronate. Hyaluricht is the first drug containing zinc bound to hyaluronic acid. Zinc participates as a cofactor in more than 70 enzymes, some of which are involved in the biochemical processes of wound healing. Thus, zinc hyaluronate has a complex effect on physiological wound healing, preventing ulcers from infection because of its antimicrobial activity against a number of bacteria. It is a clear sterile solution with physiological osmolality and pH 5 – 6. Hyaluricht does not affect the skin around ulcer and does not stick to the wound (Illes et al. 2002). Hyaluronic acid is a component of advanced therapy medical products produced by Fidia, Italy, such as HYALOGRAFT 3D™ and LASER SKIN™, which are autologous dermal and epidermal replacement, respectively.

3.8 Iodine

Iodine has been used for many years to treat wounds as an antiseptic. As iodine is a strong oxidizing agent and could cause wound irritation when applied in high concentration, the pharmaceutical companies invested in last 60 years to the development of safe forms of iodine application, e.g. by using iodophors with slow release of iodine. It is active against many bacteria, viruses and fungi and it may also increase the healing rate (Selvaggi et al. 2003; Cooper 2007). Polyvinyl pyrrolidone – iodine preparation in hydrogel was reported to improve healing by increasing wound moisture and by preventing bacterial infection. The epithelialization of meshed skin grafts was increased in human patients after hydrogel application (Vogt et al. 2006). Cadexomer iodine is a promising treatment to clear *Staphylococcus aureus* cells within biofilm from skin lesions of exudative or infectious wounds and to prevent wound exacerbation (Akiyama et al. 2004). Wound dressings containing either silver or iodine (Aquacel Ag and Iodozyme) exerted an antimicrobial effect against the biofilms of *Pseudomonas aeruginosa* and *S. aureus*, although the iodine dressing was more efficacious under the experimental conditions employed (Thorn et al. 2009). Epithelium of chronic venous ulcers grew faster after treatment with cadexomer iodine when compared to standard dressing (Ormiston et al. 1985). Besides supporting epithelialization, iodine preparations may influence cytokine production by macrophages (Moore et al. 1997) and modulate the redox environment of wounds (Schmidt et al. 1995).

3.9 Hyiodine

The mixture of HA and iodine complex KI_3 (Hyiodine) was used by Sobotka et al. (2006, 2007) to treat chronic non-healing wounds in diabetic patients. Clinical improvement was found in a majority of patients. Accelerated healing of chronic wounds treated with Hyiodine was also reported by Ajemian et al. (Ajemian et al. 2007; Brenes et al. 2011). Complex of HA and iodine was found to be safe and effective in healing sternal wound dehiscence (Brenes et al. 2011). Hyiodine is a novel preparation used for wound treatment that supports wound hydration. The concentration of iodine in Hyiodine is lower (0.1%) in comparison to Betadine (~1% of iodine).

4 Methods

4.1 Animals

4.1.1 Experiments with permanent wounds in Wistar rats

Wistar rats (Biotest, Konárovice) weighing about 350 g and $9-10$ weeks old were used. The work with animals was done according to the acknowledged project under current rules of "*§ 11 Vyhláška č. 207/2004 Sb. (o ochraně, chovu a využití pokusných zvířat)*". The project was acknowledged by the Ethics Committee of Medical Faculty in Hradec Králové and by the Committee for Animal Protection of Ministry of Education, Youth and Sport of Czech Republic on 15th of May 2005. The work was divided into 3 experiments with 25 animals. Three animals were removed from the experiment due to removal of the ring implant. In each of 3 experiments, the animals were divided into 5 groups with n = 5 animal making together $n = 14-15$. In each group 0.6 ml of the solution was applied on the wound with a syringe. Groups were following:

- SALINE: a control group, treated with physiological solution (Medicamenta).
- HA11: treated with very low molecular weight (m.w.) hyaluronan with 11 kDa m.w. in average (1.5% solution, Contipro, filter sterilized).
- HA1200: treated with hyaluronan with 1200 kDa m.w. in average (1.5% solution, Contipro, sterilized by autoclaving at 120 °C during 15 min).
- KI3 (KI/I_2): treated with dissolved Lugol's solution (0.1% I_2/0.15% KI). KI – Sigma, 30315, puriss., Ph.Eur.; I_2 – Riedel-de Haen, 03002, puriss, Ph.Eur.
- HYIO: treated with Hyiodine (1.5% sterile autoclaved solution of 1200 kDa hyaluronan with addition of 0.1% I_2 and 0.15% KI, Contipro Dolní Dobrouč).

4.1.1.1 Experiments with contractile wounds in Wistar rats

40 Male Wistar rats (Biotest), $9-10$ weeks old and weighing $300-380$ g were housed in individual cages and fed commercial pelleted diet *ad libitum*. They were maintained in an air-conditioned room at 22 °C. The experiments were approved by the Ethics Committee of the Faculty of Medicine in Hradec Králové.

- 16 rats were observed until full wound closure (2 groups, n = 8),
- 24 rats were used for the histological assessment of wound tissue (2 groups, 4 time intervals – 3, 7, 11, 15 days, n = 3). In desired time interval the rats were euthanized and the wound tissue was taken for the histological analysis.

Groups were following:

- SALINE: a control group, treated with physiological solution (Medicamenta).
- HYIO: treated with Hyiodine (1.5% sterile autoclaved solution of 1200 kDa HA with addition of 0.1% I_2 and 0.15% KI, Contipro Dolní Dobrouč).

In each group 1 ml of the solution was applied on the gauze with a syringe and then applied on the wound.

4.1.2 ZDF animals and work with ZDF animals

Male and female ZDF rats that originated from Charles River (USA) were purchased from Anlab (Prague, Czech Republic) in March 2006. For the purposes of experiment the offsprings were bred in a vivarium at the Faculty of Medicine in Hradec Králové by mating non-obese heterozygous (fa/+) carrier parents or by mating fa/fa males with fa/+ females. This resulted in approximately 25% and 50% obesity rates, respectively. During the experiments with wounds, the rats were housed in individual cages. All animals were fed standard laboratory diet ST-1 (8% kcal fat, Velaz, Lysá nad Labem, Czech Republic) until the age of 6 – 8 weeks. Diabetes was then induced by feeding high fat diet (Peterson 2007) *ad libitum*: PURINA 5008 (17% kcal fat, IPS Supplies) was used for males and C13004 (48% kcal fat, Research Diets, New Brunswick, NJ, USA) was fed to females. Animals were considered to be diabetic when their non – fasting glucose levels reached 14 mmol/l in males and 9 mmol/l in females and when they possessed obese phenotype. Animals were maintained in an air – conditioned room at $22^{o}C$ with an automatic light/dark cycle. The experiments were approved by the Ethics Committee of the Faculty of Medicine in Hradec Králové (9.1.2006) and by committee of Ministry of Education, Youth and Sport of Czech Republic.

4.1.2.1 Experiments

As ZDF animals were difficult to breed and were bred continuously in smaller numbers, there were many small experiments that were combined. In one experiment, animals with similar age and diabetic status were used. Totally 24 experiments with 2 – 12 animals in each experiment were done without bandage (air exposed wound) and 30 experiments with 2 – 16 animals in each experiment were done with bandage (bandaged wound).

For both sexes these groups were created:

- Non – diabetic: control group – lean animals with genotype +/+ or fa/+,
- Diabetic: diabetes mellitus group – obese animals with genotype fa/fa.

4.2 Diets

4.2.1 Purina 5008 and RD 13004

Animals were fed high fat diet from 6 − 8 week of life. Males were fed Purina 5008 (16% of kcal fat), (Peterson 2007). Females were fed with RD 13004 (48% kcal of fat), (Peterson 2007).

4.2.2 H1 and HZ2

Diets H1 and HZ2 were developed as a potential replacement for the C13004 in order to induce high hyperglycemia. Diet C13004 induced only mild levels of hyperglymia (see further on), and this was also confirmed by the supplier of the diet. The difference between H1 and HZ2 was the content of the fat. Another reason for developing an alternative diet to C13004 was high price and shipping costs. Tab. 2 shows the composition and nutritional values of H1 in comparison with C13004 and HZ2.

C13004 composition	%	protein	fat	fiber	saccharides	moisture	ash	total
Purina 5015	65%	18,9%	11%	2,2%	52,20%	10%	6%	100%
maltodextrin 42	5%	0%	0%	0%	96%	4%	0%	100%
Homilc 7-60	30%	7%	60%	0%	27%	3%	3,60%	100%
total C13004		14,4%	25,2%	1,43%	46,8%	7,6%	4,98%	100%

H1	%	protein	fat	fiber	saccharides	moisture	ash	total
ST1 (non-granulated)	60%	24%	3,5%	3,7%	50,5%	11,8%	6,5%	100,0%
lard (pork)	25%	0,2%	99,5%	0%	0%	0,2%	0,1%	100,0%
cornstarch	5%	0,3%	0,05%	0,9%	90,3%	8,3%	0,1%	100,0%
sugar (white)	10%	0%	0%	0%	100%	0%	0%	100,0%
total H1		14,5%	27,0%	2,3%	44,8%	7,5%	3,9%	100%

HZ2	%	protein	fat	fiber	saccharides	moisture	ash	total
ST1 (non-granulated)	50%	24,00%	3,50%	3,70%	50,50%	11,80%	6,50%	100%
lard (pork)	35%	0%	99,5%	0%	0%	10%	0%	100%
cornstarch	5%	0%	0%	1%	91,3%	8,3%	0,1%	100%
sugar (white)	10%	0%	0%	0%	100%	0%	0%	100%
total HZ2		12,0%	36,6%	1,9%	39,8%	9,8%	3,3%	100%

Tab. 2: Composition and nutritional values of diets C13004 (Labdiets), H1 and HZ2. Nutritional values of components were obtained from the component's specification sheets or from National Nutrient Database for Standard Reference Release 25 (http://ndb.nal.usda.gov/) or from http://www.lucy.cz/energeticke-tabulky/.

4.3 Genotypization of ZDF animals

ZDF animals were genotyped by using a PCR followed by a cleavage by restriction endonuclease MspI (Sudre et al. 2002). The method is described below. The DNA was obtained by using Viagen Direct PCR solution or QIAGEN DNeasy kit. The photographs of gels were taken by a camera Canon 300D.

4.3.1 Materials and chemicals

- Primers (Generi Biotech, Hradec Králové)

  sZDFfa1: 5'-CGT ATG GAA GTC ACA GAT GAT GGT AAT-3'

  sZDFfa2: 5'-CCT CTC TTA CGA TTG TAG AAT TCT CT-3'

- Reagents for PCR (Taq polymerase Fermentas, EP0401, Vilnius, dNTP Mix 10 nM)

- Restriction endonuclease Msp I (Fermentas, ER0541)

- Materials for DNA extraction: Viagen Direct PCR or QIAGEN DNeasy

- Materials for agarose electrophoresis : DNA ladder (FastRuler™ Ultra Low Range DNA Ladder, ready-to-use: 10, 20, 50, 100, 200 bp, Fermentas or Fermentas – SM1233 Ultra Low Range DNA Ladder (Biogen)

- PCR thermocycler (Biometra)

4.3.2 PCR amplification of gene for leptin receptor

Master Mix (MM) was prepared for desired number of reactions according to Tab. 3. MM was divided by 24 µl to the PCR tubes and 1 µl of genomic DNA (approximately 100 ng) was added to each tube.

Chemical	volume (µl) for one reaction	volume (µl) for 10 reactions
10x polymerase buffer	2.5	25
primer sZDFfa1 (10 µM) – 40 pmol	4	40
primer sZDFfa2 (10 µM) – 40 pmol	4	40
50x dNTP Mix (10 mM each)	0.5	5
Taq polymerase	0.2	2
MgCl2 (25 mM)	2.5	25
water (suitable for PCR)	10.3	103
Genomic DNA – 100 ng	1	10x1
Total	25	250

Tab. 3: Preparation of Master Mix for PCR reaction.

DNA was amplified in the thermocycler using temperature program for ZDF genotyping (see Tab. 4). The product of PCR reaction (5 µl) was analyzed on 3% agarose gel at 70 V for 1 hour (TAE buffer) with a suitable DNA ladder. 118 bp bands were expected.

95 °C – initial denaturation	2 min	
95 °C – denaturation	30 s	33 x
64 °C – annealing	1 min	33 x
72 °C – elongation	30 s	33 x
72 °C – final elongation	2 min	

Tab. 4: Temperature program for genotypization of ZDF animals.

4.3.3 Restriction cleavage of PCR product

For each sample the mixture of 20 µl of PCR reaction solution with 1 µl of Tango Buffer and 1 µl MspI nuclease (30 U/µl) was prepared. After mixing and short spin the tube was incubated for 1 hour at 37 °C in the thermocycler. 11 µl of mixture was used for 4% agarose gel electrophoresis at 70 V for 1 hour and 30 min (TAE buffer), with a suitable ladder.

4.3.4 Analysis of results

Bands for the +/+ (wild type) genotype had 118 bp in size, for +/fa genotype had size 118, 79 and 39 bp and for fa/fa genotype had size 79 and 39 bp, thus allowing genotypization.

4.4 Measurement of glycemia

A drop of blood was collected from the tail vein. Portable glucose meter, Accu-Chek Go was used for glucose measurement using a drop of blood according to a procedure bellow.

4.4.1 Materials

- Laboratory rat
- Blood glucose meter Accu-Chek Go (Roche)
- Blood glucose test strips (Roche)
- Needle (23G), syringe, gauze, Ajatin (disinfection solution)
- Sampling container

4.4.2 Procedure

Rat was inserted into a sampling container and its tail was cleansed under a stream of warm water (about 40 °C) and wipe-dried. After the localization of the tail veins the needle was inserted into the tail vein at the back of the tail. Minimally 10 µl of blood was sampled by an outflow. A new test strip was inserted into the glucose meter and as soon as a flashing drop appeared on the display, the tip of the strip was inserted into a drop of blood. Once the drop was aspirated, the sound indicated correct sampling and the display showed the level of glucose in mmol/l. Excess blood on rat's tail was removed with gauze and rinsed with a disinfectant solution (Ajatin).

4.5 Creation of a permanent wound and granulation tissue collection

The permanent wounds (Fig. 4) were created as described by (Rudas 1960). The details of the procedure are described below.

Fig. 4: The picture of permanent wound. In the upper part an implanted plastic ring without the cover is shown.

4.5.1 Materials

- Rat
- Nembutal (pentobarbital 50 mg/ml), ether
- Clippers
- Pliers (bone rongeurs 19 mm)
- Plastic rings into the wound, nylon wound cap
- Surgical thread
- Superglue

4.5.2 Procedure of permanent wound induction

The rats were anesthetized by applying a solution of Nembutal intraperitoneally at a dose of 1 ml per kg of rat weight. The rats were attached on the operational board (stomach

down) and their coat on the back was shaved with clippers. A fold of skin was made by gripping it in two fingers and the skin was cut out at a distance of about 6 cm from the ear using pliers and scissors. This procedure should create regular circular wound, approximately 18 - 20 mm in diameter. The wound should not bleed. 4 threads were sewn into the skin about 3 mm from the edge of wound, each at intervals of 90 degrees. Plastic ring was inserted into the wound. Threads were inserted into the holes in the ring and the ring was attached carefully with threads at the back of the rat. The superglue was applied to the top of the ring and the nylon cap was stuck to the ring. The cap was attached to the ring by tying it with a thread. The solution was applied to influence the formation of granulation tissue by syringe and needle. Every day 0.6 ml of the solution was applied for seven days. Application was made with a syringe and a needle piercing through a nylon cap.

4.5.3 Sampling of the granulation tissue

The rat was put in a container to inhale the ether until the rat stopped breathing. The plastic ring was removed by cutting off all the threads holding it. The fibro-vascular granulation tissue in the size of the internal ring radius and height of about 1 - 2 mm was cut out carefully, using surgical curved scissors. It was important not to cause the discharge of blood to the tissue. The whole tissue was weighted. The half of the tissue was put to buffered formaldehyde for histological analysis. The rest of the tissue was cut into small pieces (approximately 50 mg ~ 4 x 4 x 3 mm) and inserted into:

1. a pre-weighed micro-vial with a screw cap (30 - 60 mg tissue is needed for hydroxyproline,
2. a tube with 0.5 ml RNA later (Qiagen) solution (about 30 mg of tissue should be immersed for RNA isolation). The tissue was incubated in RNA latter for 24 hours at 4 °C in order to penetrate the sample. Then, the sample was stored at -20 °C.

4.6 Induction of contractile wounds, tissue sampling

Full-thickness, 2 cm large in diameter, excisional wounds were made on the back of experimental animals. Procedure of wound induction, substances application and sampling are described below in detail.

4.6.1 Materials and chemicals

- laboratory rat
- Nembutal (pentobarbital 50 mg/ml, dose 50 mg/kg) or ketamine (100 mg/ml) and xylasine (20 mg/ml), dose 75 and 5 mg/kg respectively, ether
- trimming clippers
- curved surgical scissors
- Luer bone rongeur forceps (19mm) - pliers
- millimeter ruler
- Digital Camera (Canon EOS D350)
- gauze compress, gauze (sterile), tape, elastic gauze
- image analysis software ImageJ (available at http://rsb.info.nih.gov/ij/)

4.6.2 Procedure

4.6.2.1 Induction of wound

The rats were anesthetized by applying a solution of nembutal intraperitoneally at a dose of 1 ml per kg rat weight or a mixture of ketamine and xylasine (3:1), 75 and 5 mg/kg, respectively. The blood was sampled with a glass capillary from retro orbital plexus. The rats were attached on the operational board (stomach down) and their coat on the back was shaved with clippers. A fold of skin was made by gripping it in two fingers and the skin was cut out at a distance of about 6 cm from the ear using pliers and scissors. This procedure should create regular circular wound, approximately 18 - 20 mm in diameter. The wound should not bleed. The millimeter ruler was put near the wound and a picture was taken with a digital camera. The substances soaked in a gauze were applied on the wound. Another gauze pad was applied on the wound, fixed with a tape, and elastic gauze (Fig. 5).

Fig. 5: Picture of the treated rat with a gauze pad, gauze and tape.

4.6.3 Application

Every one to three days (according to plan of experiment) the treatment was applied and the bandage was changed. In case of monitoring of diabetes impact on healing no curative treatment is applied.

4.6.4 Sampling the tissue

The rat was put into a container to inhale the ether until the rat stopped breathing. The rats were euthanized by cervical dislocation. After the removal of the bandage a picture of the wound with crust was taken. If possible, the crust was removed carefully and stored for further analysis. The picture of the wound without the crust was taken. Fibro-vascular granulation tissue also with 3 mm of uninjured skin was cut out carefully, using surgical curved scissors. The tissue was split into two halves. The first half was put to buffered formaldehyde for histological analysis. The uninjured skin was cut off from the second half and the remaining granulation tissue was weighted. The tissue was cut into small triangular pieces (approximately 50 mg ~ similarly to cutting of pizza slides) and inserted into:

1. a pre-weighed micro-vial with a screw cap (30 - 60 mg tissue was needed for hydroxyproline,
2. a tube with 0.5 ml RNA later (Qiagen) solution (about 30 - 50 mg of tissue was immersed for RNA isolation). The tissue was incubated in RNA latter for 24 hours at 4 °C in order to penetrate the sample. Then, the sample was stored at -20 °C.

During the experiment, especially during first 3 days, it was important that rats were kept on dust-free bedding. For this purpose, filter paper or paper wood pulp was used as an absorbent.

4.7   Photographing wounds, wound size analysis

4.7.1   Photographing the wound

Photographs of wounds were taken every one to three days. If the bandage was applied, photographs were taken at each bandage change. When photographing the wound, a millimeter ruler was placed approximately 5 mm from the wound edge . Wound surface and ruler was in one plane.

4.7.2   Measuring the wound

The picture of the wound was open in *ImageJ* software. The image calibrated using a known length (2 – 4 cm):

i)   the option *straight line selection* was selected;

ii)   the line with a known distance (on ruler) was selected ;

iii) the function   *Analyze → Set Scale → Known Distance* was used with the length of the calibration line, e.g. 3 cm - see Fig. 6;

The scale of image in pixels/cm was automatically calculated.
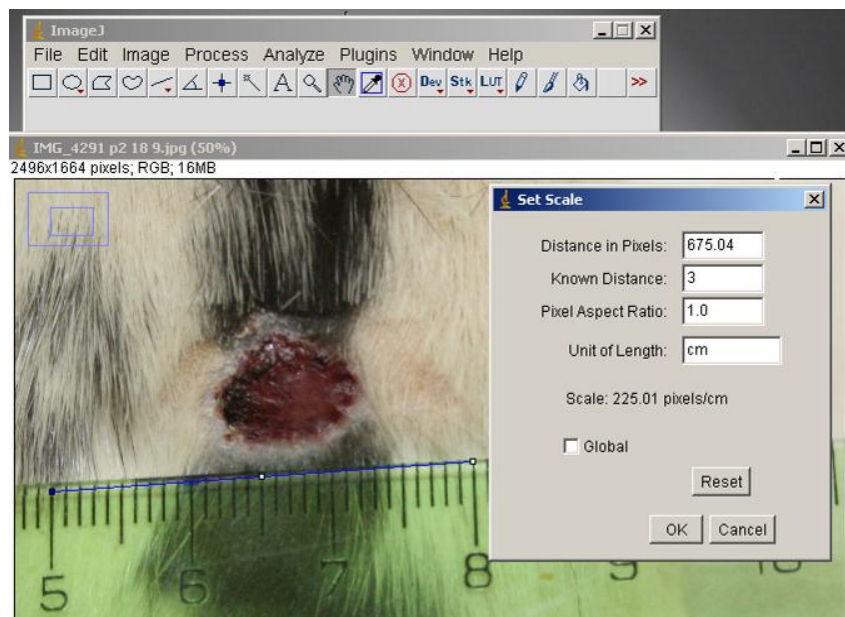
Fig. 6: Calibration of pictures.

A border line was made around the wound using function *Polygon Selection* (Fig. 7). The function Analyze → Measure was selected. The program calculated wound area in cm^2 and showed it in a table. The procedure was repeated with next pictures and the table with results was copied to MS Excel.
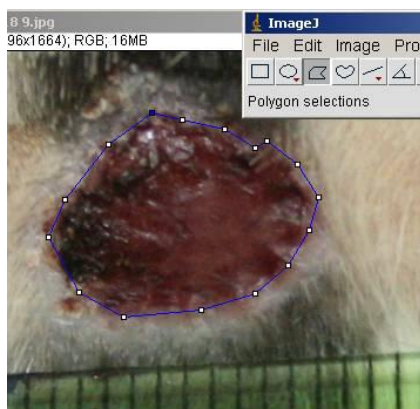
Fig. 7: Border-line selection around the wound

4.8 Hydroxyproline determination

Approximately every seventh amino acid in collagen is hydroxyproline. Other proteins with the exception of elastin are practically hydroxyproline-free. Hydroxyproline content was determined by the method of (Hurych et al. 1962). The details of the procedure are described below.

4.8.1 Chemicals and materials

- CAP 4X (citrate-acetate buffer)   1000 ml pH= 6.3, conserved with two drops of toluene
    - 50 g citric acid.H_2O p.a. (Penta, 27490 1)
    - 12 ml glacial acetic acid (Lachner)
    - 120 g sodium acetate.$3H_2O$ p.a. (Penta, 71193 1)
    - 34 g NaOH
- CAP 1X (citrate-acetate buffer): 250ml CAP 4x with 750 ml of distilled water
- PCAP (propanol-citrate-acetate buffer) – 100 ml
    - 30 ml propanol
    - 20 ml H_2O
    - 50 ml CAP 4X
- 0.84% solution of chloramine-T (Sigma – Riedel-de Haen, cat.no. 31224) in PCAP
- 5% PDAB (p-dimethylaminobenzaldehyd, Sigma-Aldrich) in propanol
- Stock solution of hydroxyproline (Sigma-Aldrich) 10000, 500 µg/ml in injection water and 8 µg/ml in CAP
- Thermoblock
- UV/VIS Spectrophotometer (Helios)

- 1,5 ml micro-tubes

4.8.2 Procedure

Hydrolysis of granulation tissue (GT) and dry mass determination

An empty polypropylene sample tube with a screw cap was weighted with 0.1 mg accuracy. The tube with the sample was weighted and the mass of wet GT (VGT) calculated. GT was dried at 80 °C in an open tube in the thermoblock until constant weight is achieved (3 hours was usually suitable). The mass of dried granulation tissue (DGT) was calculated. % dry weight was calculated as a ratio of DGT/VGT. 6M HCl was added to the tube in 1:100 ratio (to 10 mg DGT 1000 µl of 6M HCl was added) and hydrolyzed for 16 hours at 105 °C in a thermoblock or in a dryer. The samples were centrifuged for 10 minutes at 10000x g. The hydrolysate was then stored in clean tubes at 4 °C.

Determination of hydroxyproline from hydrolysate

Chloramine-T, PDAB and stock solutions of hydroxyproline for the calibration curve were prepared fresh. Standard solutions were prepared using two-fold serial dilution in CAP (Tab. 5).

S 0 - blank	S 0.5	S 1	S 2	S 4	S 8
250 µl CAP	250 µl S 1	250 µl S 2	250 µl S 4	250 µl HYP 8	250 HYP 8
	250 µl CAP	250 µl CAP	250 µl CAP	250 µl CAP	

Tab. 5: Dilution of hydroxyproline standards.

2.5 µl of GT hydrolysate was diluted with 247.5 µl of CAP 1X. 250 µl of solution of chloramine-T was added and incubated for 20 minutes at room temperature. 250 µl of 3M $HClO_4$ was added, mixed thoroughly and incubated for 5 minutes at room temperature. 250 µl of PDAB solution was added, mixed and incubated for 20 minutes at 60 °C in the thermoblock. After cooling down for 20 minutes at room temperature the samples were measured for the absorbance at 560 nm against blank. The concentration was calculated using the calibration curve. The absorbance of most concentrated standard was usually around 0.8.

4.8.3 Protein and uronic acid determination

The crust with jelly-like exudate was extracted with 0.5 mol ⁄ L NaOH at 60 °C for 2 h (Simeon et al. 2000). The mixture was neutralized and ethanol was added to the final concentration of 80% (v ⁄ v). After centrifugation, the precipitate was redissolved in 0.5 mol ⁄ L NaOH and used for protein and uronic acid determinations. Protein was measured using a commercial protein assay (DC Protein Assay; Bio-Rad,) with bovine serum albumin (Sigma) as a standard. The carbazole method (Bitter et al. 1962) was used to determine uronic acid levels, and D-glucuronic acid (BDH Biochemicals) was used as a standard.

4.8.4 Polyacrylamide gel electrophoresis

Protein samples were boiled with dithiothreitol and SDS, applied to 8% acrylamide gel and electrophoresed. For the samples, 30 µg of rat serum or plasma proteins, 30 µg of proteins extracted from the crust ⁄ exudate, or 15 µg of bovine serum albumin (Sigma) were used. After resolution, the proteins were stained with Coomassie Blue.

4.9 Determination of leptin, insulin, PAI-1, IL-6 and CRP in plasma

The blood was taken from the orbital plexus into the heparinized tubes with a separation gel (Sarsted Microvette). Heparinized blood was centrifuged at 13000 rpm for 5 minutes. ELISA kits for proteins/peptides determination were used according to the recommendation of manufacturers.

- Mercodia Rat Insulin ELISA (10-1113-01)
- Alpco, Salem, USA (45-IL6RT-E01.1) and Bender MedSystem rat IL6 ELISA (BMS625)
- American Diagnostica Imunoclone Rat PAI-1 ELISA kit (601)
- Leptin rat ELISA: Biovendor, Brno, Czech Republic (RD291001200R)
- CRP (c-reactive protein) rat ELISA: Biovendor, Brno, Czech Republic (RH951CRP01R)

The determinations by ELISA were done by Mgr. Tkáčová under the supervision of author of the present thesis. Detailed procedures and the results are a part of her diploma thesis.

4.10 Malondialdehyde measurement using HPLC

The measurement was done in co-operation with the Department of Pharmacology, Faculty of Medicine in Hradec Králové by Miloš Hroch, MSc., PhD. In short, the analysis was based on alkali hydrolysis (6M NaOH), de-proteination with perchloric acid (35% v/v) and addition of derivatization reagent (5mM dinitrophenylhydrazine in HCl). The analysis of

product was done on Agilent HPLC equipment with a UV/VIS detector on a column with reverse phase separation EC NUCLEOSIL 100-5 C18 (4.6x125mm).

4.11   Histological analysis of uninjured skin

The skin that was removed during the wound induction was used for the histological analysis of uninjured skin. Tissue was fixed in 10% neutral buffered formalin (4% formaldehyde) for several days at 4 °C and embedded in paraffin. Six μm sections were stained at the Department of Histology and Embryology, Faculty of Medicine in Hradec Králové (Jana Holerová). The tissue was stained with blue trichrome for collagen and also with haematoxylin and eosin.

4.12   Histological analysis of granulation tissue

Wound biopsies that included wound tissue and approximately 3 mm of surrounding uninjured skin were fixed in 10% neutral buffered formalin for several days at 4 °C and embedded in paraffin. Six μm sections were cut at the center of the wound, perpendicularly to the wound surface. Tissue sections were stained with haematoxylin and eosin or with blue trichrome.

4.13   Image analysis of histological sections

For the image analysis the samples were scanned with a scanner Epson Perfection V700 Photo, using resolution 4800 dpi, (1890 pixel/cm). Software ImageJ (NIH) was calibrated with this value. Samples were analyzed for: length of epithelization tongue, fat content in tissue (wound, skin), granulation tissue content, and thickness of crust (wound), fat layer and dermis (skin) using image analysis with ImageJ.

4.14   Processing and statistical evaluation of data

Data were accumulated into MS Excel. Graphs were made in this program and where suitable, the differences between groups were evaluated using unpaired t-statistical test.

4.15   Isolation of RNA

A slice of granulation tissue (without surrounding intact skin, without wound crust) was homogenized in the lysis buffer (Qiagen) with Ultra-turrax (IKA). A part of the homogenate was extracted using the RNeasy Fibrous Tissue Mini-Kit (Qiagen).

4.16 Microarray analysis

4.16.1 Microarray chip design

The software OligoArray 2.1 was used to design oligonucleotide probes for microarray. Whole genome *Rattus norvegicus* mRNA database was obtained from the ftp server of The National Center for Biotechnology Information (NCBI) from the address ftp://ftp.ncbi.nih.gov/genomes/R_norvegicus/RNA/. Input parameters for probes selection were as described in Tab. 6.

Probe length	48-52 bp
GC content	30% - 70%
Melting temperature of probe	86 – 90 °C
Melting temperature of secondary structures of probes - limits for probe rejection	65 °C
Max. distance of probe from 3' end	4000 bp
Minimal distance between probes	50 bp
Forbidden sequences	AAAAA, TTTTT, CCCCC, GGGGG

Tab. 6: Parameters for OligoArray 2.1 for probe design.

The list of genes is shown in Tab. 7. These genes were used in the first part of this study (effect of Hyiodine and hyaluronic acid in Wistar rats). Genes shown in Tab. 7 with changes shown in Tab. 8 were used in the second part of this study, in the studies of wound repair on ZDF rats.

name	gene symbol	REFSEQ ID
Hyaluronan metabolism		
hyaluronan synthase1 (LOC282821)	HAS1	NM_172323
hyaluronan synthase 2 (Has2)	HAS2	NM_013153
hyaluronan synthase 3 (Has3)	HAS3	NM_172319
hyaluronidase 1 (Hyal1)	hyal1	NM_207616
hyaluronidase 2 (Hyal2)	hyal2	NM_172040
hyaluronidase 3 (Hyal3)	hyal3	NM_207599
CD44 antigen (Cd44)	cd44	NM_012924
hyaluronan mediated motility receptor (Hmmr)	RHAMM	NM_012964
toll-like receptor 4 (Tlr4)	TLR4	NM_019178
Apoptosis / Cell cycle		
CD47 antigen (Rh-related antigen, integrin-associated signal transducer)	IAP4 = CD 47	NM_019195
inhibitor of apoptosis protein 1 (Birc3)	BIRC3	NM_023987
apoptosis inhibitor 2 (Api2)	API2	NM_021752
Bcl2-associated X protein (Bax)	bax	NM_017059
v-myc avian myelocytomatosis viral oncogene homolog (Myc)	c-myc	NM_012603
Bcl-x alpha	bcl-x alpha	U72350
B-cell leukemia/lymphoma 2 (Bcl2)	bcl-2	NM_016993
caspase 3 (Casp3)	caspase-3	NM_012922
caspase-8 (Casp8)	caspase-8	NM_022277
tumor protein p53 (Tp53)	p53	NM_030989
proliferating cell nuclear antigen (Pcna)	PCNA	NM_022381
p21 (CDKN1A)-activated kinase 2 (Pak2)	p21	NM_053306
Cytoskelet		
desmin (Des)	desmin	NM_022531
glial fibrillary acidic protein (Gfap)	GFAP	NM_017009
mitogen activated protein kinase 1 (Mapk1)	MAPK1	NM_053842
NO metabolism		
Rattus norvegicus nitric oxide synthase 2, inducible (Nos2)	iNOS, NOS2	NM_012611
nitric oxide synthase 3, endothelial cell (Nos3)	NOS3	NM_021838
ECM / ligamentous proteins		
neural cell adhesion molecule 1 (Ncam1)	N-CAM	NM_031521
vitronectin (Vtn)	Vtn	NM_019156
thrombospondin 2 (TSP-2)	Tsp-2	XM_214778
thrombospondin 1 (Tsp1)	Tsp-1	AF309630
secreted acidic cysteine rich glycoprotein (Sparc)	SPARC	NM_012656
reelin (Reln)	Reln	NM_080394
secreted phosphoprotein 1 (Spp1)	spp1 Opn	NM_012881
alpha-2-macroglobulin (A2m)	a2m	NM_012488
fibulin 5 (Fbln5)	Fbln-5	NM_019153
fibulin 2 (Fbln2)	Fbln-2	XM_232197
laminin, beta 2 (Lamb2)	lamb2	NM_012974
fibronectin 1 (Fn1)	Fn1	NM_019143
fibrillin-1 (Fbn1)	Fbn1	NM_031825
fibrillin-2 (Fbn2)	Fbn2	NM_031826
elastin (Eln)	Eln	XM_341061
procollagen, type I, alpha 2 (Col1a2)	Col1a2	NM_053356
collagen, type III, alpha 1 (Col3a1)	Col3a1	XM_343563
collagen, type V, alpha 1 (Col5a1)	Col5	NM_134452
similar to alpha-3 type IV collagen (LOC363265)	col4	XM_343607
collagen, type XVIII, alpha 1 (Col18a1)	col18a1	XM_241632

name	gene symbol	REFSEQ ID
Proteases and inhibitors		
matrix metalloproteinase 2 (72 KDa type IV collagenase) (Mmp2)	mmp-2	NM_031054
matrix metalloproteinase 3 (Mmp3)	mmp-3	NM_133523
matrix metalloproteinase 7 (Mmp7)	mmp-7	NM_012864
matrix metalloproteinase 9 (gelatinase B, 92-kDa type IV collagenase)	mmp-9	NM_031055
matrix metalloproteinase 13 (Mmp13)	mmp-13	XM_343345
matrix metalloproteinase 12 (Mmp12)	mmp-12	NM_053963
matrix metalloproteinase 14 (membrane-inserted) (Mmp14)	mmp-14	NM_031056
mannose-binding protein associated serine protease-1 (Masp1)	P100=masp1	NM_022257
tissue inhibitor of metalloproteinase 1 (Timp1)	TIMP1	NM_053819
tissue inhibitor of metalloproteinase 2 (Timp2)	TIMP2	NM_021989
tissue inhibitor of metalloproteinase 3 (Timp3)	TIMP3	NM_012886
Proteoglycans		
aggrecan 1 (Agc1)	Agc1	NM_022190
biglycan (Bgn)	bgn	NM_017087
decorin (Dcn)	Dcn	NM_024129
lumican (Lum)	lum	NM_031050
syndecan 1 (Sdc1)	sdc1	NM_013026
syndecan 3 (Sdc3)	sdc3	NM_053893
syndecan 4 (Sdc4)	sdc4	NM_012649
heparan sulfate core protein precursor (HSPG) (Perlecan)	plc	XM_233606
Cytokines a growth factors		
connective tissue growth factor (Ctgf)	CTGF	NM_022266
endothelin 1 (Edn1)	Edn1	NM_012548
fibroblast growth factor 2 (Fgf2)	FGF2	NM_019305
interleukin 1 beta (Il1b)	IL1b	NM_031512
interleukin 4 (Il4)	IL-4	NM_201270
interleukin 6 (Il6)	IL-6	NM_012589
interleukin 10 (Il10)	IL-10	NM_012854
interleukin 12b (Il12b)	IL-12b	NM_022611
neurotrophin 3 (Ntf3)	NT-3	NM_031073
platelet derived growth factor, alpha (Pdgfa)	PDGFa	NM_012801
Platelet-derived growth factor (Pdgfb)	PDGFb	XM_343293
transforming growth factor, beta 1 (Tgfb1)	TGFb1	NM_021578
transforming growth factor, beta 3 (Tgfb3)	TGFb3	NM_013174
tumor necrosis factor superfamily, member 2 (Tnf)	TNFa	NM_012675
vascular endothelial growth factor (Vegf)	VEGF	NM_031836
insulin-like growth factor 1 (Igf1)	Igf1	NM_178866
relaxin 1 (Rln1)	Rln1	NM_013413
House keeping		
actin, beta (Actb)	Actb	NM_031144
Rat 18S rRNA sequence	18S RNA	X01117
glyceraldehyde-3-phosphate dehydrogenase (Gapd)	GAPD	NM_017008.2
Receptors		
transforming growth factor, beta receptor 3 (Tgfbr3)	Beg= TGFBR3	NM_017256
intercellular adhesion molecule 1 (Icam1)	ICAM-1	NM_012967
laminin receptor 1 (67kD, ribosomal protein SA)	Lamr1	NM_017138
Integrin, alpha 5 (fibronectin receptor, alpha)	Itga5	XM_235707
integrin, alpha 6 (Itga6)	Itga6	XM_215984
integrin beta 1 (Itgb1)	Itgb1	NM_017022
integrin beta 3 (Cd61)	Itgb3	NM_153720

Tab. 7: List of assayed transcripts, their abbreviations and reference numbers according to NCBI used in the study of wound repair.

name	gene symbol	REFSEQ ID	group
ADDED			
galectin-1	Lgals1	NM_019904	Receptors
galectin-3	Lgals3	NM_031832	Receptors
hsp-47	gp46	NM_017173.1	ECM / ligamentous proteins
laminin M (α2)	Lama2	XM_219866	ECM / ligamentous proteins
plasminogen	plg	NM_053491.1	ECM / ligamentous proteins
plasminogen activator	Plat	NM_013151	ECM / ligamentous proteins
plasminogen activator inhibitor (Rattus norvegicus serine (or cysteine) peptidase inhibitor, clade E, member 1 (Serpine1))	PAI-1	NM_012620.1	ECM / ligamentous proteins
tissue transglutaminase, 2 (C polypeptide)	Tgm2	NM_019386	ECM / ligamentous proteins
transforming growth factor, beta 2	Tgfb2	NM_031131	Cytokines a growth factors
Rattus norvegicus nitric oxide synthase 1, neuronal (Nos1)	Nos1	NM_052799	NOS
PREDICTED: Rattus norvegicus matrix metalloproteinase 1b (interstitial collagenase) (predicted)	mmp1	XM_235849	Proteases and inhibitors
Rattus norvegicus matrix metallopeptidase 10 (Mmp10)	mmp10	NM_133514	Proteases and inhibitors
Rattus norvegicus bone morphogenetic protein 6 (Bmp6)	bmp6	nm_013107	Cytokines a growth factors
PREDICTED: Rattus norvegicus chondroitin sulfate proteoglycan 2 (Cspg2)	versican	XM_215451.4	Proteoglycans
Rattus norvegicus macrophage expressed gene 1 (Mpeg1)	mpeg1	NM_022617	Inflammation
Rattus norvegicus S100 calcium binding protein A9 (calgranulin B) (S100a9).	mrp14	NM_053587	Inflammation
Rattus norvegicus syndecan 2 (Sdc2).	sdc2	NM_013082	Proteoglycans
Rattus norvegicus plasminogen activator, urokinase (Plau)	plau	NM_013085	Proteases and inhibitors
Rattus norvegicus matrix metallopeptidase 8 (Mmp8)	mmp8	NM_022221	Proteases and inhibitors
Rattus norvegicus secretory leukocyte peptidase inhibitor (Slpi)	slpi	NM_053372.1	Proteases and inhibitors
Rattus norvegicus gremlin 1 homolog, cysteine knot superfamily (Xenopus laevis) (Grem1)	grem1	NM_019282.1	Cytokines a growth factors
Rattus norvegicus angiopoietin 1 (Angpt1).	angpt1	NM_053546.1	Cytokines a growth factors
PREDICTED: Rattus norvegicus angiopoietin 2 (Angpt2).	angpt2	XM_344544.3	Cytokines a growth factors
PREDICTED: Rattus norvegicus tumor necrosis factor alpha induced protein 6 (Tnfaip6).	Tnfaip6	XM_001065494	Cytokines a growth factors
Rattus norvegicus laminin, alpha 3 (Lama3)	lama3	NM_173306.1	ECM / ligamentous proteins
PREDICTED: Rattus norvegicus laminin, beta 3 (Lamb3)	lamb3	XM_223087.4	ECM / ligamentous proteins
PREDICTED: Rattus norvegicus lamimin, gamma 2 (Lamc2)	lamc2	XM_213902.4	ECM / ligamentous proteins
PREDICTED: Rattus norvegicus laminin, beta 1 (predicted) (Lamb1_predicted)	lamb1	XM_216679.4	ECM / ligamentous proteins
PREDICTED: Rattus norvegicus laminin, gamma 1 (Lamc1)	lamc1	XM_341133.3	ECM / ligamentous proteins
REMOVED			
inhibitor of apoptosis protein 1 (Birc3)	BIRC3	NM_023987	Apoptosis / Cell cycle
apoptosis inhibitor 2 (Api2)	API2	NM_021752	Apoptosis / Cell cycle
caspase-8 (Casp8)	caspase-8	NM_022277	Apoptosis / Cell cycle
tumor protein p53 (Tp53)	p53	NM_030989	Apoptosis / Cell cycle
desmin (Des)	desmin	NM_022531	Cytoskelet
glial fibrillary acidic protein (Gfap)	GFAP	NM_017009	Cytoskelet

Tab. 8: List of assayed transcripts, their abbreviations and reference numbers according to NCBI. Changes in microarray design for the study of wound repair in ZDF rats.

4.16.2 cDNA synthesis, biotin-dUTP labeling, hybridization

The procedure was based on the recommendation of the manufacturer (Bioscience, Jena − previously Clondiag). After the binding of random primers, RNA was transcribed to the cDNA using reverse transcriptase MuMLV (Fermentas) and 4 deoxyribonucleotides (Abgene) plus biotin labeled deoxyuridintriphosfate (Fermentas). cDNA was then hybridized with the probes on the array tube (AT) chip surface, which contained immobilized 50 bp DNA oligonucleotides probes specific for selected genes. Detailed procedure is described below.

4.16.2.1 Materials

- 20x SSPE, 20x SSC (Invitrogen)
- 3DNA buffer : 250 mM Na_2HPO_4(Penta, p.a), 4,5% SDS (Amresco), 1 mM EDTA (Sigma), 1xSSC, pH = 7.2
- HRP-streptavidine conjugate (Pierce, 1 mg/ml, 21130)
- Blocker Casein in PBS (1% casein, Pierce, 37528)
- deoxy nucleotides (100 mM, AB gene)
- YM-30 columns (Millipore)
- True Blue peroxidase substrate (KPL, 71-00-67, 10ml)

4.16.2.2 cDNA synthesis and purification procedure

The mixture of 26 µl of RNA with 3 µl of random hexamer primers (Invitrogen, 3 µg/µl) was prepared. RNA was denatured by incubation at 65 °C for 10 minutes, and then was put on ice. During the denaturation RT-mix was prepared for all the samples according to Tab.9. 21 µl of RT-mix was added to every tube with RNA mixture.

Reagent	Volume [µl]
5x RT buffer (Fermentas)	10
Nucleotide mix(5 mM dATP, 5 mM dGTP, 5 mM dCTP, 3 mM dTTP)	1.5
Biotin-dUTP 1 mM (Fermentas)	3
MuMLV- RT – 200U/µl (Fermentas)	2
RNAse free H_2O (Qiagen)	4.5
Total 1x RT-mix volume 21 µl	21
Total volume (RTmix + RNA sol. + hexamers)	50

Tab. 9: cDNA master mix for microarray for one reaction

The reaction was done in a thermocycler at 25 °C for 10 minutes, then at 42 °C for 120 minutes. 10 µl of NaOH (1M) was added and incubated at 65 °C in thermocycler for 10 minutes to denaturate RNA. Meanwhile 430 µl of ddH_2O was added to YM-30 columns. 10 µl of 1M HCl was added to tubes with cDNA to neutralize the solution. Neutralized cDNA solution was applied on the columns prefilled with H_2O. Columns were centrifuged at 13000 g at 20 °C for 8 minutes, the permeate was removed and 450 µl of ddH_2O was added to columns to wash cDNA. Last centrifugation/washing step was repeated once more. The eluate of cDNA was transferred to clean tubes. If necessary the eluate was concentrated in a freeze dryer connected to a vacuum pump. The volume was adjusted with H_2O to 12 µl. cDNA concentration and purity was measured at UV/VIS spectrophotometer at 260 and 280 nm using 2 µl cDNA.

4.16.2.3 Hybridization procedure

Array tubes were prewashed twice with 500 µl of 3DNA buffer (30 °C / 5min and 50 °C / 5min) in thermomixer at 550 rpm. 10 µl of labeled cDNA was mixed with 90 µl, denaturated at 95 °C and cooled on ice of one minute. Then the solution was added to array tube (AT) and hybridized overnight at 50 °C in thermomixer at 550 rpm. After the hybridization ATs were washed with 500 µl of 2xSSC + 0.2% SDS at 30 °C for 5 min then with 2xSSC at the room temperature for 5 min and finally with 0.2xSSC at room temperature for 5 min. The unspecific background was blocked with 500 µl of 0.1% casein in 6xSSPE + 0.1% SDS at 30 °C for 30 min. 2 µl the HRP-streptavidin conjugate (1:100 in PBS) with 98 µl 3DNA buffer at 30 °C was added for 30 min. In all incubation steps ATs were incubated at 550 rpm in the thermomixer.

4.16.2.4 Washing and signal capturing procedure

The washing procedure was done according to Tab. 10. Cleansing of the bottom of AT with a micro-fiber cloth and checking in AT reader. The enzyme reaction was started by adding 100 µl of True Blue peroxidase substrate. The signal of the array is captured in AT reader (ATR 01, CloneDiag) with open tubes. The AT reader was controlled using IconoClust array imaging software. The signal was captured at 25 °C for 15 minutes in 1 minute intervals. The images were analyzed using IconoClust software and bad spots were manually removed. The data were exported to MS Excel.

2xSSC+0.01% Triton	500 µl	RT (room temp.)/5 min	550 rpm on vortex
2. 2xSSC	500 µl	RT/5 min	550 rpm on vortex
3. 0.2xSSC	500 µl	RT/5 min	550 rpm on vortex

Tab. 10: Washing steps of AT procedure

4.17 Analysis of mRNA gene expression using quantitative RT-PCR

4.17.1 Materials

- High-Capacity cDNA Archive kit (Applied Biosystems, PN 4322171)
- total RNA (1 µg)
- Universal TaqMan Master mix, No Amperase UNG (Applied Biosystems, PN 4324018)
- Fluorescent TaqMan probes with primers - Gene Expression Assay (Applied Biosystems, PN 4331182)
- Real-time PCR instrument able to detect fluorescent probes labeled with VIC a FAM (Applied Biosystems ABI 7500 FAST, ABI 7900)
- SDS software 1.3.1 (Applied Biosystems)
- MicroAmp Fast 96-Well Reaction Plate (0.1 mL, Applied Biosystems, PN 4346907)
- Optical adhesive cover for 96-well plate (Applied Biosystems)

Applied Biosystems Gene Expression assays probes/primers sets were used in this study (Tab. 11).

Gene (rat)	Assay ID	RefSeq accession number
rac1 subunit of NADPH oxidase	Rn01412765_m1	NM_134366
rac2 subunit of NADPH oxidase	Rn01504461_g1	NM_001008384
catalase	Rn00560930_m1	NM_012520
glutathion reductase 1	Rn00588153_m1	NM_053906
glutathion peroxidase 1/7	Rn00577994_g1	NM_030826
superoxide dismutase 1, cytoplasm	Rn00566938_m1	NM_017050
superoxide dismutase 2, mitochondrial	Rn00566942_g1	NM_017051.2
superoxide dismutase 3, extracellular	Rn00563570_m1	NM_012880.1
thioredoxin1	Rn00587437_m1	NM_053800
heme oxygenase 1	Rn00561387_m1	NM_012580.2
p22-phox subunit of NADPH oxidase	Rn00577357_m1	NM_024160
myeloperoxidase	Rn01460205_m1	XM_220830

Tab. 11: List of analyzed genes using TaqMan® Gene Expression assays.

4.17.2 Procedure

4.17.2.1 Synthesis of cDNA (reverse transcription of RNA)

The RT premix was prepared according to the Tab. 12 and 50 µl of the RT premix was pipetted to each tube. 1 µg of RNA in total volume of 50 µl was added to each reaction and incubated in a thermocycler at 25 °C for 10 min, then at 37 °C for 120 min.

Reagent	1 reaction [µl]
10x RT buffer	10
25x dNTP mixture	4
10x Random primers	10
Multiscribe RT (50 U/µl)	5
RNase free H_2O	21
total PREMIX	50
RNA 1 µg	50
total reaction volume	100

Tab. 12: Preparation of premix for cDNA synthesis from RNA.

4.17.3 Realtime-PCR amplification

Every cDNA sample was diluted with water in ratio 1:10 and calibration samples also in ratios 1:100 and 1:1000. The master mix was prepared with probe according to Tab. 13.

Reagent	1 reaction [µl]
2 X TaqMan master mix	10
probe + primers	1
Total master mix volume	11

Tab. 13 : Preparation of TaqMan probe PCR reaction.

11 µl of the master mix was added to each well of the plate. 9 µl of diluted cDNA was added to wells. The plate was sealed and put into the qPCR instrument. The program ABI SDS using absolute quantification module was used. Standard thermal program was used as follows : 50 °C - 2 min, 95 °C - 10 min and 40 cycles (95 °C - 15 s, 60 °C - 1 min). Data were analyzed using SDS software with absolute quantification module. Calibration curve was calculated from the signal of three dilutions of the calibration sample (quantity was made equal to 1 for 1:10 dilution, 0.1 for 1:100 dilution and 0.01 for 1:1000 dilution).

4.18 Immunohistochemistry

The immunohistochemistry procedures were done in part by Vlasta Tkáčová (as a part of her diploma thesis and her summer job at the Faculty of Medicine in Hradec Králové) and Burak Tahmazoglu (as a part of his summer fellowship at the Faculty of Medicine in Hradec Králové) under the tuition and supervision of the author of this thesis.

4.18.1 Chemicals and materials

- Xylene (P-Lab), ethanol p.a. (Lach-Ner), hydrogen peroxide p.a. (Riedel-de Haën), bovine fetal serum (Gibco), citric acid p.a. (Lach-Ner), sodium citrate p.a. (Lach-Ner), hydrochloric acid (Penta), sodium chloride (Lach-Ner), sodium hydrogen phosphate dihydrate p.a. (Fluka), potassium dihydrogen phosphate (Lachema), formaldehyde (Sigma)
- Polyclonal rabbit antibody IgG against IL-6 (Abcam, ab6672)
- Polyclonal rabbit antibody IgG against MPO (Abcam, ab9535)
- Goat polyclonal antibody against MMP-3 (Santa Cruz Biotechnology, Santa Cruz, CA, USA, sc-31074)

- Rabbit polyclonal antibody against MMP-13 (Santa Cruz, sc-30073)

- DakoCytomation LSAB+ System – HRP; Biotinylated link universal, Streptavidin-HRP (DakoCytomation, K0690)

- DAB Substrate – Chromogen system; DAB chromogen, DAB substrate buffer (DakoCytomation – K3466)

- DPX mountant for histology (Fluka)

- Hematoxylin solution according to Mayer (Sigma, 51275)

- PBS buffer (NaCl 9.0 g ; KH_2PO_4 0.144 g; $Na_2HPO_4.2H_2O$ 0.528 g per liter , pH 7.4)

- Citrate buffer
  - Solution A: 0.63 g of citric acid in 30 ml of distilled water
  - Solution B: 1.32 of sodium citrate in 45 ml of distilled water
  - Fresh solution of citrate buffer was prepared by adding 9 ml of solution A to 41 ml of solution B, adding 450 ml of distilled water. pH was adjusted to 6.0.

- Casein blocking solution 1% (Pierce #37528)

- Microscope Nikon Eclipse 80i with objectives (4x, 20x, 60x), camera Nikon DS-Fi1

- Nis – Elements AR 3.0 software and camera drivers: Nikon DS-U2/L2 USB, 5.03

4.18.2 Procedure

Hydration and paraffin removal was done by incubating samples in xylene for 3 x 5 min, 100% ethanol for 5 min, 96% ethanol for 5 min, 80% ethanol for 5 min, 75% ethanol for 5 min and finally in distilled water for 5 min. Antigen demasking was done by boiling in microwave oven in citrate buffer at 800 W / 2.5 min and then at 200 W / 12.5 min. The unspecific peroxidase reaction in samples was blocked by 3% H_2O_2 for 15 min. Then samples were washed three times in PBS for 5 min and in 5% serum or 0.25% casein blocking solution for 30 min. Samples were incubated with PBS solution of antibody for 1 h at 1:50 dilution for MPO, at 1:400 for IL-6, at 1:200 for MMP-3 and 1:100 for MMP-13. Slides were washed in PBS three times for 5 min. For the attachment of secondary antibody, the samples were incubated in biotinylated link universal solution for 15 min and then washed in PBS buffer 3 times for 5 min. Samples were then incubated with enzyme conjugate streptavidin HRP for 15 min and washed in PBS buffer 3 times for 5 min. Stain development was performed with DAB chromogen during 10 min incubation for MPO and 4 min for others antigens. Samples were washed twice for 2 minutes with PBS. Nucleus was stained with hematoxylin for 5 min followed by a wash with tap water for 10 min. Samples were dehydrated by an incubation in

75% ethanol for 5 min, 80% ethanol for 5 min, 96% ethanol for 5 min, 100% ethanol for 5 min and xylene 3 x 5 min. Then the slides were mounted and covered with cover slip. The samples were observed and images were captured using Microscope Nikon Eclipse 80i with camera settings as follows: contrast – high, white autobalance, autoexposition AE+1, high quality capture resolution (2560 x 1920, 5 MPix).

5   Results

5.1   Part 1: Effects of hyaluronan and iodine on wound contraction and granulation tissue formation in rat skin wounds

5.1.1   Determination of wound contraction

Wound contraction in control rats was rapid in the first week of the experiment and it was almost complete by day 15 when less than 5% of the wound area was not covered with epithelium. The contraction was significantly accelerated in the first few days by the mixture of HA1200 and KI_3 (Hyiodine) treatment. The wound area in control rats on day 5 was 60% of the original size. When the wounds were treated with Hyiodine, this percentage was reached almost 2 days earlier (Fig. 8).
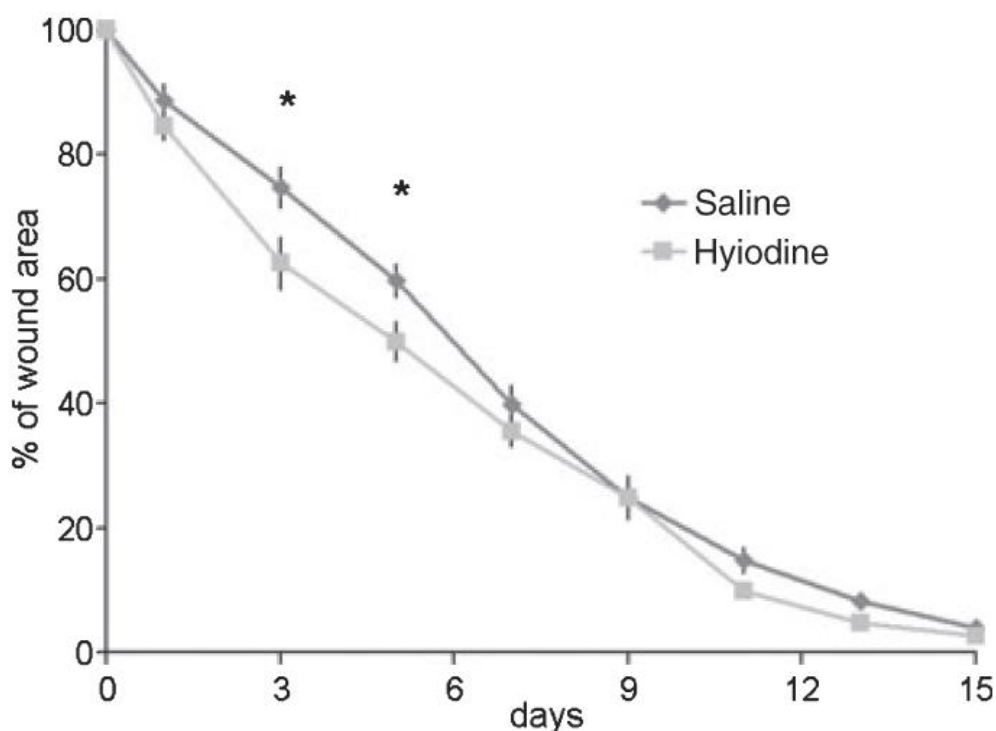
Fig. 8: Wound area as a percentage of the original area measured immediately after wounding. Data are show as means ± SEM, * significant results.

5.1.2 Appearance of the contractile wounds

The appearance of wound on day 3 and day 5 is illustrated in Fig. 9. The wounds treated with Hyiodine did not adhere to the bandage and bleeding was little compared to control group (Fig. 9).
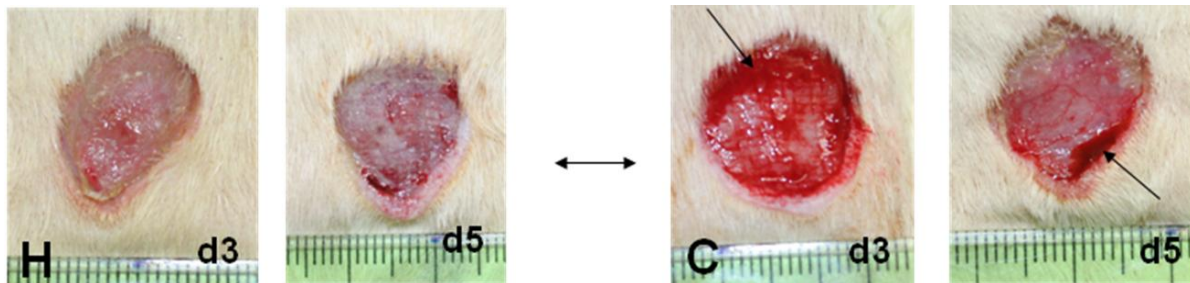
Fig. 9: Photographs of wounds treated with Hyiodine (H) vs. control (C, saline). Note the increased bleeding after the removal of bandage in control group (arrow).

5.1.3 Histological analysis of contractile wounds

Fig. 10 shows the thickening of the epithelium in the wound on day 7 of Hyiodine treatment. The thickness of the epithelial layer measured immediately after wounding was 30 μm. It increased to 102 μm in both saline and Hyiodine treated wounds on day 3. However, it was 109 μm and 146 μm, respectively, in saline and in Hyiodine treated wounds on day 7. The difference was statistically significant.
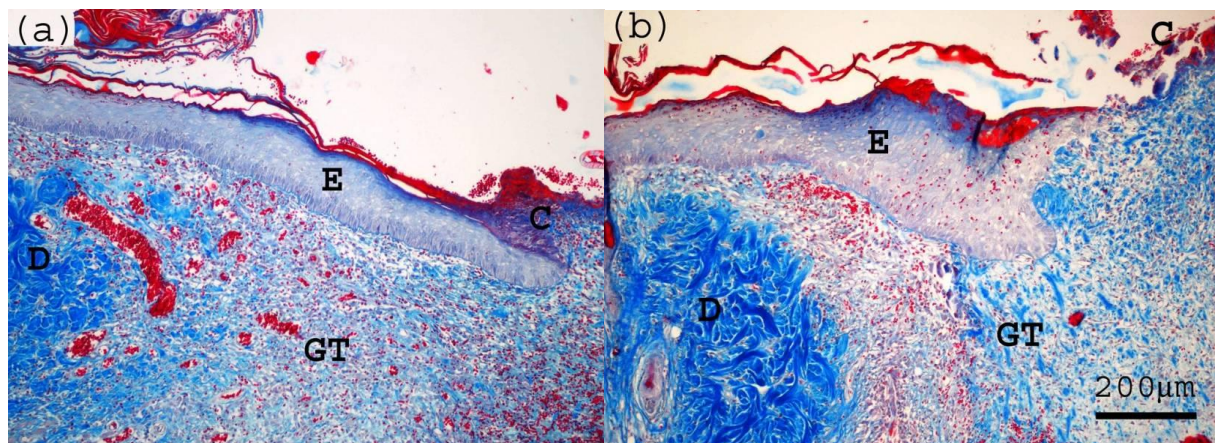
Fig. 10: Histological sections of saline (a) and Hyiodine (b) treated wounds stained with blue trichrome; E - epithelium, C - crust, GT - granulation tissue, D - dermis.

5.1.4 Analysis of the granulation tissue from permanent wound

Seven-day treatment of GT with the mixture of HA1200 and KI_3 (Hyiodine) resulted in 18% increase in the wet weight of the GT compared to saline treatment. The changes caused by HA1200 and by KI_3 alone were smaller and were not statistically significant. The concentration of hydroxyproline, the index of collagen, was decreased by Hyiodine treatment when compared to saline or other solutions but little changes were found in total hydroxyproline content (Tab. 14).

Granulation tissue	Saline	HA11	HA1200	HA1200 plus KI_3 (Hyiodine)	KI_3
Weight (mg)	363 ± 18	410 ± 16	375 ± 14	428 ± 17 [a]	409 ± 27
% dry weight	16.0 ± 0.9	16.1 ± 0.7	16.1 ± 0.6	15.9 ± 0.8	18.3 ± 1.2
Hyp concentration (mg/g)	4.03 ± 0.22	3.99 ± 0.19	4.25 ± 0.24	3.66 ± 0.14 [b]	3.88 ± 0.22
Hyp content (mg)	1.45 ± 0.09	1.63 ± 0.09	1.58 ± 0.09	1.56 ± 0.08	1.56 ± 0.11

Tab. 14: Changes in granulation tissue weight, dry weight and hydroxyproline (hyp) content after treatment of the wounds with saline, hyaluronan, iodine or Hyiodine. Means ± SEM. Statistical significance ($p < 0.05$). a) Hyiodine vs. saline, b) Hyiodine vs. HA1200.

5.1.5 Analysis of the crust and exudate of permanent wound

The crust was formed on the top of the granulation tissue. It could not be separated from the exudate gel that was abundant especially after Hyiodine treatment (Fig. 11).
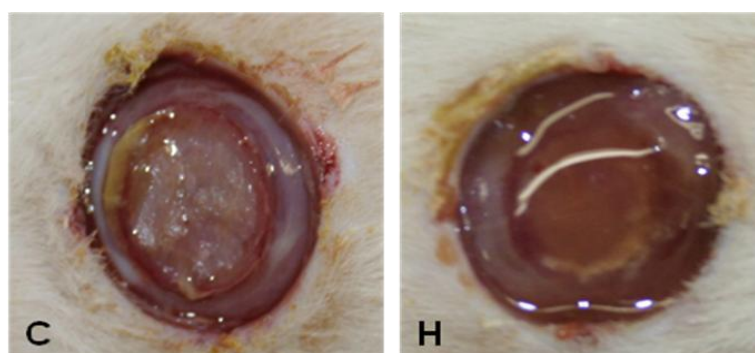
Fig. 11: Photograph of permanent wound on day 7, after the removal of plastic ring, C – control wound, H – wound treated with Hyiodine. Note the presence of moist gel on the top of Hyiodine treated wound.

HA1200 caused a 37% increase in the crust/exudate weight and KI_3 alone did not have any effect. When applied together, these substances increased the weight of the layer by 351% (Tab. 15). Proteins and uronic acids were extracted from the crust/exudate with hot alkali.

Protein concentration was similar in all groups but the total amount of protein was by far the highest in the Hyiodine group, 349% when compared with saline. The source of the protein might be blood plasma. We therefore studied the composition of the protein mixture by SDS-PAGE. Fig. 12 shows that the protein pattern of 4 different exudate samples resembled that of plasma and serum. The band at 66 kDa corresponding to albumin was prominent.
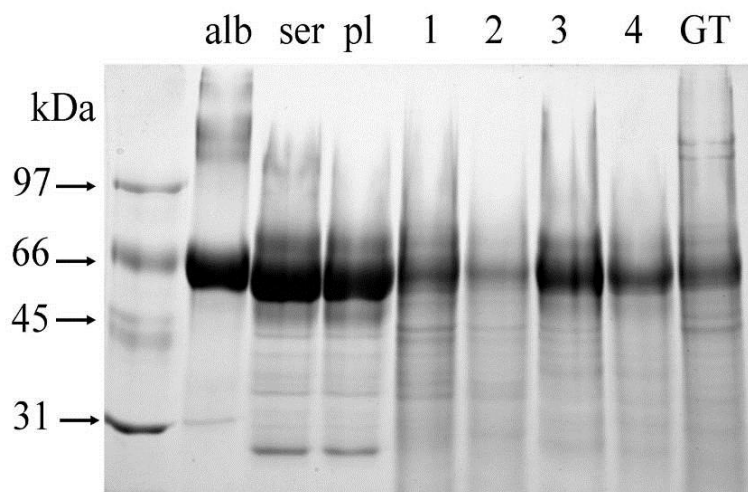
Fig. 12: SDS-PAGE of proteins contained in the crust/exudate. alb – bovine serum albumin, ser – rat blood serum, pl – rat blood plasma, 1,2,3,4 – different samples of crust/exudate after treatment with Hyiodine, GT – granulation tissue.

Total uronic acid content in dried crust/exudate was increased about 3fold by HA1200 and 14fold by Hyiodine when compared to saline (Tab. 15).

Crust/exudate	Saline	HA11	HA1200	HA1200 + KI$_3$ (Hyiodine)	KI$_3$
Weight (mg)	95.0± 19.9	153.3 ± 22.3	130.0 ± 31.0	428.0 ± 81.2 [a,c,d]	96.1 ± 25.1
Protein concentration (% dry weight)	90.6 ± 9.2	91.4 ± 5.9	93.8 ± 6.8	92.5 ± 9.5	85.3 ± 8.9
Protein content (mg)	36.8 ± 7.1	38.7 ± 5.6	36.6 ± 9.0	128.3 ± 27.0 [a,b,c]	48.2 ± 11.3
Uronic acid concentr. (% dry weight)	1.38 ± 0.22	1.25 ± 0.14	2.83 ± 0.52	4.07 ± 0.64 [a,b,d]	1.42 ± 0.20
Uronic acid content (mg)	0.37 ± 0.06	0.49 ± 0.05	1.08 ± 0.34	5.10 ± 0.94 [a,b,c,d]	0.53 ± 0.10

Tab. 15: Changes in the weight, protein and uronic acids content in the crust and exudate after treatment with saline, hyaluronan, iodine or Hyiodine. Means ± SEM. Statistical significance ($p < 0.05$). a) Hyiodine vs. saline, b) Hyiodine vs. HA11, c) Hyiodine vs. HA1200, d) Hyiodine vs. KI$_3$.

5.1.6 Gene expression analysis in granulation tissue by DNA arrays

The mean expression of 92 genes studied was made equal to 1. Studied genes were cell cycle regulators, cytokines and growth factors, part of ECM, proteinases and their inhibitors and receptors. The results of their expression are shown in Tab. 16. No statistically significant differences were found by DNA arrays when Hyiodine- and saline-treated tissues were compared. Nonetheless, it was observed that many ECM proteins and proteoglycans mRNAs were highly expressed in the granulation tissue (collagens 1, 3 and 5, fibrilin-1, fibronectin, osteonectin, osteopontin, thrombospondin-1, vitronectin, biglycan, decorin, lumican, perlecan).

Substance	Group	saline	HA11	HA1200	KI$_3$	HYIO
API2	Apoptosis / Cell cycle	0.09	0.12	0.17	0.07	0.11
bax	Apoptosis / Cell cycle	0.83	0.92	0.97	0.72	0.74
bcl-2	Apoptosis / Cell cycle	**2.58**	**2.36**	**2.24**	**2.57**	**2.52**
bcl-x alpha	Apoptosis / Cell cycle	**1.93**	**1.81**	**1.72**	**1.90**	**1.99**
BIRC3	Apoptosis / Cell cycle	0.07	0.08	0.12	0.04	0.08
caspase-3	Apoptosis / Cell cycle	0.51	0.57	0.60	0.39	0.47
caspase-8	Apoptosis / Cell cycle	0.10	0.10	0.14	0.07	0.15
c-myc	Apoptosis / Cell cycle	**1.05**	**1.14**	**1.08**	**0.98**	**1.08**
IAP4	Apoptosis / Cell cycle	**1.06**	**0.98**	**0.91**	**0.87**	**0.94**
p21	Apoptosis / Cell cycle	0.57	0.55	0.55	0.48	0.53
p53	Apoptosis / Cell cycle	0.20	0.22	0.27	0.20	0.22
PCNA	Apoptosis / Cell cycle	0.38	0.39	0.40	0.34	0.36
CTGF	Cytokines a growth factors	0.15	0.13	0.16	0.11	0.14
Edn1	Cytokines a growth factors	0.17	0.15	0.20	0.15	0.18
FGF2	Cytokines a growth factors	0.67	0.47	0.56	0.54	0.62
Igf1	Cytokines a growth factors	0.69	0.65	0.62	0.64	0.56
IL-10	Cytokines a growth factors	0.26	0.21	0.27	0.20	0.22
IL-12b	Cytokines a growth factors	0.08	0.06	0.10	0.07	0.08
IL1b	Cytokines a growth factors	0.10	0.13	0.16	0.09	0.13
IL-4	Cytokines a growth factors	0.08	0.09	0.09	0.10	0.10
IL-6	Cytokines a growth factors	0.19	0.20	0.21	0.14	0.20
NT-3	Cytokines a growth factors	0.10	0.07	0.06	0.04	0.12
PDGFa	Cytokines a growth factors	0.24	0.25	0.25	0.18	0.23
PDGFb	Cytokines a growth factors	**2.34**	**2.17**	**2.20**	**2.46**	**2.36**
Rln1	Cytokines a growth factors	0.23	0.16	0.19	0.14	0.19
TGFb1	Cytokines a growth factors	0.66	0.73	0.75	0.58	0.62
TGFb3	Cytokines a growth factors	0.26	0.20	0.26	0.19	0.22
TNFa	Cytokines a growth factors	0.24	0.22	0.32	0.22	0.27
VEGF	Cytokines a growth factors	**1.56**	**1.89**	**1.79**	**2.06**	**2.13**
desmin	Cytoskelet	**3.20**	**3.23**	**3.16**	**3.55**	**3.35**
GFAP	Cytoskelet	0.13	0.08	0.14	0.13	0.10

a2m	ECM proteins	0.67	0.61	0.70	0.47	0.55
col18a1	ECM proteins	0.61	0.60	0.58	0.61	0.59
Col1a2	ECM proteins	**3.15**	**3.35**	**3.23**	**3.52**	**3.09**
Col3a1	ECM proteins	**2.97**	**3.19**	**3.13**	**3.47**	**2.99**
col4	ECM proteins	0.31	0.31	0.30	0.25	0.31
Col5	ECM proteins	**1.87**	**1.97**	**1.86**	**1.88**	**1.85**
Eln	ECM proteins	**1.34**	**1.33**	**1.32**	**1.27**	**1.40**
Fbln-2	ECM proteins	0.67	0.56	0.62	0.57	0.59
Fbln-5	ECM proteins	0.23	0.21	0.27	0.17	0.20
Fbn1	ECM proteins	**2.46**	**2.60**	**2.43**	**2.80**	**2.70**
Fbn2	ECM proteins	0.26	0.25	0.24	0.18	0.24
Fn1	ECM proteins	**1.06**	**1.04**	**1.12**	**1.10**	**1.19**
lamb2	ECM proteins	0.15	0.09	0.13	0.11	0.13
Reln	ECM proteins	**1.07**	**0.87**	**0.92**	**0.98**	**0.90**
SPARC – ON	ECM proteins	**3.12**	**3.38**	**3.21**	**3.63**	**3.28**
spp1 - OPN	ECM proteins	**2.69**	**3.00**	**2.90**	**2.66**	**2.82**
Tsp-1	ECM proteins	**1.20**	**1.03**	**1.05**	**1.14**	**1.14**
Tsp-2	ECM proteins	0.80	0.76	0.71	0.70	0.73
Vtn	ECM proteins	**1.15**	**1.08**	**1.03**	**1.02**	**0.98**
18S RNA	House keeping	**2.74**	**2.78**	**2.84**	**2.92**	**2.58**
Actb	House keeping	**2.97**	**3.13**	**3.15**	**3.29**	**2.79**
GAPD	House keeping	0.43	0.35	0.46	0.40	0.34
cd44	Hyaluronan metabolism	0.43	0.48	0.46	0.34	0.47
HAS1	Hyaluronan metabolism	0.49	0.43	0.48	0.40	0.48
HAS2	Hyaluronan metabolism	0.32	0.36	0.38	0.27	0.32
HAS3	Hyaluronan metabolism	0.00	0.02	0.02	0.01	0.02
hyal1	Hyaluronan metabolism	0.54	0.50	0.57	0.45	0.53
hyal2	Hyaluronan metabolism	**1.68**	**1.75**	**1.65**	**1.98**	**2.09**
hyal3	Hyaluronan metabolism	**1.28**	**1.02**	**1.13**	**1.00**	**1.01**
RHAMM	Hyaluronan metabolism	**1.20**	**1.10**	**1.00**	**0.93**	**1.09**
TLR4	Hyaluronan metabolism	0.12	0.12	0.17	0.09	0.13
iNOS	NOS	0.35	0.33	0.37	0.21	0.33
NOS3	NOS	0.07	0.07	0.12	0.08	0.10
mmp-12	Proteinases and inhibitors	0.32	0.33	0.48	0.26	0.34
mmp-13	Proteinases and inhibitors	0.65	0.52	0.59	0.50	0.63
mmp-14	Proteinases and inhibitors	**1.74**	**1.81**	**1.77**	**1.63**	**1.70**
mmp-2	Proteinases and inhibitors	**1.38**	**1.48**	**1.42**	**1.58**	**1.64**
mmp-3	Proteinases and inhibitors	0.19	0.16	0.18	0.14	0.22
mmp-7	Proteinases and inhibitors	0.75	0.65	0.69	0.65	0.66
mmp-9	Proteinases and inhibitors	0.07	0.07	0.10	0.08	0.12
P100	Proteinases and inhibitors	0.54	0.51	0.48	0.45	0.48
TIMP1	Proteinases and inhibitors	**2.04**	**1.94**	**1.90**	**2.06**	**1.98**
TIMP2	Proteinases and inhibitors	**2.89**	**2.86**	**2.83**	**3.19**	**3.02**
TIMP3	Proteinases and inhibitors	0.49	0.45	0.49	0.41	0.43
Agc1	Proteoglycans – ECM	0.00	0.02	0.01	0.00	0.02
bgn	Proteoglycans – ECM	**1.20**	**1.08**	**1.18**	**1.05**	**1.12**
Dcn	Proteoglycans – ECM	**1.64**	**1.66**	**1.58**	**1.47**	**1.66**

lum	Proteoglycans – ECM	**2.75**	**2.93**	**2.84**	**2.94**	**2.86**
plc	Proteoglycans – ECM	**3.34**	**3.42**	**3.39**	**3.77**	**3.35**
sdc1	Proteoglycans – transmemb.	0.45	0.37	0.44	0.42	0.42
sdc3	Proteoglycans – transmemb.	0.08	0.06	0.10	0.07	0.09
sdc4	Proteoglycans – transmemb.	0.38	0.42	0.45	0.30	0.42
Beg	Receptors	**1.27**	**1.14**	**1.17**	**1.16**	**1.16**
ICAM-1	Receptors	0.59	0.61	0.59	0.47	0.58
Itga5	Receptors	**2.36**	**2.51**	**2.41**	**2.55**	**2.52**
Itga6	Receptors	0.61	0.62	0.60	0.52	0.56
Itgb1	Receptors	**1.19**	**1.13**	**1.11**	**1.09**	**1.09**
Itgb3	Receptors	0.32	0.34	0.37	0.27	0.35
Lamr1	Receptors	**1.81**	**1.86**	**1.73**	**1.88**	**1.87**
N-CAM	Receptors	**1.60**	**1.61**	**1.46**	**1.40**	**1.50**
MAPK1	Signal transduction	0.23	0.21	0.26	0.17	0.21
average		**1.00**	**1.00**	**1.00**	**1.00**	**1.00**

Tab. 16: Gene expression of selected genes in granulation tissue on day 7. For full gene names please refer to the methods. Values of highly expressed genes are bold (expression value > 1 in saline group). n = 14 - 15.

5.1.7 Gene expression analysis in granulation tissue by quantitative RT-PCR

Selected genes expression was also analyzed by qPCR. The results are shown in Tab. 17. None of the studied genes were significantly differentially expressed in none of the studied groups. MMP-7 and osteopontin were non-significantly elevated in HA1200 group and MMP-13 was slightly elevated in Hyiodine group.

GENE	Saline	HA11	HA1200	HYIO	KI3
MMP-2	0.89±0.06	0.99±0.09	0.837±0.07	0.83±0.07	0.969±0.09
MMP-7	4.32±1.22	4.9±1.53	7.27±1.83	2.65±0.54	2.14±0.53
MMP-13	0.37±0.08	0.24±0.06	0.37±0.10	0.58±0.20	0.41±0.14
Osteopontin	0.58±0.08	0.56±0.15	0.84±0.18	0.50±0.09	0.42±0.07
COL1A2	0.39±0.06	0.42±0.08	0.34±0.13	0.33±0.10	0.34±0.11
VEGF	1.27±0.18	1.39±0.17	1.32±0.24	1.33±0.25	1.27±0.17
HYAL-2	1.13±0.08	1.24±0.10	1.11±0.06	1.04±0.06	1.11±0.06

Tab. 17: Relative gene expression of selected genes in granulation tissue on day 7 as assayed by qPCR. Means ± SEM are shown. n = 14 - 15.

5.2 Part 2: Zucker Diabetic Fatty rat – a new model of impaired cutaneous wound repair with type II diabetes mellitus and obesity

5.2.1 Animal breeding

During the study it was necessary to optimize the conditions of ZDF animal breeding. We had very good results in breeding non-diabetic carrier (fa/+) males with non-diabetic carrier females (fa/+). In this case, the progeny was expected as follows: 25% of the offspring diabetic, 50% non-diabetic carriers, 25% non-diabetic non-carriers. It was also possible to interbreed diabetic male with non-diabetic carrier females. In this case the offspring were expected to be 50% of diabetic animals and 50% of non-diabetic carriers. The breeding was possible if the diabetes-predisposed males were young enough (usually < 15 week). Alternatively, it was possible to apply the food restriction (*ad libitum* regime was replaced with the recommended standard dose regime). In this case, rats did not become significantly obese and phenotypically diabetic and hence their fertility was better. In this section the term diabetic signifies the genotype (diabetes in not necessarily manifested in young animals).

5.2.2 Genotypization of ZDF animals

Typical results of genotypization are shown in Fig. 13 and Fig. 14. DNA for leptin receptor gene was first amplified by PCR and then the amplified fragment was cleaved by a restriction enzyme at the site of the potential mutation. In case of *lepr* mutation, the amplified part of the gene was cleaved and new bands appeared on the electrophoretogram (Fig. 14).
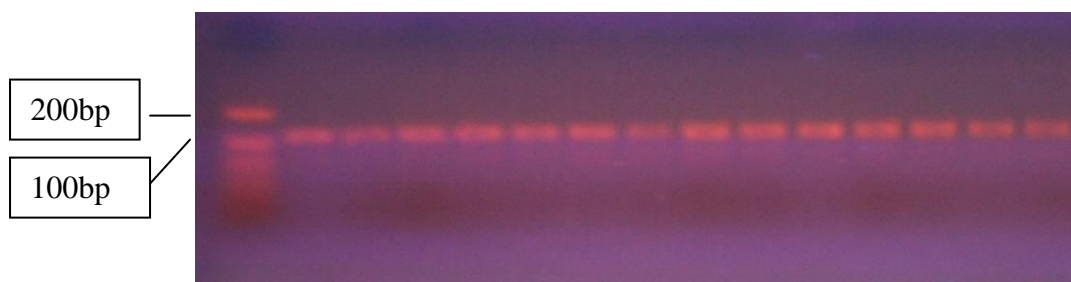

Fig. 13: The results of PCR reaction. The product has 118bp. The ladder is located on the left with 200bp/100bp/50bp/20bp/10bp fragments.
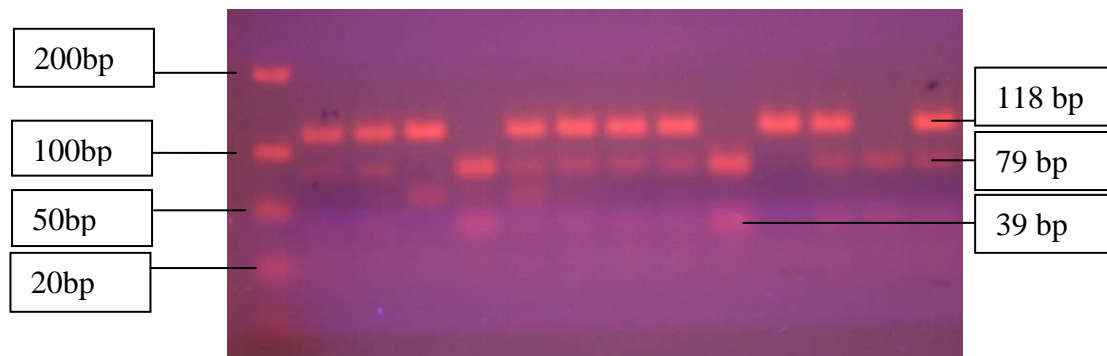
Fig. 14: Electrophoresis image after enzymatic cleavage of PCR fragment with MspII. Bands for +/+ genotype are in region of 118 bp, for +/fa genotype in region 118, 79 and 39bp and for fa/fa genotype in region 79 and 39bp. The ladder is located on the left with 200bp/100bp/50bp/20bp/10bp fragments.

The expected rate of genotype of progeny from carriers breeding was confirmed by PCR-RFLP genotypization (Tab. 18).

genotype	amount	rate %
+/+	18	26.5%
fa/+	32	47.1%
fa/fa	18	26.5%
total	68	100%

Tab. 18: Summary of numbers of offspring obtained from breeding of fa/+ and fa/+ animals.

5.2.3 Development of diabetes in ZDF rats

Non-fasting glycemia was increased in diabetic males and usually began to increase significantly at the age of 12-14 weeks. It was 3fold higher at the age of about 20 weeks (Fig. 15). However, the increase in glycemia was individual; there were animals in whom we observed high glycemia as early as the age of 12 weeks. In some animals glycemia began to increase at later age.
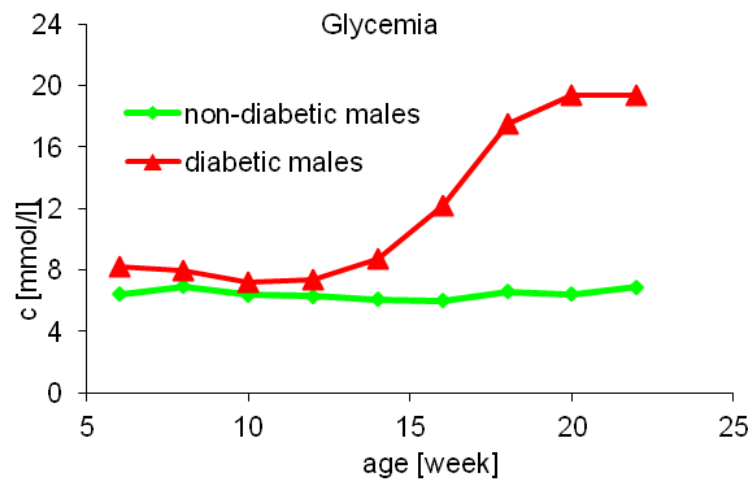

Fig. 15: Changes in blood glycemia in ZDF males fed by Purina 5008. Means of five animals are shown.

Non-fasting glycemia was increased in diabetic females during the development of diabetes, however, it did not increase to such an extent as in males. It reached the level of approximately 50% higher compared to controls at the age of 20 weeks (Fig. 16).
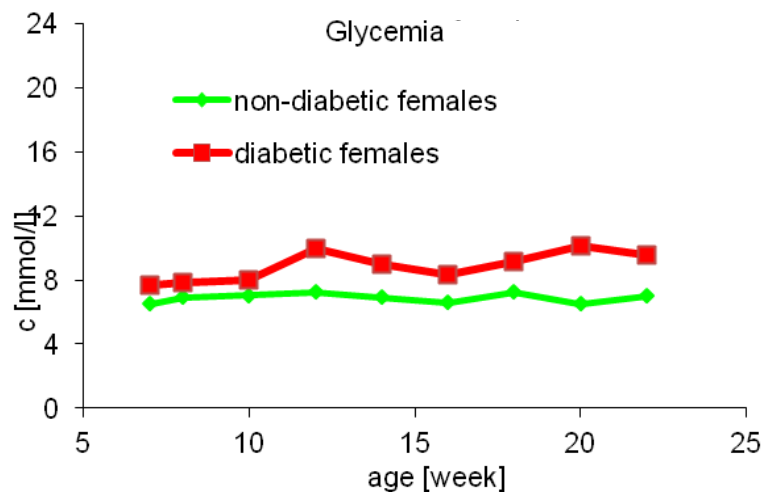

Fig. 16: Development of blood glycemia in ZDF females fed with C13004. The means of five animals are shown.

5.2.3.1 Modification of diet and the effect on glycemia

The diet had a profound effect on the development of glycemia. The diets H1 and HZ2 with high content of saturated fat were able to induce high glycemia in female ZDF animals (Fig. 17). Please refer to the Materials and methods for the composition of H1 and HZ2.

As early as after 6 weeks of feeding the special diet the glycemia was more than double that of the controls in H1 and HZ2 groups. At the end of the treatment the glycemia reached the values > 20 mmol/l, which is comparable with the levels observed in obese diabetic males fed PURINA 5008 at the age of 20 weeks.
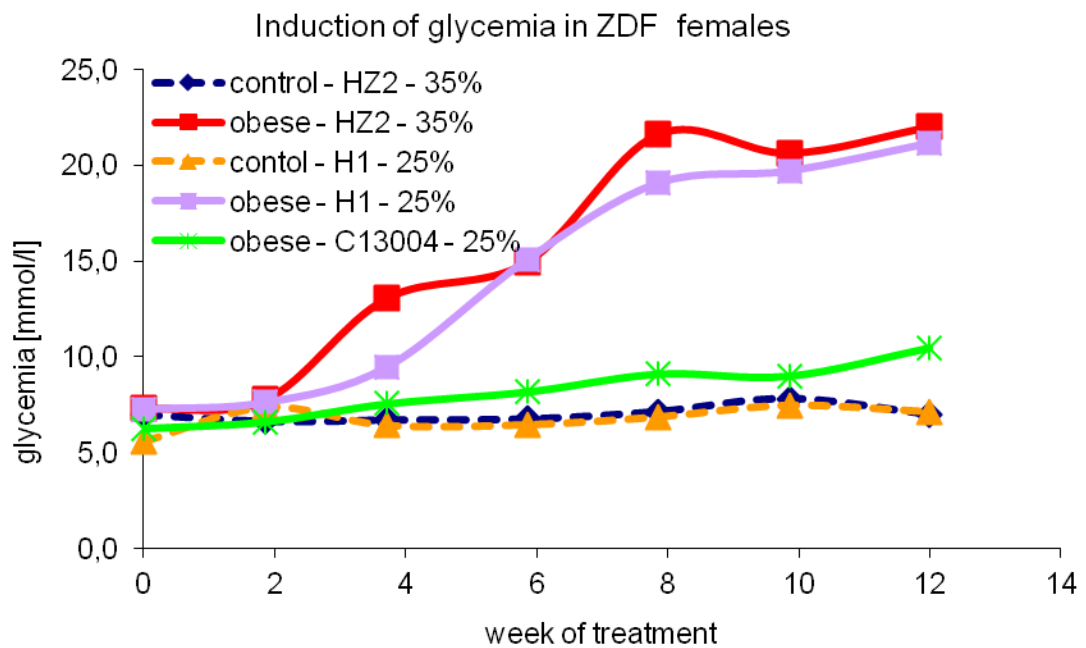

Fig. 17: The development of glycemia in ZDF females and the effect of "home-made" high-fat diet. The graph shows changes in glycemia with time as influenced by different diets H1, H2 a C13004. Dashed lines indicate non-diabetic control animals. Animals were 6 - 8 weeks old at the start of the treatment, n = 6, means are shown.

5.2.4   Physiology of ZDF rats

5.2.4.1   Growth curve of animals

As shown in Fig. 18 there was an expected difference in the growth curves of diabetic and non-diabetic animals. The animals had similar weights at the age of 5 weeks. The difference was significant ($p < 0.05$) at the age of 11 weeks and further on. The difference increased until the age of about 13 weeks. Then, the difference increased at a slower pace. At the age of about 20 weeks the difference tended to be constant. After the age of 22 weeks it was observed that diabetic animal weight stagnated or even decreased (not shown) and non-diabetic animals tended to grow slowly. This was probably the results of severe metabolic problems. Animals had already very high glycemia and could not utilize glucose and insulin properly.
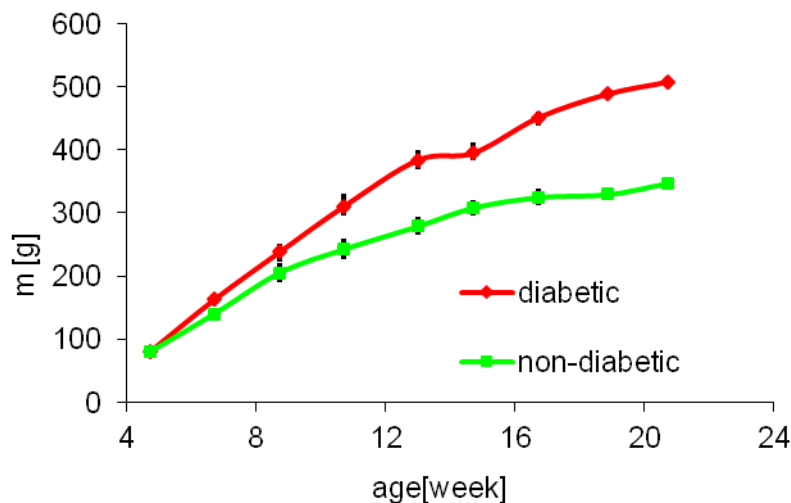
Fig. 18: Typical weight curve of ZDF males. n = 4, means ± SEM.

The weight of 5 weeks old females was similar in both groups. The difference was significant ($p < 0.05$) at the age of 7 weeks and further on. The difference in weight increased at a steady pace during whole period of observation. After 22 weeks of age the difference between control and obese animals continued to increase (not shown). Females did not show signs of metabolic deterioration at such an extent that was observed in males.
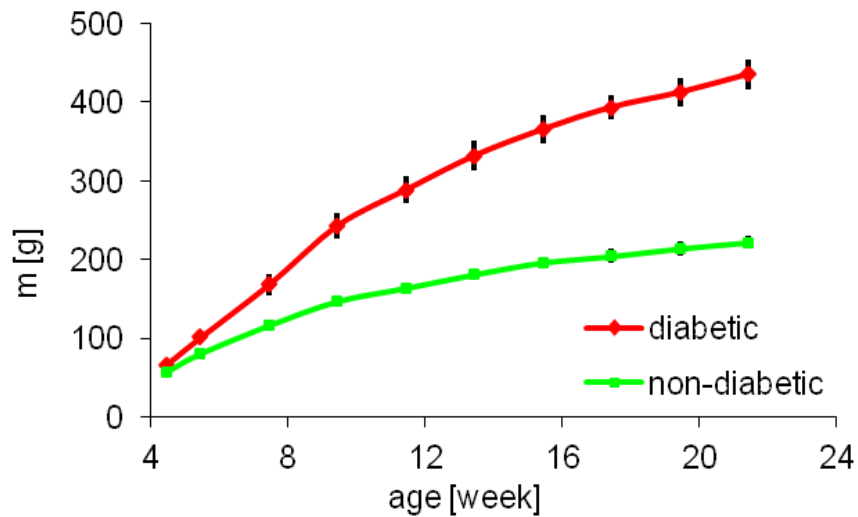

Fig. 19: Typical weight curve of ZDF females. n = 4, means ± SEM.

5.2.4.2 Physiological and blood parameters of ZDF animals

The body weight of diabetic animals was increased in both sexes and it was more pronounced in females, doubling that of control (Tab. 19). Elevated glucose levels, on the other hand, were more pronounced in diabetic males. Diabetes in the ZDF rats was associated with higher levels of plasma insulin, PAI-1, leptin and CRP (Tab. 19) compared to controls. Levels of MDA were elevated in males (Tab. 19) and correlated with glycemia (R = 0.82, not shown). Levels of interleukin-6 were not elevated in diabetic groups (Tab. 19).

	Non-diabetic males	Diabetic males	Ratio	Non-diabetic females	Diabetic females	Ratio
Weight (g) n = 13-18	363 ± 7	466 ± 13 **	1.3	218 ± 4	436 ± 7 **	2.0
Glucose (mmol/l) n = 13-18	6.7 ± 0.2	17.8 ± 0.7 **	2.7	7.3 ± 0.3	11.4 ± 0.3 **	1.6
Insulin (ng/ml) n = 11-14	1.28 ± 0.08	10.8 ± 1.48 **	8.4	1.63 ± 0.15	17.6 ± 1.64 **	10.8
PAI-1 (ng/ml) n = 9-11	2.45 ± 0.17	4.89 ± 0.75 **	2	2.62 ± 0.21	5.06 ± 0.71 **	1.93
Interleukin-6 (pg/ml) n = 10-12	62.7 ± 3.0	64.0 ± 5.1	1.02	64.4 ± 6.3	62.5 ± 4.6	0.97
C-reactive protein (μg/ml) n = 7-10	45.5 ± 5	62.5 ± 10.2	1.37	30.4 ± 3.3	47.4 ± 5.3 *	1.57
Leptin (ng/ml) n = 12-16	5.05 ± 0.44	39.1 ± 3.29 **	7.7	2.85 ± 0.39	51.4 ± 5.13 **	18.0
Malondialdehyd (μmol/l) n = 6	3.95 ± 0.29	7.44 ± 0.94 **	1.88	4.26 ± 0.3	4.52 ± 0.34	1.06

Tab. 19: Parameters of ZDF animals at the age of 18 - 20 weeks. Data are expressed as mean ± SEM, *: $p < 0.05$, **: $p < 0.01$ (diabetic animals compared to non-diabetic controls).

5.2.5 Wound closure of bandaged wounds in ZDF rats.

The appearance of bandaged wounds is shown in Fig. 20. On day 0 there was visible underlying fat tissue in diabetic wounds. On day 5 and day 10 wounds were larger in diabetic animals than in the control ones. When the wounds were covered with gauze dressing, the crust formation was suppressed (Fig. 20) as the exudate was absorbed by the gauze. During the changes of gauze dressing the crust was usually removed with gauze and new crust formed afterwards.
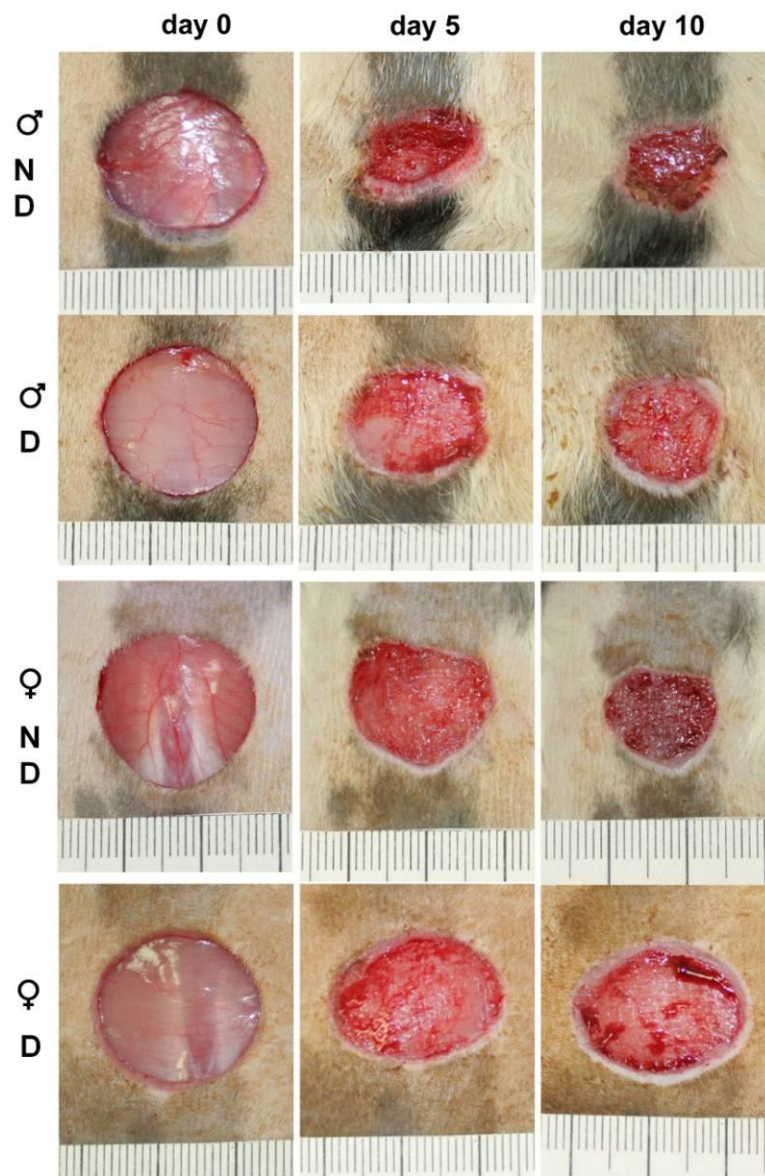
Fig. 20: Healing of excisional wounds in ZDF males and females. A: Photographs of bandaged wounds on day 0, day 5, and day 10. ND : non-diabetic animals, D : diabetic animals.

Fig. 21 and Fig. 22 show that the healing progress of diabetic wounds was retarded in both sexes, resulting in healing times about 80% longer in males and 60% in females.

Fig. 21: Wound healing of bandaged wounds - ZDF females. n = 5, mean ± SEM.
**: p < 0.01, *: p < 0.05 (diabetic vs. non-diabetic)
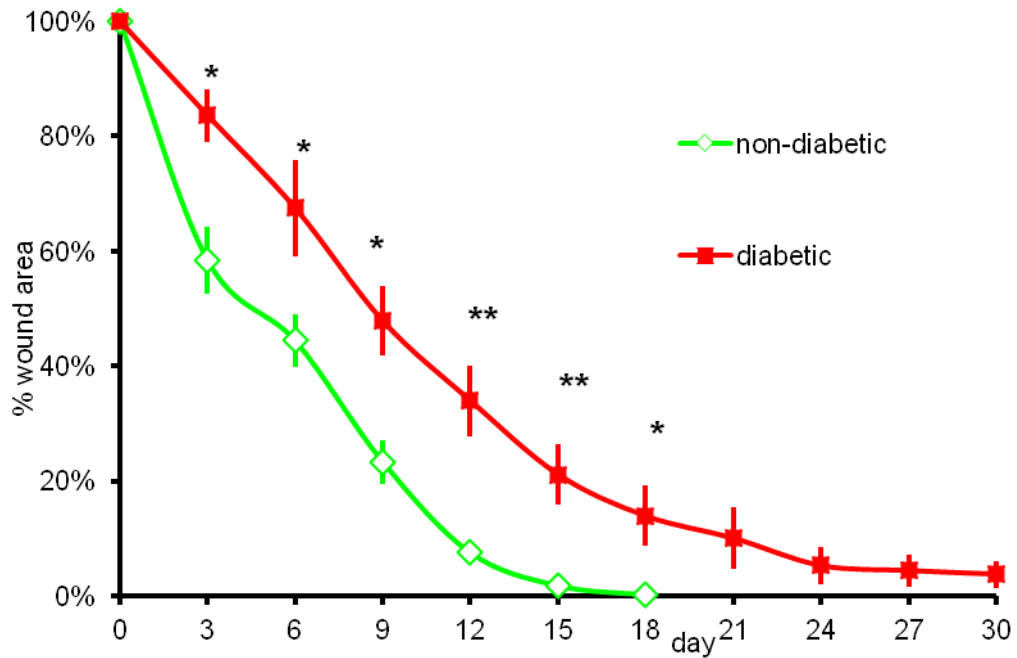
Fig. 22: Healing of bandaged wounds - ZDF males. n = 6 - 7, mean ± SEM. **: p < 0.01,
*: p < 0.05 (diabetic vs. non-diabetic).

5.2.6 Wound closure of non-bandaged wounds in ZDF rats.

Fig. 23 illustrates the macroscopic appearance of non-bandaged wounds. Wound size diminution in diabetic males was significantly retarded during 10 days after wounding. The wounds were covered with a crust that was more pronounced in diabetic rats (Fig. 23).

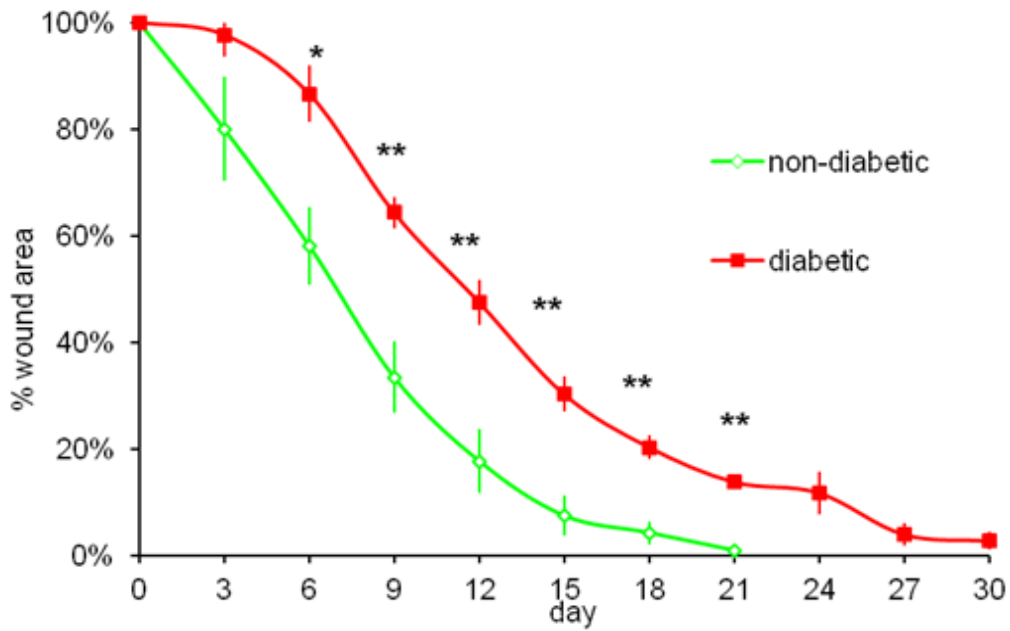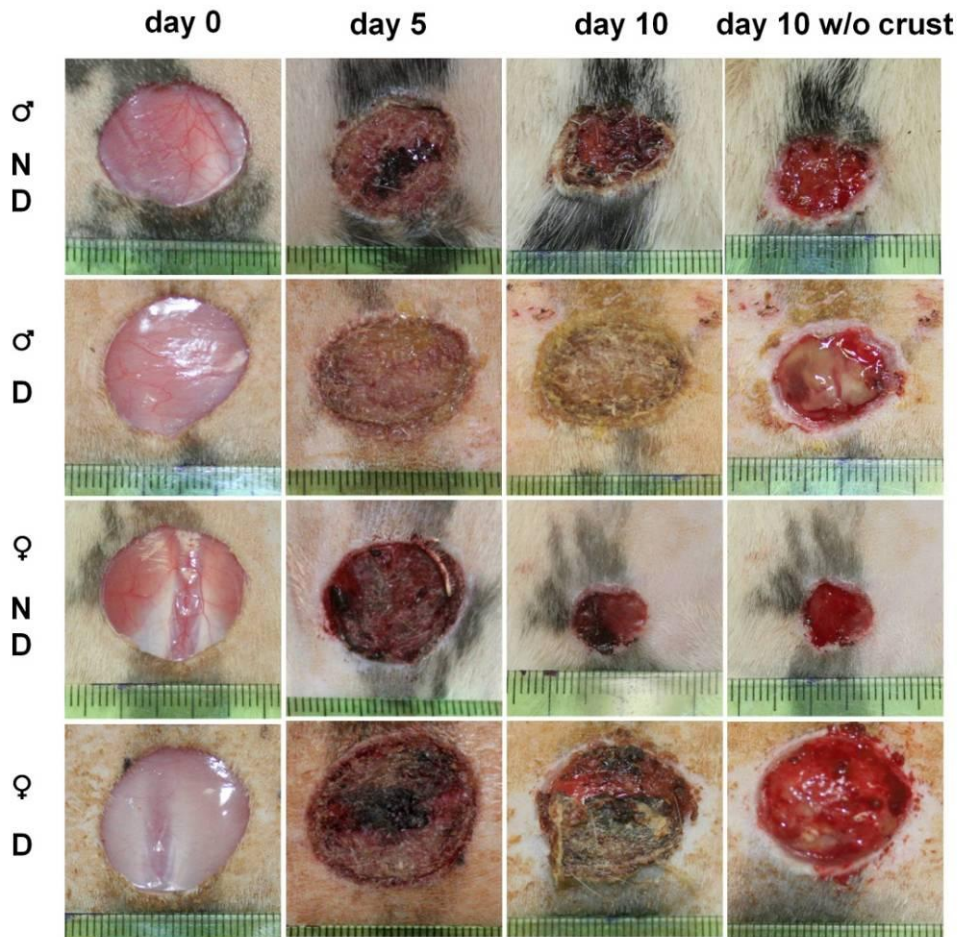

Fig. 23: Healing of excisional wounds. Photographs of wounds on day 0, day 5, day 10 and day 10 without crust that was removed. Note large crusts over diabetic wounds on day 10. ND : non-diabetic, D : diabetic.

In males, the wounds had a tendency to increase in size (peak on day 3, 106% of original size) and diminished to below their original size by day 6, whereas non-diabetic wounds were already 80% of their original size (Fig. 24).

Fig. 24: Wound size changes of excisional wounds – males. Data are shown as means ± SEM. n = 9 - 12. **: $p < 0.01$ (diabetic animals compared to non-diabetic controls).

In diabetic females, the wound size diminution was even more profoundly retarded. The wounds tended to increase in size (peak on day 5, 128% of original size) diminishing below to their original size by day 8, whereas non-diabetic wounds were already half of their original size at that time (Fig. 25).

At the end of the experiment, on day 10, the male diabetic wounds were about 50% larger and female diabetic wounds were about 150% larger than control non-diabetic wounds.

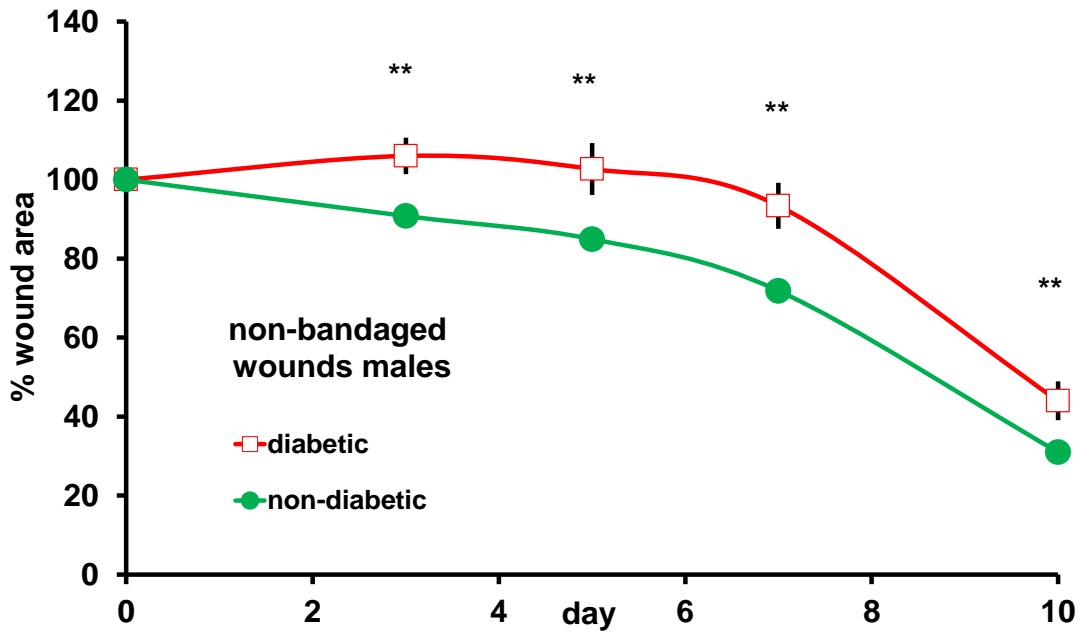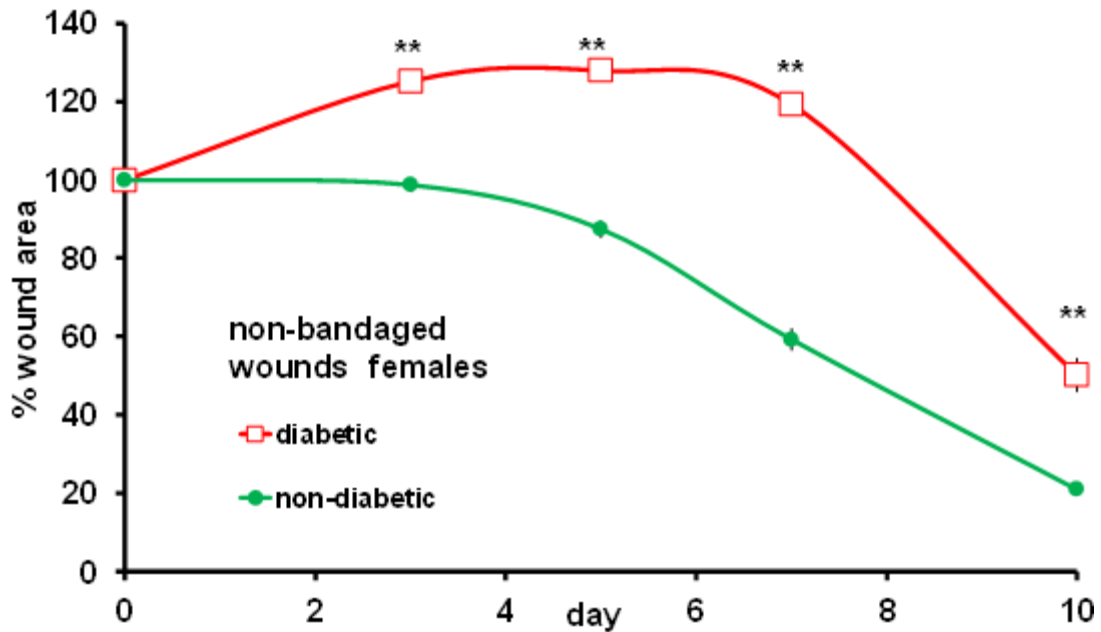Fig. 25: Wound size changes of excisional wounds – females. Data are shown as means ± SEM. n = 8 - 10, **: p < 0.01 (diabetic animals compared to non-diabetic controls).

In each group, the non-bandaged wound started to heal more slowly in comparison to the bandaged wound – the bandage helped initial contraction (please compare Fig. 25 Fig. 25 vs. Fig. 21, and Fig. 24 vs. Fig. 22).

5.2.7 Histological analysis of adipose, epithelial, granulation and dermal tissue.

The unwounded dermis on the back of animals was slightly thinner in diabetic animals, notably in males by 30% (Tab. 20). Diabetic skin contained a thick layer of underlying adipose tissue, most notably in females (Tab. 20, Fig. 26A). As a result the wounds in the diabetic females were deeper. The wound tissue retrieved on day 5 contained a significant amount of adipose tissue in both non-diabetic $((37 \pm 5)\%)$ and diabetic animals $((70 \pm 3)\%)$ with significantly $(p < 0.01)$ greater amount in diabetic animals (Fig. 26B). Fibrous granulation tissue was thicker in non-diabetic animals and it covered the entire surface of the wound, whereas in diabetic animals the granulation tissue had been infiltrated by adipose tissue and covered the wound only partially, mainly at the periphery (Fig. 26B). On day 5, the thickening of new epithelium near the wound edge was clearly observed, however with little migration over the wound. The wound tissue retrieved on day 10 (Fig. 26C) generally contained more granulation and fibrous tissue, and less adipose tissue compared to day 5. The granulation tissue in diabetic animals was poorly developed and irregular (tissue was not organized in a single continuous fibrous layer parallel to wound

surface), and was infiltrated by adipose tissue (Fig. 26C). Diabetic wounds were characterized by an increased amount of crust (red in Fig. 26, Tab. 20). Large amount of poly-morphonuclear infiltration was found under and inside the crust of diabetic animals. The proportion of adipose tissue in wound tissue was 4 to 5 times higher in diabetic than in non-diabetic animals (Tab. 20). The crust was 2 and 3 times thicker in diabetic animals in males and females, respectively (Tab. 20). Interestingly, the total length of the epithelial tongue over the wound was significantly increased in diabetic animals by 50% (Tab. 20).

	non-diabetic males	diabetic males	non-diabetic females	diabetic females
Dermis thickness in unwounded skin [μm]	1668 ± 52	1159 ± 44**	758 ± 23	683 ± 27
Adipose tissue thickness in unwounded skin [μm]	58 ± 19	509 ± 104**	45 ± 6	1204 ± 213**
Adipose tissue in wound tissue [%]	7.4 ± 2.6	32.1 ± 10*	7.2 ± 2.4	34.2 ± 4.2**
Crust thickness [μm]	421 ± 47	806 ± 59**	280 ± 29	915 ± 176**
Epithelial tongues [mm]	2.1 ± 0.2	3.2 ± 0.2*	2.3 ± 0.1	3.4 ± 0.2**

Tab. 20: Histological assessment of uninjured skin and wound tissue on day 10 in ZDF rats. Data are shown as means ± SEM. *: $p<0.05$, **: $p < 0.01$ (diabetic animals compared to non-diabetic controls, $n = 5$). Length of epithelial tongues is a sum of epithelial tongues lengths from both sides of a histological sample.
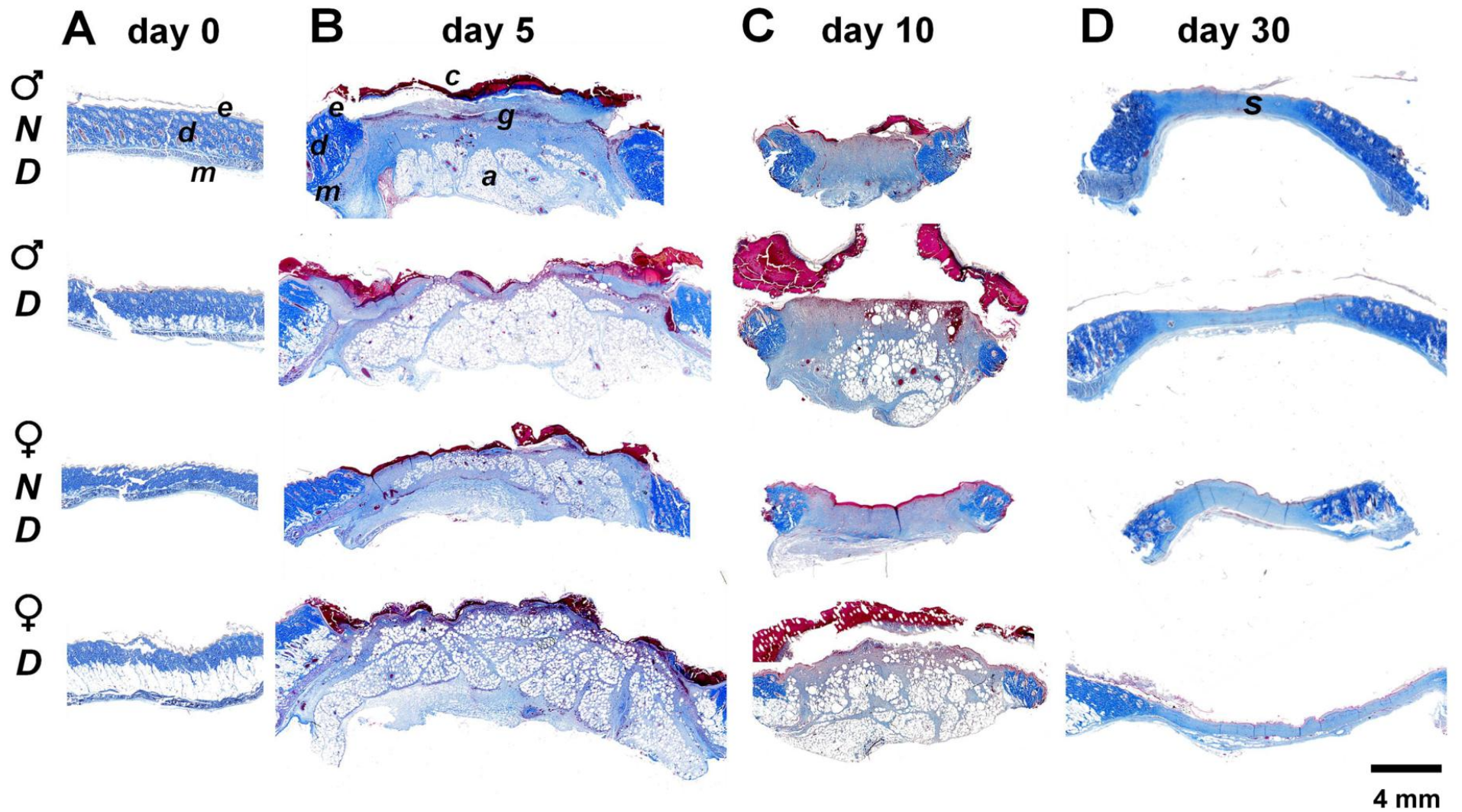
Fig. 26: Histological and immunohistochemical image of skin and wound tissue, blue trichrome-staining (1x magnification), A: skin on day 0, B: wound tissue on day 5, C: wound tissue on day 10, D: healed wound - scar on day 30. *D* - diabetic, *ND* - non-diabetic, *e* - epithelium, *d* - dermis, *m* - muscle layer, *c* -crust, *g* - granulation tissue, *a* - adipose tissue, *s* - scar.

5.2.8 Analysis of scar tissue

The wounds were closing by secondary intention, with significant contraction and resulted in the formation of scar tissue (Fig. 27) composed of newly formed collagenous tissue covered with new epithelium.

Fig. 27: Photographs of healed wounds – scars on day 30. Note that diabetic scars are larger than scars of non-diabetic animals. ND stands for non-diabetic, D stands for diabetic.

The healed diabetic scars were thinner (Fig. 26D). Scars formed only 26% and 15% of original wound surface in non-diabetic males and females respectively (Tab. 21). Scar size in diabetic animals was significantly increased: by 40% in males and by 140% in females (Tab. 21, Fig. 27). Contribution of epithelization on overall healing is equal to scar size (Fig. 28). Thus it was concluded that epithelization made significantly increased contribution to wound repair in diabetic animals (Tab. 21), most notably in diabetic females.
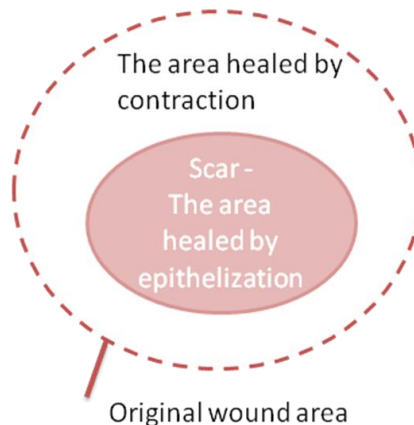

Fig. 28. The schematics of contribution of epithelization and contraction to overall process of wound repair.

	Males ND	Males D	Ratio D/ND	Females ND	Females D	Ratio D/ND
Contribution of epithelization to overall healing (scar size) n = 6, [% of original wound area]	26 ± 2	37 ± 2 **	1.4	15 ± 2	36 ± 3 **	2.4
Contribution of contraction to overall healing. n = 6, [% of original wound area]	74 ± 2	63 ± 2 **	0.85	85 ± 2	64 ± 3 **	0.75
Fresh scar strength, n = 4, [g/mm]	71 ± 5.8	39 ± 8.3 *	0.55	47 ± 3.6	26 ± 3.2 *	0.55

Tab. 21: Contribution of contraction and epithelization to overall process of wound repair. % epithelization = size of scar/size of original wound, % contraction = 100% – % epithelization. Data are means ± SEM. *: $p < 0.05$, **: $p < 0.01$ (diabetic compared to non-diabetic). D (diabetic), ND (non-diabetic).

5.2.9 Hydroxyproline

Hydroxyproline content per gram of wet tissue was lowered significantly in the skin of diabetic females. Accumulation of hydroxyproline during diabetic wound healing on days 5 and 10 was lowered to approximately half that in healthy controls (Tab. 22). Lowered accumulation could be caused by lower collagen production or more likely by partial expulsion/substitution of fibrous tissue by adipose tissue in wounds (Fig. 26 B,C).

Experimental group	Day 0 - skin	Day 5	Day 10
Non-diabetic males	19.6 ± 1.42	3.33 ± 0.36	7.10 ± 0.85
Diabetic males	17.6 ± 1.42	1.61 ± 0.56 *	2.68 ± 0.41 **
Non-diabetic females	24.5 ± 3.54	2.27 ± 0.15	5.17 ± 0.51
Diabetic females	10.9 ± 2.54 *	1.21 ± 0.46 *	3.15 ± 0.28 **

Tab. 22: Concentration of hydroxyproline (mg/g of wet tissue) in skin and wounds. Data are shown as means ± SEM. n = 4 - 6 (day 0, day 5), n = 9 - 11 (day 10). *: $p < 0.05$, **: $p < 0.01$ (diabetic animals compared to non-diabetic controls).

5.2.10 mRNA analysis: DNA-arrays and real-time RT-PCR.

Using DNA-array analysis, simultaneously studying expression of 115 genes, it was shown that gene expression differed between diabetic and non-diabetic animals in wound tissue on day 10. In diabetic males the most up-regulated mRNAs were those of IL-6 and PAI-1, while tropoelastin mRNA was down-regulated (Tab. 23) when compared to controls. In female wounds the expression pattern was different. The mRNA levels of MMP-3 and MMP-13 were notably up-regulated in the diabetic group (Tab. 24). Other significantly changed gene expressions are shown in Tab. 23 and Tab. 24.

Gene – males	mRNA expression ratio of diabetic to non-diabetic animals
Interleukin-6 (NM_012589)	1.38 *
Plasminogen activator inhibitor-1 (NM_012620)	1.23
MMP-3 (stromelysin-1, NM_133523)	1
MMP-13 (collagenase-3, M60616)	0.94
Tropoelastin (NM_012722)	0.71*
MMP-12 (macrophage metalloelastase, NM_053963)	0.68*
Interleukin-10 (NM_012854)	1.15*

Tab. 23: Relative gene expression of selected genes in granulation tissue in males on day 10 as assayed by DNA array (totally assayed 115 genes), ratio = gene expression in diabetic animals/gene expression in non-diabetic animals, n = 7 - 8, *: $p < 0.05$, **: $p < 0.01$ (diabetic animals compared to non-diabetic controls).

Gene – females	mRNA expression ratio of diabetic to non-diabetic animals
Interleukin-6 (NM_012589)	0.93
Plasminogen activator inhibitor-1 (NM_012620)	1.20
MMP-3 (stromelysin-1, NM_133523)	2.52**
MMP-13 (collagenase-3, M60616)	1.5**
Tropoelastin (NM_012722)	0.96
iNOS (nitric oxide synthase 2, inducible, NM_01261)	0.69 *
Laminin gama 2 (XM_213902.4)	0.4 **
calgranulin B (MRP14, NM_053587)	0.79*
Plasminogen (NM_053491.1)	0.73 *
Tumor necrosis factor alpha (NM_012675)	0.72 *

Tab. 24 : Relative gene expression of selected genes in granulation tissue on day 10 in females as assayed by DNA array (totally assayed 115 genes), ratio = gene expression in diabetic animals/gene expression in non-diabetic animals, n = 7 - 8, *: $p < 0.05$, **: $p < 0.01$ (diabetic animals compared to non-diabetic controls).

As shown by real-time PCR analysis, the mRNA levels of IL-6, myeloperoxidase (MPO), p22-phox and rac2 subunits of NADPH-oxidase were up-regulated in males on day 10. The expression of tropoelastin and type I procollagen was down-regulated (Tab. 25). In females, the levels of IL-6, MPO, MMP-3 and MMP-13 were substantially up-regulated in diabetic wound tissue (Tab. 25).

Gene	Males mRNA expression ratio (diabetic to non-diabetic animals)	Females mRNA expression ratio(diabetic to non-diabetic animals)
Inflammation		
Interleukin-6 (NM_012589)	3.30 *	2.76 *
Interleukin-1β (NM_031512)	1.54	1.15
Connective tissue metabolisms		
Plasminogen activator inhibitor-1 (NM_012620)	1.17	1.17
MMP-3 (stromelysin-1, NM_133523)	1.33	5.70 **
MMP-13 (collagenase-3, M60616)	1.31	1.99 *
Tropoelastin (NM_012722)	0.39 *	0.83
Type I procollagen alpha II (NM_53356)	0.7*	0.85
Metabolism of reactive oxygen species		
Myeloperoxidase (XM_220830)	2.40 **	4.10 **
P22-phox –NADPH oxidase (NM_024160)	1.39 *	1.04
Rac2-NADPH oxidase (NM_001008384)	1.64 **	1.11

Tab. 25: Relative gene expression of selected genes in granulation tissue on day 10 as assayed by quantitative RT-PCR, ratio = gene expression in diabetic/gene expression in non-diabetic animals, n = 10 - 14. *: $p < 0.05$, **: $p < 0.01$ (diabetic animals compared to non-diabetic controls).

5.2.11 Immunohistochemistry

5.2.11.1 Myeloperoxidase and interleukin-6

Immunohistochemical staining showed increased MPO (Fig. 29A, B) and IL-6 (Fig. 29C, D) positive signals at the very top inflammatory layer of diabetic wounds. This layer was composed mainly of pus and wound exudate. IL-6 positive signal was found in immune cells (Fig. 30A) and in granulation tissue fibroblasts. MPO was found in PMN cells and macrophage-like cells (Fig. 30B, C).

5.2.11.2 Matrix metalloproteinases 3 and 13

MMP-3 staining was more intense in wound tissue of diabetic females compared to control (Fig. 29G, H). Wound fibroblasts located on the top of granulation tissue under inflammatory layer were MMP-3 positive (Fig. 31D). Some immune cells and giant cells were also positive (Fig. 31C). The tip of the epithelial tongue was MMP-3 negative or very weak positive.

MMP-13 staining was elevated in granulation tissue of diabetic females compared to control (Fig. 29E, F). MMP-13 was strongly positive in the epithelial cells at the bottom of the new epidermis leading edge (Fig. 31B). These positive epithelial cells were in contact with granulation tissue and were present in all studied groups. Fibroblastic cells inside the top layer of the granulation tissue were also MMP-13 positive and were parallel to would surface (Fig. 31A). This layer was located under the very top inflammatory layer.

Fig. 29 : Immunohistochemical image of wound tissue, peroxidase staining, wound on day 10 (4x magnification). A: Interleukin-6 in non-diabetic male wound, B: Interleukin-6 in diabetic male wound, C: Myeloperoxidase in non-diabetic wound, D: Myeloperoxidase in diabetic wound, E: Collagenase-3 (MMP-13) in female non-diabetic wound, F: MMP-13 in female diabetic wound. G: Stromelysin-1 (MMP-3) in female non-diabetic wound, H: MMP-3 in diabetic female wound. *e* - epithelium, *d* - dermis, *m* - muscle layer, *c* - crust, *g* - granulation tissue, *a* - adipose tissue. Representative illustrative images from four to five stained tissues are shown.
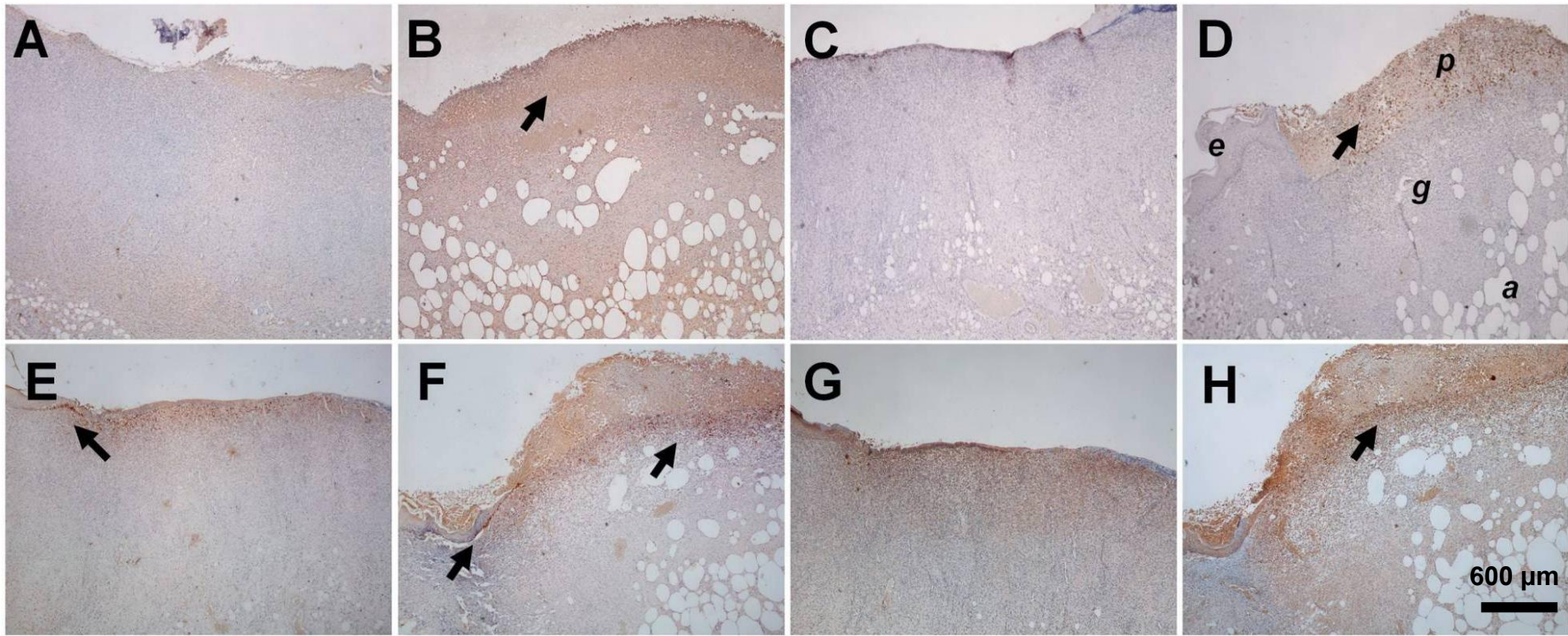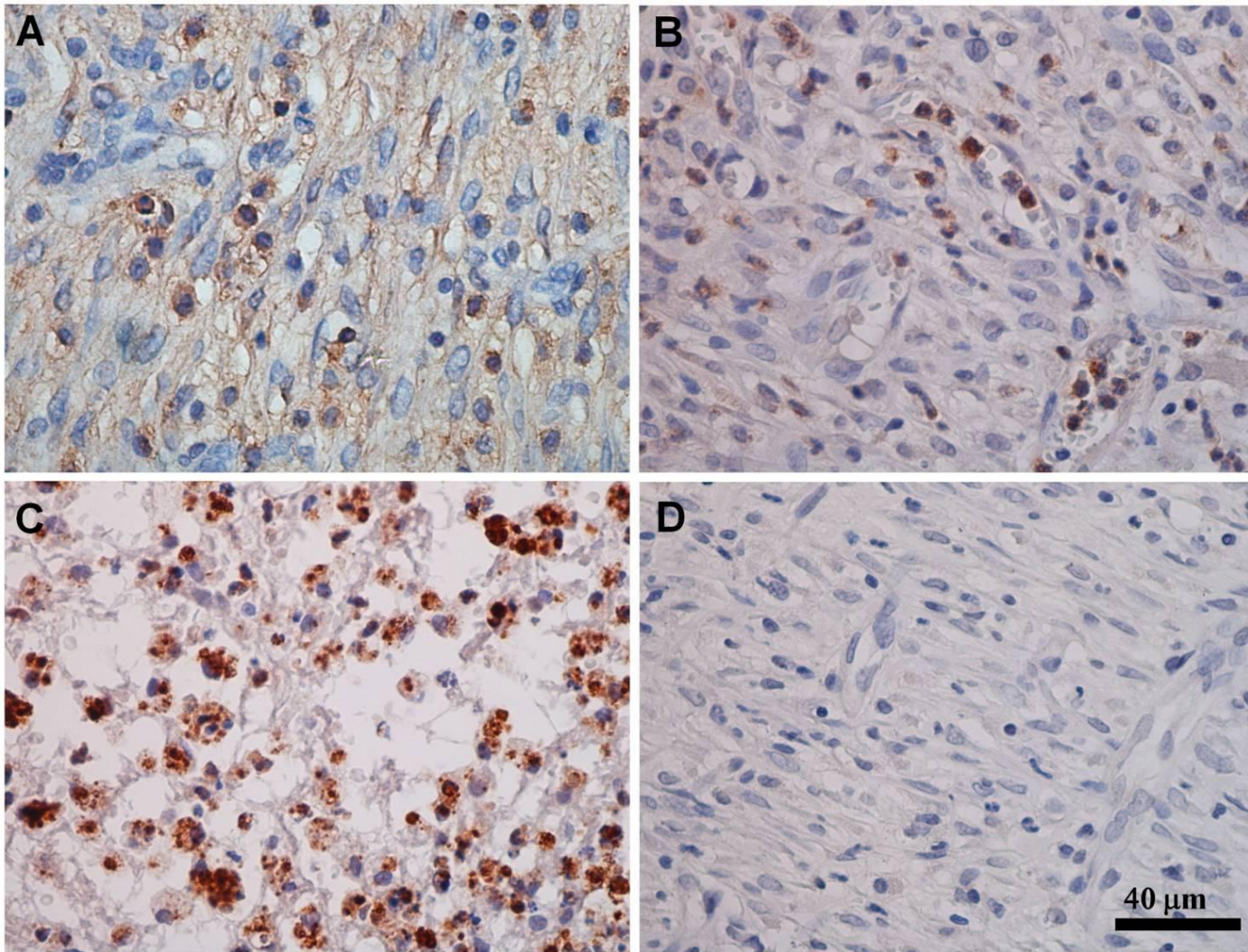
Fig. 30: Immunohistochemical image of wound tissue, peroxidase staining, wound on day 10 (60x magnification). A: Interleukin-6 in immune cells, B: myeloperoxidase in PMN cells, C: myeloperoxidase in macrophage-like cells in the wound pus, D: granulation tissue - negative control without antibody. Representative illustrative images from four to five stained tissues are shown.
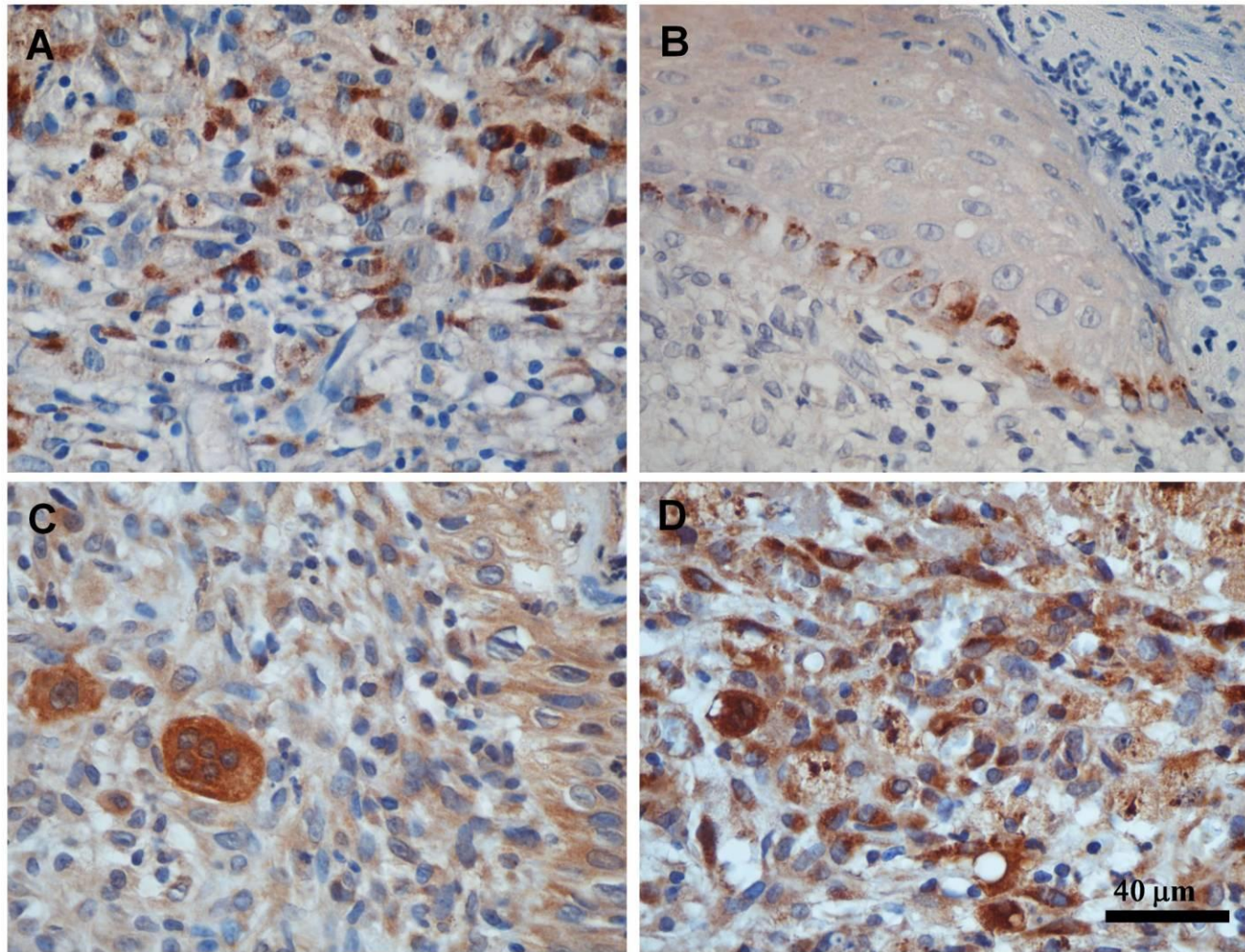
Fig. 31 : Immunohistochemical image of wound tissue, peroxidase staining, wound on day 10 (60x magnification). A: MMP-13 in fibroblast-like cells on the top of granulation tissue, B: MMP-13 in epithelial cells at the tip of newly forming epithelial tongue, C: MMP-3 in multi-nucleated giant cell in the granulation tissue, D: MMP-3 in fibroblastic cell on the top of granulation tissue. Representative illustrative images from four to five stained tissues are shown.

6 Discussion

6.1 Part 1: Hyaluronan, Hyiodine - a potential for wound healing

Hyiodine, the combination of hyaluronate and iodine, is a novel product combining high m.w. HA and iodine. It was reported that the complex of hyaluronate-iodine had beneficial effect on wound repair in diabetic foot ulcers and hard-to-heal wound of different etiology (Sobotka et al. 2006; Sobotka et al. 2007). However, the exact mechanism of its action on wound repair is unknown. High m.w. HA has beneficial effects on wound healing (Balazs et al. 2000). It is highly viscous and when it was applied on rat skin wounds in our experiments, it made wound redressing easier because Hyiodine soaked gauze did not stick to the wound. Hyiodine applied on the wounds immediately after skin excision accelerated wound contraction in the first days of healing. Later on the course of wound closure was similar in the Hyiodine-treated and saline-treated group. The influence of added HA may be greatest in the proliferative phase of healing. The antiseptic properties of iodine may be more important in humans than in rats.

Wounds treated with Hyiodine showed thickened epithelium on day 7. HA is a component of granulation tissue but its synthesis is not limited to mesenchymal cells. HA is contained in normal epidermis and it is synthesized by epidermal keratinocytes. Epidermal injury activates hyaluronan synthases in keratinocytes and causes an increase in epidermal HA. Keratinocyte migration is retarded when hyaluronan synthesis is blocked (Tsuboi et al. 1992). Exogenous HA may support epithelial hyperplasia (Arnold et al. 1995). The role of iodine in wound healing is not clear (Selvaggi et al. 2003), but PVP-iodine hydrogel was reported to improve epithelialization (Vogt et al. 2006).

Hyiodine application did not change collagen accumulation in the granulation tissue. The expression of other ECM components, proteinases and cytokines was not changed when studied on mRNA level. Together, expression of 92 genes were studied, however it is now known that thousands of genes are differentially expressed during the wound repair in comparison to uninjured skin (Roy et al. 2007; Roy et al. 2008; Greco et al. 2010). It is possible that several important targets had been missed in our selection. Therefore, for the future clarification of the mode of action, the whole-genome wide approach is more advisable.

Iodine greatly potentiated the ability of HA1200 to stimulate exudate formation. The protein composition of the exudate reminded of that of rat plasma with a prominent albumin band suggesting that a large part of exudate came from the plasma. Uronic acid content in the exudate was also increased. HA is a normal component of wound fluid, but plausibly some HA applied on the wound have been retained on its surface. The nature of the interaction between iodine and HA is not clear. Iodine may bind to the glycosaminoglycan or it may oxidize it. The action of HA may be more powerful or its absorption may be slowed down and the effect of HA may be protracted in the presence of iodine.

6.2 Part 2: Characteristics of cutaneous healing of diabetic and obese ZDF rats

ZDF rat is a well-known model of type II diabetes with obesity. This work shows characteristics of skin repair in ZDF male and female rats. Wound size diminution was impaired by DM and obesity in both sexes. The start of the closure was slightly slower in females and wound size increased significantly in the first phase of wound repair in diabetic females. This could be caused by the relatively higher wound severity due to the smaller body size of females, different diet, different skin composition or hormonal distinction. Diabetic animals had different skin composition, containing more adipose tissue compared to non-diabetic counterparts.

Diabetic wounds were accompanied by inflammation and were covered by larger crusts. During the healing, diabetic wounds were filled with a large amount of adipose tissue, poorly filled with granulation tissue and their contraction was impaired. Whereas non-diabetic wounds were almost entirely closed by contraction, in diabetic wounds, the epithelization had a more pronounced contribution to repair. Consequently, diabetic animals developed larger scars. Different fibroblast phenotype in adipose as opposed to dermal tissue could provide different paracrine stimulation of epithelium. Adipose tissue could influence wound healing by limiting cell migration or by its adipokine production. The retardation in contraction could be mediated through physical changes such as tension in skin due to obesity. The organization of fibroblasts and myofibroblasts network could be impaired by abundant adipose tissue (Goodson et al. 1986; Bauer et al. 2004). Generally speaking, wound healing in humans is known to be accomplished mainly by granulation tissue formation and epithelization with little wound contraction. Thus healing with increased contribution of epithelization that was observed in diabetic animals resembles partially this manner of healing.

Lower hydroxyproline concentrations and slightly lower type I collagen mRNA expression in granulation tissue was most probably caused by a displacement of collagen producing fibroblastic cells by adipocytes. The study of obese insulin resistant JCR rat showed impaired wound repair, contraction and wound collagen content (Bauer et al. 2004) comparable to our results. In our study, diabetic males had very high increase in blood glucose and relatively low increase in body weight. On the other hand, diabetic females showed a high increase in body weight and a relatively low increase in blood glucose compared to non-diabetics. We

observed impaired wound repair in both sexes and therefore we propose that both factors (high obesity and high glucose) had negative effect on wound repair. Most probably the combination of high obesity and high glycemia would result in even higher impairment of wound repair due to cumulating effect. Together their study (Bauer et al. 2004) and our study suggest that obesity significantly impairs wound healing and that this parameter is as least as important as hyperglycemia. On the other hand, similar work on db/db mice concluded that the variability of wound closure for individual mice did not correlate with severity of obesity, hyperglycemia, hyperinsulinemia, or insulin resistance (Trousdale et al. 2009).

We noticed a substantial difference in healing between bandaged and non-bandaged (open) wound. The bandaging increased the contraction in early phases of wound repair. This could be caused by the tension of the bandage, a barrier being formed against particles or microbial infection, wound moisture retention or exudate removal support. On the other hand, a bandage could cause animal stress. Animals had a natural tendency to scratch and to try to remove the bandage. As a result of these conditions the animals sometimes decreased their weight by up to 10% when bandaged. Furthermore, anesthesia was needed at every change of dressing and the fragile tissue adhering to the gauze pad could have been damaged. A portion of the crust that merged with the gauze was removed during the dressing change.

ZDF rat differs from other diabetes rodent models. Although type I DM is clinically less frequent when compared to type II, streptozotocine-induced type I diabetic rodent is the most widespread model for experimental research of diabetic wound. This model has limitations such as potential kidney, liver, pancreas toxicity of streptozotocine, and impaired weight gain (Greenhalgh 2003). An obese type II diabetic db/db mice, exhibited severe wound healing impairment compared to streptozotocine-induced diabetic mouse, which healed quite similarly to control non-diabetic mouse (Keswani et al. 2004; Michaels et al. 2007). Rate of wound area diminution was also similar between diabetic and non-diabetic rat in recent study (Dogan et al. 2009). In our work, epithelization played an important role in diabetic rats, as wound contraction was impaired. The length of epithelization tongue was increased. Increased epithelization could be caused by high levels of insulin (Apikoglu-Rabus et al. 2010) present in diabetic ZDF rats. Therefore the use of the present model for studying impaired epithelization is limited. The model we report could be modified for further studies by lowering rat insulin levels. Also increased leptin levels in diabetic rats could play a role in this phenomena, as leptin influences epithelial cells *in vitro* and *in vivo* and epithelial tongue in wounds expresses leptin receptors (LEPR) (Frank et al. 2000). In db/db mice, epithelization

was severely disturbed (Wall et al. 2002) and leptin levels were reported to be increased (Sahai et al. 2004) alike in ZDF rats. This difference in epithelization could be explained by different mutations of LEPR in ZDF fa/fa rats and in db/db mice (C57BL/KS-Leprdb/J). In ZDF rats there is a point missense mutation in residue 269. A protein with leptin binding activity and intact signaling domain is produced, however with dimer formation impairment (Phillips et al. 1996). In the case of db/db mice an aberrant splicing variant of LEPR with a 106 nucleotides insertion and prematurely terminated dysfunctional intra-cellular domain is present (Chen et al. 1996). This suggests that leptin dependent epithelial cell promotion might be functional in ZDF rats (due to probable different mechanism of LEPR formation and function in epithelial cells than in the hypothalamus) and dysfunctional in the case of db/db mice (due to a missing intracellular domain in the receptor). To prove this hypothesis it would be necessary to do another *in vivo* study and to compare the responsiveness of cutaneous epithelial cells from ZDF rats and from db/db mice to leptin.

Our study showed different patterns of the expression of several genes, some of them connected to inflammation, thus supporting observed abundant inflammation in diabetic animals. However, the question of whether diabetic wounds are inflamed due to deregulated endogenous inflammation control or higher susceptibility to microbial infection remains unresolved. We have shown increased expression of IL-6 in diabetic wounds and established its spatial distribution on the very top of the wound. Surprisingly, the levels of adipokine IL-6 in the plasma of both healthy and diabetic unwounded animals were similar even in diabetic females, whose body weight was double that of their non-diabetic counterparts. The role of IL-6 is complex. IL-6 is essential in the regulation of early immune response to trauma that is necessary for proper wound repair (McFarland-Mancini et al. 2010). It is produced by fibroblasts, keratinocytes, neutrophils and macrophages (Mateo et al. 1994) and its deficiency leads to impaired healing (Lin et al. 2003; McFarland-Mancini et al. 2010). However, a surfeit of IL-6 can slow down tissue repair (Gallucci et al. 2001) and decrease fibroblast proliferation (Mateo et al. 1994). IL-6 levels were elevated in patients with diabetic ulcers (Fu et al. 1999). It can be extrapolated from the research on liver regeneration, where a short-term application of IL-6 was shown to be beneficial and a prolonged application negative, that a prolonged expression of IL-6 in diabetic wounds might also be detrimental to wound healing. In contrast to our results, the IL-6 levels were suppressed in wound fluids of streptozotocine-diabetic mice (Fahey et al. 1991).

We have observed higher levels of MMP-3 and MMP-13 mRNA, and immunohisto-chemical signal in diabetic females. Abundant expression of metalloproteinases could be partially responsible for lower collagen (hydroxyproline) content in diabetic wounds. MMP-13 degrades native fibrilar collagens and to some extent proteoglycans and other extracellular matrix components while the main substrates of MMP-3 are gelatin, laminin, fibronectin and proteoglycans. Over-expression of wound MMPs can lead to proteolytic tissue damage (Lobmann et al. 2002). In chronic wounds, MMP-3 was expressed by keratinocytes located above the basement membrane behind the leading edge of the hyperproliferative epithelium and was also detected in the granulation tissue (Saarialho-Kere et al. 1994). In our experiments, MMP-3 was not present in the epithelium, but we have detected MMP-3 in the granulation tissue in rats. MMP-3 has a role in wound contraction and activation of the contraction phenotype in fibroblasts (Bullard et al. 1999). *In vitro*, MMP-1 and MMP-3 can be induced by a shock via IL-6 autocrine stimulation in dermal fibroblasts (Park et al. 2004) and IL-6 can increase the MMP-13 gene expression in rat fibroblasts (de la Torre et al. 2005). We hypothesize that the abundant presence of IL-6 in diabetic wounds could cause the increased expression of MMP-3 and MMP-13. As MMP-1 is not present in rat tissues, rat MMP-13 is considered to play a predominant role in matrix degradation, comparable to the role of MMP-1 in humans (Okazaki et al. 2001). In chronic human wounds, MMP-13 was detected exclusively in fibroblasts in deep wound bed and not in migrating keratinocytes (Vaalamo et al. 1997). MMP-1 is produced by migrating epithelial cells (Parks 1999). In ZDF rats, MMP-13, playing similar role as human MMP-1, was clearly detected in keratinocytes located near wound edge and in upper layers wound fibroblasts. Also MMP-8 (neutrophil collagenase) and MMP-9 (type IV collagenase) were elevated in human chronic wounds in comparison to early acute wounds (Lobmann et al. 2002). In our study, we did not observe increased MMP-9 or MMP-8. MMP-9 is required for normal progression of wound closure (Kyriakides et al. 2009). However, its abundant presence was shown to interfere with epithelization, basement membrane and keratinocyte migration (Reiss et al. 2010). The reason why we did not observe impairments in epithelization could be partially explained by the finding that MMP-9 levels were normal in diabetic rats. The limitation of our study is that only one time interval (day 10) was used for the analysis of mRNA and proteins using imunohistochemistry.

7 Conclusion

7.1 Conclusion – Part 1

Positive action of hyaluronan-iodine complex observed on hard-to-heal wounds in diabetic patients was supported by our animal model study. Hyiodine speeded up the process of wound closure in the early phase of healing. The positive effect could be mediated by an effect on wound epithelium. Accentuated exudation keeps the wound moist and makes wound redressing easier. The influence of HA is supported by iodine that was not only a mere disinfectant but potentiated some effects of HA. The formation of granulation tissue and its main component, collagen, was not changed as was not the mRNA expression of the set of studied genes.

7.2 Conclusion – Part 2

The present work revealed an impaired mode of cutaneous healing, and the structure of wound tissue in obese diabetic and lean non-diabetic ZDF rats. This model could be useful for further studies of molecular changes in wound repair caused by obesity and diabetes. The reported results warrant further research into the regulation and resolution of inflammation response, the role of adipose tissue, the deregulation of MMPs during wound repair in ZDF rats. Also the role of leptin and its receptor in epithelization could be studied on molecular level. Obese ZDF rats seem to be a suitable model for the testing substances designed to influence tissue repair and are proposed as a novel model of impaired cutaneous wound repair with type II diabetes mellitus and obesity.

8 References

Abatangelo, G., Martelli, M. and Vecchia, P. Healing of hyaluronic acid-enriched wounds: histological observations. *J Surg Res*, 1983, vol. 35, no. 5, p. 410-416.

Ahmed, N. Advanced glycation endproducts--role in pathology of diabetic complications. *Diabetes Res Clin Pract*, 2005, vol. 67, no. 1, p. 3-21.

Ajemian, M. S., Macaron, S. and Brenes, R. Hyaluronate-iodine (hyiodine) complex in the treatment of non-healing wounds. *J Am Coll Surg*, 2007, vol. 205, no. 3, p. S55.

Akiyama, H., Oono, T., Saito, M. and Iwatsuki, K. Assessment of cadexomer iodine against Staphylococcus aureus biofilm in vivo and in vitro using confocal laser scanning microscopy. *J Dermatol*, 2004, vol. 31, no. 7, p. 529-534.

Apikoglu-Rabus, S., Izzettin, F. V., Turan, P. and Ercan, F. Effect of topical insulin on cutaneous wound healing in rats with or without acute diabetes. *Clin Exp Dermatol*, 2010, vol. 35, no. 2, p. 180-185.

Armstrong, D. G. and Jude, E. B. The role of matrix metalloproteinases in wound healing. *J Am Podiatr Med Assoc*, 2002, vol. 92, no. 1, p. 12-18.

Arnold, F., Jia, C., He, C., Cherry, G. W., Carbow, B., Meyer-Ingold, W., Bader, D. and West, D. C. Hyaluronan, heterogeneity, and healing: the effects of ultrapure hyaluronan of defined molecular size on the repair of full-thickness pig skin wounds. *Wound Repair Regen*, 1995, vol. 3, no. 3, p. 299-310.

Bakker, K. *International Consensus on the Diabetic Foot*. Brussels, International Working Group on the Diabetic Foot, 1999.

Balazs, E. A. and Larsen, N. E. Hyaluronan : Aiming for Perfect Skin Regeneration. *Scarless Wound Healing*. G. H. Garg and M. T. Longaker (ed.). New York, Marcell Dekker, 2000, p. 143-160.

Bassilian, S., Ahmed, S., Lim, S. K., Boros, L. G., Mao, C. S. and Lee, W. N. Loss of regulation of lipogenesis in the Zucker diabetic rat. II. Changes in stearate and oleate synthesis. *Am J Physiol Endocrinol Metab*, 2002, vol. 282, no. 3, p. E507-513.

Bauer, B. S., Ghahary, A., Scott, P. G., Iwashina, T., Demare, J., Russell, J. C. and Tredget, E. E. The JCR:LA-cp rat: a novel model for impaired wound healing. *Wound Repair Regen.*, 2004, vol. 12, no. 1, p. 86-92.

Birch, M., Tomlinson, A. and Ferguson, M. W. Animal Models for Adult Dermal Wound Healing, *Fibrosis Research : Methods and Protocols. Methods in Molecular Medicine.* 2005, vol. 117, p. 223-235.

Bitter, T. and Muir, H. M. A modified uronic acid carbazole reaction. *Anal Biochem*, 1962, vol. 4, no., p. 330-334.

Blakytny, R., Jude, E. B., Martin Gibson, J., Boulton, A. J. and Ferguson, M. W. Lack of insulin-like growth factor 1 (IGF1) in the basal keratinocyte layer of diabetic skin and diabetic foot ulcers. *J Pathol*, 2000, vol. 190, no. 5, p. 589-594.

Brem, H. and Tomic-Canic, M. Cellular and molecular basis of wound healing in diabetes. *J Clin Invest*, 2007, vol. 117, no. 5, p. 1219-1222.

Brenes, R. A., Ajemian, M. S., Macaron, S. H., Panait, L. and Dudrick, S. J. Initial experience using a hyaluronate-iodine complex for wound healing. *Am Surg*, 2011, vol. 77, no. 3, p. 355-359.

Brenes, R. A., Sobotka, L., Ajemian, M. S., Manak, J., Vyroubal, P., Slemrova, M., Adamkova, V., Zajic, J. and Dudrick, S. J. Hyaluronate-iodine complex: a new adjunct for the management of complex sternal wounds after a cardiac operation. *Arch Surg*, 2011, vol. 146, no. 11, p. 1323-1325.

Brown, J. A. The role of hyaluronic acid in wound healing's proliferative phase. *J Wound Care*, 2004, vol. 13, no. 2, p. 48-51.

Buck, D. W., 2nd, Jin da, P., Geringer, M., Hong, S. J., Galiano, R. D. and Mustoe, T. A. The TallyHo polygenic mouse model of diabetes: implications in wound healing. *Plast Reconstr Surg*, 2011, vol. 128, no. 5, p. 427e-437e.

Bullard, K. M., Mudgett, J., Scheuenstuhl, H., Hunt, T. K. and Banda, M. J. Stromelysin-1-deficient fibroblasts display impaired contraction in vitro. *J Surg Res*, 1999, vol. 84, no. 1, p. 31-34.

Burrow, J. W., Koch, J. A., Chuang, H. H., Zhong, W., Dean, D. D. and Sylvia, V. L. Nitric oxide donors selectively reduce the expression of matrix metalloproteinases-8 and -9 by human diabetic skin fibroblasts. *J Surg Res*, 2007, vol. 140, no. 1, p. 90-98.

Carthy, J. M., Boroomand, S. and McManus, B. M. Versican and CD44 in in vitro valvular interstitial cell injury and repair. *Cardiovasc Pathol*, 2011, vol., no.

Clark, R. A., Folkvord, J. M. and Wertz, R. L. Fibronectin, as well as other extracellular matrix proteins, mediate human keratinocyte adherence. *J Invest Dermatol*, 1985, vol. 84, no. 5, p. 378-383.

Clark, R. A., Nielsen, L. D., Welch, M. P. and McPherson, J. M. Collagen matrices attenuate the collagen-synthetic response of cultured fibroblasts to TGF-beta. *J Cell Sci*, 1995, vol. 108 (Pt 3), no., p. 1251-1261.

Clark, R. A. F. Wound Repair : Overview and General Consideretion. *The Molecular and Cellular Biology of Wound Repair*. R. A. F. Clark (ed.). New York, Springer, 1996, p. 3-50.

Coleman, D. L. and Eicher, E. M. Fat (fat) and tubby (tub): two autosomal recessive mutations causing obesity syndromes in the mouse. *J Hered*, 1990, vol. 81, no. 6, p. 424-427.

Cooper, R. A. Iodine revisited. *Int Wound J*, 2007, vol. 4, no. 2, p. 124-137.

Corsetti, J. P., Sparks, J. D., Peterson, R. G., Smith, R. L. and Sparks, C. E. Effect of dietary fat on the development of non-insulin dependent diabetes mellitus in obese Zucker diabetic fatty male and female rats. *Atherosclerosis*, 2000, vol. 148, no. 2, p. 231-241.

Cross, S. E., Naylor, I. L., Coleman, R. A. and Teo, T. C. An experimental model to investigate the dynamics of wound contraction. *Br J Plast Surg*, 1995, vol. 48, no. 4, p. 189-197.

Danis, R. P. and Yang, Y. Microvascular retinopathy in the Zucker diabetic fatty rat. *Invest Ophthalmol Vis Sci*, 1993, vol. 34, no. 7, p. 2367-2371.

Davidson, J. M. Animal models for wound repair. *Arch Dermatol Res*, 1998, vol. 290 Suppl, p. S1-11.

Davidson, J. M. Experimental Animal Wound Models. *Wounds*, 2001, vol. 13, no. 1, p. 9-23.

Day, R. and Mascarenhas, M. Signal Transduction Associated with Hyaluronan. *Chemistry and Biology of Hyaluronan*. H. Garg (ed.). Oxford, Elsevier, 2004, p. 153-188.

de la Torre, J. I. and Chambers, J. A. (2008, 9.10.2008). *Chronic Wounds*. Retrieved 10.6.2011, from http://emedicine.medscape.com/article/1298452-overview#showall.

de la Torre, P., Diaz-Sanjuan, T., Garcia-Ruiz, I., Esteban, E., Canga, F., Munoz-Yague, T. and Solis-Herruzo, J. A. Interleukin-6 increases rat metalloproteinase-13 gene expression through Janus kinase-2-mediated inhibition of serine/threonine phosphatase-2A. *Cell Signal*, 2005, vol. 17, no. 4, p. 427-435.

Deskins, D. L., Ardestani, S. and Young, P. P. The polyvinyl alcohol sponge model implantation. *J Vis Exp*, 2012, no. 62.

Dogan, S., Demirer, S., Kepenekci, I., Erkek, B., Kiziltay, A., Hasirci, N., Muftuoglu, S., Nazikoglu, A., Renda, N., Dincer, U. D., Elhan, A. and Kuterdem, E. Epidermal growth factor-containing wound closure enhances wound healing in non-diabetic and diabetic rats. *Int Wound J*, 2009, vol. 6, no. 2, p. 107-115.

Doillon, C. J. and Silver, F. H. Collagen-based wound dressing: effects of hyaluronic acid and fibronectin on wound healing. *Biomaterials*, 1986, vol. 7, no. 1, p. 3-8.

Dorsett-Martin, W. A. Rat models of skin wound healing: a review. *Wound Repair Regen*, 2004, vol. 12, no. 6, p. 591-599.

Engerman, R. L. and Kramer, J. W. Dogs with induced or spontaneous diabetes as models for the study of human diabetes mellitus. *Diabetes*, 1982, vol. 31, no. Suppl 1 Pt 2, p. 26-29.

Fahey, T. J., 3rd, Sadaty, A., Jones, W. G., 2nd, Barber, A., Smoller, B. and Shires, G. T. Diabetes impairs the late inflammatory response to wound healing. *J Surg Res*, 1991, vol. 50, no. 4, p. 308-313.

Feinberg, R. N. and Beebe, D. C. Hyaluronate in vasculogenesis. *Science*, 1983, vol. 220, no. 4602, p. 1177-1179.

Finegood, D. T., McArthur, M. D., Kojwang, D., Thomas, M. J., Topp, B. G., Leonard, T. and Buckingham, R. E. Beta-cell mass dynamics in Zucker diabetic fatty rats. Rosiglitazone prevents the rise in net cell death. *Diabetes*, 2001, vol. 50, no. 5, p. 1021-1029.

Frank, S., Stallmeyer, B., Kämpfer, H., Kolb, N. and Pfeilschifter, J. Leptin enhances wound re-epithelialization and constitutes a direct function of leptin in skin repair. *J Clin Invest*, 2000, vol. 106, no. 4, p. 501-509.

Fu, X. B., Yang, Y. H. and Sun, T. Z. Transforming growth factor beta 1 and interleukin 6 mRNA expression in wound tissues of patients with diabetic ulcers. *Zhongguo Xiu Fu Chong Jian Wai Ke Za Zhi*, 1999, vol. 13, no. 5, p. 259-262.

Galasso, U., Fiumano, F., Cloro, L. and Strati, V. Use of hyaluronic acid in the therapy of varicose ulcers of the lower limbs. *Minerva Chir*, 1978, vol. 33, no. 21, p. 1581-1596.

Galiano, R. D., Michaels, J. t., Dobryansky, M., Levine, J. P. and Gurtner, G. C. Quantitative and reproducible murine model of excisional wound healing. *Wound Repair Regen*, 2004, vol. 12, no. 4, p. 485-492.

Gallagher, K. A., Liu, Z. J., Xiao, M., Chen, H., Goldstein, L. J., Buerk, D. G., Nedeau, A., Thom, S. R. and Velazquez, O. C. Diabetic impairments in NO-mediated endothelial progenitor cell mobilization and homing are reversed by hyperoxia and SDF-1 alpha. *J Clin Invest*, 2007, vol. 117, no. 5, p. 1249-1259.

Gallo, R. L. and Bernfield, M. Proteoglycans and Their Role in Wound Repair. *The Molecular and Cellular Biology of Wound Repair*. R. A. F. Clark. New York, Springer, 1996, p. 475-492.

Gallucci, R. M., Sugawara, T., Yucesoy, B., Berryann, K., Simeonova, P. P., Matheson, J. M. and Luster, M. I. Interleukin-6 treatment augments cutaneous wound healing in immunosuppressed mice. *J Interferon Cytokine Res*, 2001, vol. 21, no. 8, p. 603-609.

Gan, D. *Diabetes Atlas, third edition*. Brussels, International Diabetic Federation, 2007.

Goodson, W. H., 3rd and Hunt, T. K. Wound collagen accumulation in obese hyperglycemic mice. *Diabetes*, 1986, vol. 35, no. 4, p. 491-495.

Greco, J. A., 3rd, Pollins, A. C., Boone, B. E., Levy, S. E. and Nanney, L. B. A microarray analysis of temporal gene expression profiles in thermally injured human skin. *Burns*, 2010, vol. 36, no. 2, p. 192-204.

Greenhalgh, D. G. Tissue repair in models of diabetes mellitus. A review. *Methods Mol Med*, 2003, vol. 78, p. 181-189.

Greenhalgh, D. G., Sprugel, K. H., Murray, M. J. and Ross, R. PDGF and FGF stimulate wound healing in the genetically diabetic mouse. *Am J Pathol*, 1990, vol. 136, no. 6, p. 1235-1246.

Greenway, S. E., Filler, L. E. and Greenway, F. L. Topical insulin in wound healing: a randomised, double-blind, placebo-controlled trial. *J Wound Care*, 1999, vol. 8, no. 10, p. 526-528.

Grinnell, F. Fibronectin and wound healing. *J Cell Biochem*, 1984, vol. 26, no. 2, p. 107-116.

Grinnell, F. Fibroblasts, myofibroblasts, and wound contraction. *J Cell Biol*, 1994, vol. 124, no. 4, p. 401-404.

Grinnell, F., Billingham, R. E. and Burgess, L. Distribution of fibronectin during wound healing in vivo. *J Invest Dermatol*, 1981, vol. 76, no. 3, p. 181-189.

Grodsky, G. M., Anderson, C. E., Coleman, D. L., Craighead, J. E., Gerritsen, G. C., Hansen, C. T., Herberg, L., Howard, C. F., Jr., Lernmark, A., Matschinsky, F. M., Rayfield, E., Riley, W. J. and Rossini, A. A. Metabolic and underlying causes of diabetes mellitus. *Diabetes*, 1982, vol. 31, no. Suppl 1 Pt 2, p. 45-53.

Hebda, P. A. and Sandulache, V. C. The Biochemistry of Epidermal Healing. *The Epidermis in Wound Healing* D. T. Rovee and H. I. Maibach (ed.). Boca Raton, CRC Press, 2004, p. 408.

Holeček, M. Komplexní regulace metbolizmu živin v nemoci. *Regulace metabolizmu cukrů, tuků, bílkovin a aminokyselin*. Praha, Grada, 2006, p. 231-264.

Hu, M., Sabelman, E. E., Cao, Y., Chang, J. and Hentz, V. R. Three-dimensional hyaluronic acid grafts promote healing and reduce scar formation in skin incision wounds. *J Biomed Mater Res B Appl Biomater*, 2003, vol. 67, no. 1, p. 586-592.

Hurych, J. and Chvapil, M. Methods of hydroxyproline determination. *Kozarstvi* 1962, vol. 12, p. 317-323.

Chen, H., Charlat, O., Tartaglia, L. A., Woolf, E. A., Weng, X., Ellis, S. J., Lakey, N. D., Culpepper, J., Moore, K. J., Breitbart, R. E., Duyk, G. M., Tepper, R. I. and Morgenstern, J. P. Evidence that the diabetes gene encodes the leptin receptor: identification of a mutation in the leptin receptor gene in db/db mice. *Cell*, 1996, vol. 84, no. 3, p. 491-495.

Chen, W. Y. and Abatangelo, G. Functions of hyaluronan in wound repair. *Wound Repair Regen*, 1999, vol. 7, no. 2, p. 79-89.

Ialenti, A. and Di Rosa, M. Hyaluronic acid modulates acute and chronic inflammation. *Agents Actions*, 1994, vol. 43, no. 1-2, p. 44-47.

Illes, J., Javor, A. and Szijarto, E. Zinc-hyaluronate: ana original organotherapeutic compound of Gedeon Richter Ltd. *Acta Pharm Hung*, 2002, vol. 72, no. 1, p. 15-24.

Iwata, Y., Yoshizaki, A., Komura, K., Shimizu, K., Ogawa, F., Hara, T., Muroi, E., Bae, S., Takenaka, M., Yukami, T., Hasegawa, M., Fujimoto, M., Tomita, Y., Tedder, T. F. and Sato, S. CD19, a response regulator of B lymphocytes, regulates wound healing through hyaluronan-induced TLR4 signaling. *Am J Pathol*, 2009, vol. 175, no. 2, p. 649-660.

Jia, C., Chen, B. and Arnold, F. The effect of ultrapure hyaluronic acid with different molecular weights on the healing of porcine full thickness skin wound. *Zhongguo Xiu Fu Chong Jian Wai Ke Za Zhi*, 1998, vol. 12, no. 4, p. 197-200.

Jiang, D., Liang, J. and Noble, P. W. Hyaluronan in tissue injury and repair. *Annu Rev Cell Dev Biol*, 2007, vol. 23, p. 435-461.

Kahn, S. E. The importance of the beta-cell in the pathogenesis of type 2 diabetes mellitus. *Am J Med*, 2000, vol. 108 Suppl 6a, p. 2S-8S.

Keswani, S. G., Katz, A. B., Lim, F. Y., Zoltick, P., Radu, A., Alaee, D., Herlyn, M. and Crombleholme, T. M. Adenoviral mediated gene transfer of PDGF-B enhances wound healing in type I and type II diabetic wounds. *Wound Repair Regen*, 2004, vol. 12, no. 5, p. 497-504.

King, S. R., Hickerson, W. L. and Proctor, K. G. Beneficial actions of exogenous hyaluronic acid on wound healing. *Surgery*, 1991, vol. 109, no. 1, p. 76-84.

Kyriakides, T. R., Wulsin, D., Skokos, E. A., Fleckman, P., Pirrone, A., Shipley, J. M., Senior, R. M. and Bornstein, P. Mice that lack matrix metalloproteinase-9 display delayed wound healing associated with delayed reepithelization and disordered collagen fibrillogenesis. *Matrix Biol*, 2009, vol. 28, no. 2, p. 65-73.

Laing, T., Hanson, R., Chan, F. and Bouchier-Hayes, D. The role of endothelial dysfunction in the pathogenesis of impaired diabetic wound healing: a novel therapeutic target? *Med Hypotheses*, 2007, vol. 69, no. 5, p. 1029-1031.

Lee, J. Y. and Spicer, A. P. Hyaluronan: a multifunctional, megaDalton, stealth molecule. *Curr Opin Cell Biol*, 2000, vol. 12, no. 5, p. 581-586.

Lee, W. N., Bassilian, S., Lim, S. and Boros, L. G. Loss of regulation of lipogenesis in the Zucker diabetic (ZDF) rat. *Am J Physiol Endocrinol Metab*, 2000, vol. 279, no. 2, p. E425-432.

Leibovich, S. J. and Ross, R. The role of the macrophage in wound repair. A study with hydrocortisone and antimacrophage serum. *Am J Pathol*, 1975, vol. 78, no. 1, p. 71-100.

Leonard, B. L., Watson, R. N., Loomes, K. M., Phillips, A. R. and Cooper, G. J. Insulin resistance in the Zucker diabetic fatty rat: a metabolic characterisation of obese and lean phenotypes. *Acta Diabetol*, 2005, vol. 42, no. 4, p. 162-170.

Lepperdinger, G., Fehrer, C. and Reitinger, S. Biodegradation of Hyaluronan. *Chemistry and Biology of Hyaluronan*. G. H. Garg (ed.). Oxford, Elsevier 2004, p. 71-82.

Li, J., Chen, J. and Kirsner, R. Pathophysiology of acute wound healing. *Clin Dermatol*, 2007, vol. 25, no. 1, p. 9-18.

Lin, Z. Q., Kondo, T., Ishida, Y., Takayasu, T. and Mukaida, N. Essential involvement of IL-6 in the skin wound-healing process as evidenced by delayed wound healing in IL-6-deficient mice. *J Leukoc Biol*, 2003, vol. 73, no. 6, p. 713-721.

Lobmann, R., Ambrosch, A., Schultz, G., Waldmann, K., Schiweck, S. and Lehnert, H. Expression of matrix-metalloproteinases and their inhibitors in the wounds of diabetic and non-diabetic patients. *Diabetologia*, 2002, vol. 45, no. 7, p. 1011-1016.

Longas, M. Hyaluronan in Aging. *Chemistry and Biology of Hyaluronan*. H. Garg. Oxford, Elsevier 2004, p. 351-365.

Loskutoff, D. J., Ny, T., Sawdey, M. and Lawrence, D. Fibrinolytic system of cultured endothelial cells: regulation by plasminogen activator inhibitor. *J Cell Biochem*, 1986, vol. 32, no. 4, p. 273-280.

Martin, A., Komada, M. R. and Sane, D. C. Abnormal angiogenesis in diabetes mellitus. *Med Res Rev*, 2003, vol. 23, no. 2, p. 117-145.

Mateo, R. B., Reichner, J. S. and Albina, J. E. Interleukin-6 activity in wounds. *Am J Physiol*, 1994, vol. 266, no. 6 Pt 2, p. R1840-1844.

McFarland-Mancini, M. M., Funk, H. M., Paluch, A. M., Zhou, M., Giridhar, P. V., Mercer, C. A., Kozma, S. C. and Drew, A. F. Differences in wound healing in mice with deficiency of IL-6 versus IL-6 receptor. *J Immunol*, 2010, vol. 184, no. 12, p. 7219-7228.

McKee, C. M., Penno, M. B., Cowman, M., Burdick, M. D., Strieter, R. M., Bao, C. and Noble, P. W. Hyaluronan (HA) fragments induce chemokine gene expression in alveolar macrophages. The role of HA size and CD44. *J Clin Invest*, 1996, vol. 98, no. 10, p. 2403-2413.

Midwood, K. S., Williams, L. V. and Schwarzbauer, J. E. Tissue repair and the dynamics of the extracellular matrix. *Int J Biochem Cell Biol*, 2004, vol. 36, no. 6, p. 1031-1037.

Mignatti, P., Rifkin, D. B., Welgus, H. G. and Parks, W. C. Proteinases and Tissue Remodeling. *The Molecular and Cellular Biology of Wound Repair*. R. A. F. Clark (ed.). New York, Plenum Press, 1996, p. 427-474.

Michaels, J., Churgin, S. S., Blechman, K. M., Greives, M. R., Aarabi, S., Galiano, R. D. and Gurtner, G. C. db/db mice exhibit severe wound-healing impairments compared with other murine diabetic strains in a silicone-splinted excisional wound model. *Wound Repair Regen*, 2007, vol. 15, no. 5, p. 665-670.

Miyake, K., Underhill, C. B., Lesley, J. and Kincade, P. W. Hyaluronate can function as a cell adhesion molecule and CD44 participates in hyaluronate recognition. *J Exp Med*, 1990, vol. 172, no. 1, p. 69-75.

Moore, K., Thomas, A. and Harding, K. G. Iodine released from the wound dressing Iodosorb modulates the secretion of cytokines by human macrophages responding to bacterial lipopolysaccharide. *Int J Biochem Cell Biol*, 1997, vol. 29, no. 1, p. 163-171.

Moseley, R., Walker, M., Waddington, R. J. and Chen, W. Y. Comparison of the antioxidant properties of wound dressing materials--carboxymethylcellulose, hyaluronan benzyl ester and hyaluronan, towards polymorphonuclear leukocyte-derived reactive oxygen species. *Biomaterials*, 2003, vol. 24, no. 9, p. 1549-1557.

Muller, F., Mutch, N. J., Schenk, W. A., Smith, S. A., Esterl, L., Spronk, H. M., Schmidbauer, S., Gahl, W. A., Morrissey, J. H. and Renne, T. Platelet polyphosphates are proinflammatory and procoagulant mediators in vivo. *Cell*, 2009, vol. 139, no. 6, p. 1143-1156.

Murashita, T., Nakayama, Y., Hirano, T. and Ohashi, S. Acceleration of granulation tissue ingrowth by hyaluronic acid in artificial skin. *Br J Plast Surg*, 1996, vol. 49, no. 1, p. 58-63.

Naggert, J. K., Fricker, L. D., Varlamov, O., Nishina, P. M., Rouille, Y., Steiner, D. F., Carroll, R. J., Paigen, B. J. and Leiter, E. H. Hyperproinsulinaemia in obese fat/fat mice associated with a carboxypeptidase E mutation which reduces enzyme activity. *Nat Genet*, 1995, vol. 10, no. 2, p. 135-142.

Nečas, E. Hojení rány. *Obecná patologická fyziologie*. Praha, Karolinum, 2005, p. 120-128.

Nemerson, Y. Tissue factor and hemostasis. *Blood*, 1988, vol. 71, no. 1, p. 1-8.

Newman, S. L., Henson, J. E. and Henson, P. M. Phagocytosis of senescent neutrophils by human monocyte-derived macrophages and rabbit inflammatory macrophages. *J Exp Med*, 1982, vol. 156, no. 2, p. 430-442.

Noble, P. W. Hyaluronan and its catabolic products in tissue injury and repair. *Matrix Biol*, 2002, vol. 21, no. 1, p. 25-29.

Noble, P. W., McKee, C. M., Cowman, M. and Shin, H. S. Hyaluronan fragments activate an NF-kappa B/I-kappa B alpha autoregulatory loop in murine macrophages. *J Exp Med*, 1996, vol. 183, no. 5, p. 2373-2378.

Okazaki, I., Watanabe, T., Hozawa, S., Niioka, M., Arai, M. and Maruyama, K. Reversibility of hepatic fibrosis: from the first report of collagenase in the liver to the possibility of gene therapy for recovery. *Keio J Med*, 2001, vol. 50, no. 2, p. 58-65.

Ormiston, M. C., Seymour, M. T., Venn, G. E., Cohen, R. I. and Fox, J. A. Controlled trial of Iodosorb in chronic venous ulcers. *Br Med J (Clin Res Ed)*, 1985, vol. 291, no. 6491, p. 308-310.

Ortonne, J. A controlled study of the activity of hyaluronic acid in the treatment of venous leg ulcers. *J Dermatol Treat*, 1996, vol. 7, no. 2, p. 75-81.

Park, C. H., Lee, M. J., Ahn, J., Kim, S., Kim, H. H., Kim, K. H., Eun, H. C. and Chung, J. H. Heat shock-induced matrix metalloproteinase (MMP)-1 and MMP-3 are mediated through ERK and JNK activation and via an autocrine interleukin-6 loop. *J Invest Dermatol*, 2004, vol. 123, no. 6, p. 1012-1019.

Parks, W. C. Matrix metalloproteinases in repair. *Wound Repair Regen*, 1999, vol. 7, no. 6, p. 423-432.

Passarini, B., Tosti, A., Fanti, P. A. and Varotti, C. Effect of hyaluronic acid on the reparative process of non-healing ulcers. Comparative study. *G Ital Dermatol Venereol*, 1982, vol. 117, no. 3, p. XXVII-XXX.

Peterson, R. G. The Zucker Diabetic Fatty (ZDF) Rat - Lessons from a Leptin Receptor Defect Diabetic Model. *Animal models of diabetes: frontiers in research*. E. Shafrir. Boca Raton, CRC Press, 2007, p. 103-118.

Peterson, R. G., Shaw, W. N., Neel, M. A., Little, L. A. and J., E. Zucker diabetic fatty as a model for non-insulindependent diabetes mellitus. *ILAR News* 1990, vol. 32, no., p. 16-19.

Phillips, M. S., Liu, Q., Hammond, H. A., Dugan, V., Hey, P. J., Caskey, C. J. and Hess, J. F. Leptin receptor missense mutation in the fatty Zucker rat. *Nat Genet*, 1996, vol. 13, no. 1, p. 18-19.

Piaggesi, A. Research development in the pathogenesis of neuropathic diabetic foot ulceration. *Curr Diab Rep*, 2004, vol. 4, no. 6, p. 419-423.

Postlethwaite, A. E., Holness, M. A., Katai, H. and Raghow, R. Human fibroblasts synthesize elevated levels of extracellular matrix proteins in response to interleukin 4. *J Clin Invest*, 1992, vol. 90, no. 4, p. 1479-1485.

Rappolee, D. A., Mark, D., Banda, M. J. and Werb, Z. Wound macrophages express TGF-alpha and other growth factors in vivo: analysis by mRNA phenotyping. *Science*, 1988, vol. 241, no. 4866, p. 708-712.

Rayment, E. A., Upton, Z. and Shooter, G. K. Increased matrix metalloproteinase-9 (MMP-9) activity observed in chronic wound fluid is related to the clinical severity of the ulcer. *Br J Dermatol*, 2008, vol. 158, no. 5, p. 951-961.

Reiss, M. J., Han, Y. P., Garcia, E., Goldberg, M., Yu, H. and Garner, W. L. Matrix metalloproteinase-9 delays wound healing in a murine wound model. *Surgery*, 2010, vol. 147, no. 2, p. 295-302.

Ren, G. Y., Dong, F. S., Wang, J. and Shi, P. K. The effect of hyaluronic acid external film on rats wound healing. *Zhonghua Zheng Xing Wai Ke Za Zhi*, 2004, vol. 20, no. 5, p. 380-383.

Rerup, C. C. Drugs producing diabetes through damage of the insulin secreting cells. *Pharmacol Rev*, 1970, vol. 22, no. 4, p. 485-518.

Roberts, A. B., Sporn, M. B., Assoian, R. K., Smith, J. M., Roche, N. S., Wakefield, L. M., Heine, U. I., Liotta, L. A., Falanga, V., Kehrl, J. H. and et al. Transforming growth factor type beta: rapid induction of fibrosis and angiogenesis in vivo and stimulation of collagen formation in vitro. *Proc Natl Acad Sci U S A*, 1986, vol. 83, no. 12, p. 4167-4171.

Rooney, P., Wang, M., Kumar, P. and Kumar, S. Angiogenic oligosaccharides of hyaluronan enhance the production of collagens by endothelial cells. *J Cell Sci*, 1993, vol. 105 (Pt 1), p. 213-218.

Roy, S., Khanna, S., Rink, C., Biswas, S. and Sen, C. K. Characterization of the acute temporal changes in excisional murine cutaneous wound inflammation by screening of the wound-edge transcriptome. *Physiol Genomics*, 2008, vol. 34, no. 2, p. 162-184.

Roy, S., Patel, D., Khanna, S., Gordillo, G. M., Biswas, S., Friedman, A. and Sen, C. K. Transcriptome-wide analysis of blood vessels laser captured from human skin and chronic wound-edge tissue. *Proc Natl Acad Sci U S A*, 2007, vol. 104, no. 36, p. 14472-14477.

Rudas, B. On the quantitative determination of granulation tissue in experimentally produced wounds. *Arzneimittelforschung*, 1960, vol. 10, no., p. 226-229.

Rybka, J. *Diabetes Mellitus - komplikace a přidružená onemocnění. Diagnostické a léčebné postupy*. Praha, Grada, 2007.

Saarialho-Kere, U. K., Pentland, A. P., Birkedal-Hansen, H., Parks, W. C. and Welgus, H. G. Distinct populations of basal keratinocytes express stromelysin-1 and stromelysin-2 in chronic wounds. *J Clin Invest*, 1994, vol. 94, no. 1, p. 79-88.

Sahai, A., Malladi, P., Pan, X., Paul, R., Melin-Aldana, H., Green, R. M. and Whitington, P. F. Obese and diabetic db/db mice develop marked liver fibrosis in a model of nonalcoholic steatohepatitis: role of short-form leptin receptors and osteopontin. *Am J Physiol Gastrointest Liver Physiol*, 2004, vol. 287, no. 5, p. G1035-1043.

Selvaggi, G., Monstrey, S., Van Landuyt, K., Hamdi, M. and Blondeel, P. The role of iodine in antisepsis and wound management: a reappraisal. *Acta Chir Belg*, 2003, vol. 103, no. 3, p. 241-247.

Shafrir, E. *Animal Models of Diabetes. Frontiers in Research.* Boca Raton, CRC Press, 2007.

Shimabukuro, M., Ohneda, M., Lee, Y. and Unger, R. H. Role of nitric oxide in obesity-induced beta cell disease. *J Clin Invest*, 1997, vol. 100, no. 2, p. 290-295.

Schmidt, R., Kirby, A. and Chung, L. Cadexomer iodine formulations may modulate the redox environment of wounds. *Iodine and wound physiology*. M. E. Hunt T (ed.). Cambridge, 1995, p. 6.1-6.26

Simeon, A., Wegrowski, Y., Bontemps, Y. and Maquart, F. X. Expression of glycosaminoglycans and small proteoglycans in wounds: modulation by the tripeptide-copper complex glycyl-L-histidyl-L-lysine-Cu(2+). *J Invest Dermatol*, 2000, vol. 115, no. 6, p. 962-968.

Sobotka, L., Smahelova, A., Pastorova, J. and Kusalova, M. A case report of the treatment of diabetic foot ulcers using a sodium hyaluronate and iodine complex. *Int J Low Extrem Wounds*, 2007, vol. 6, no. 3, p. 143-147.

Sobotka, L., Velebny, V., Smahelova, A. and Kusalova, M. Sodium hyaluronate and an iodine complex--Hyiodine--new method of diabetic defects treatment. *Vnitr Lek*, 2006, vol. 52, no. 5, p. 417-422.

Stadelmann, W. K., Digenis, A. G. and Tobin, G. R. Physiology and healing dynamics of chronic cutaneous wounds. *Am J Surg*, 1998, vol. 176, no. 2A Suppl, p. 26S-38S.

Sudre, B., Broqua, P., White, R. B., Ashworth, D., Evans, D. M., Haigh, R., Junien, J. L. and Aubert, M. L. Chronic inhibition of circulating dipeptidyl peptidase IV by FE 999011 delays the occurrence of diabetes in male zucker diabetic fatty rats. *Diabetes*, 2002, vol. 51, no. 5, p. 1461-1469.

Škrha, J. Diabetes mellitus a oxidační stres. *Diabetologie*. J. Perušičová. Praha, Triton, 2005, p. 13-36.

Tammi, R., Pasonen-Seppanen, S., Kolehmainen, E. and Tammi, M. Hyaluronan synthase induction and hyaluronan accumulation in mouse epidermis following skin injury. *J Invest Dermatol*, 2005, vol. 124, no. 5, p. 898-905.

Thorn, R. M., Austin, A. J., Greenman, J., Wilkins, J. P. and Davis, P. J. In vitro comparison of antimicrobial activity of iodine and silver dressings against biofilms. *J Wound Care*, 2009, vol. 18, no. 8, p. 343-346.

Tolg, C., Hamilton, S. and Turley, E. The Role of the Hyaluronan Receptor RHAMM in Wound Repair and Tumorogenesis. *Chemistry and Biology of Hyaluronan*. H. Garg. Oxford, Elsevier 2004, p. 125-142.

Tomanek, R. J. and Schatteman, G. C. Angiogenesis: new insights and therapeutic potential. *Anat Rec*, 2000, vol. 261, no. 3, p. 126-135.

Torregrossa, F. and Caroti, A. Clinical verification of the use of topical hyaluronic acid under non-adhesive gauze in the therapy of torpid ulcers. *G Ital Dermatol Venereol*, 1983, vol. 118, no. 4, p. XLI-XLIV.

Trousdale, R. K., Jacobs, S., Simhaee, D. A., Wu, J. K. and Lustbader, J. W. Wound closure and metabolic parameter variability in a db/db mouse model for diabetic ulcers. *J Surg Res*, 2009, vol. 151, no. 1, p. 100-107.

Tsuboi, R., Shi, C. M., Rifkin, D. B. and Ogawa, H. A wound healing model using healing-impaired diabetic mice. *J Dermatol*, 1992, vol. 19, no. 11, p. 673-675.

Vaalamo, M., Mattila, L., Johansson, N., Kariniemi, A. L., Karjalainen-Lindsberg, M. L., Kahari, V. M. and Saarialho-Kere, U. Distinct populations of stromal cells express collagenase-3 (MMP-13) and collagenase-1 (MMP-1) in chronic ulcers but not in normally healing wounds. *J Invest Dermatol*, 1997, vol. 109, no. 1, p. 96-101.

Vazquez, J. R., Short, B., Findlow, A. H., Nixon, B. P., Boulton, A. J. and Armstrong, D. G. Outcomes of hyaluronan therapy in diabetic foot wounds. *Diabetes Res Clin Pract*, 2003, vol. 59, no. 2, p. 123-127.

Vogt, P. M., Reimer, K., Hauser, J., Rossbach, O., Steinau, H. U., Bosse, B., Muller, S., Schmidt, T. and Fleischer, W. PVP-iodine in hydrosomes and hydrogel--a novel concept in wound therapy leads to enhanced epithelialization and reduced loss of skin grafts. *Burns*, 2006, vol. 32, no. 6, p. 698-705.

Vrabec, J. T. Tympanic membrane perforations in the diabetic rat: a model of impaired wound healing. *Otolaryngol Head Neck Surg*, 1998, vol. 118, no. 3 Pt 1, p. 304-308.

Wall, S. J., Bevan, D., Thomas, D. W., Harding, K. G., Edwards, D. R. and Murphy, G. Differential expression of matrix metalloproteinases during impaired wound healing of the diabetes mouse. *J Invest Dermatol*, 2002, vol. 119, no. 1, p. 91-98.

Weigel, P. H. The hyaluronan Synthases. *Chemistry and Biology of Hyaluronan*. H. Garg (ed.). Oxford, Elsevier 2004, p. 553-567.

Weigel, P. H., Frost, S. J., McGary, C. T. and LeBoeuf, R. D. The role of hyaluronic acid in inflammation and wound healing. *Int J Tissue React*, 1988, vol. 10, no. 6, p. 355-365.

Weigel, P. H., Fuller, G. M. and LeBoeuf, R. D. A model for the role of hyaluronic acid and fibrin in the early events during the inflammatory response and wound healing. *J Theor Biol*, 1986, vol. 119, no. 2, p. 219-234.

West, D. C., Hampson, I. N., Arnold, F. and Kumar, S. Angiogenesis induced by degradation products of hyaluronic acid. *Science*, 1985, vol. 228, no. 4705, p. 1324-1326.

Woodley, D. T., Bachmann, P. M. and O'Keefe, E. J. Laminin inhibits human keratinocyte migration. *J Cell Physiol*, 1988, vol. 136, no. 1, p. 140-146.

Yamada, K. M. and Clark, R. A. F. Provisional Matrix. *The Molecular and Cellular Biology of Wound Repair*. R. A. F. Clark. New York, Plenum Press, 1996, p. 51-94.

9   Supplements

Slavkovsky R, Kohlerova R, Tkacova V, Jiroutova A, Tahmazoglu B, Velebny V, Rezacova M, Sobotka L, Kanta J. *Zucker diabetic fatty rat: a new model of impaired cutaneous wound repair with type II diabetes mellitus and obesity*. Wound Repair Regen. 2011 Jul-Aug;19(4):515-25. Epub 2011 Jun 7. PubMed PMID: 21649785.

Slavkovsky R, Kohlerova R, Jiroutova A, Hajzlerova M, Sobotka L, Cermakova E, Kanta J. *Effects of hyaluronan and iodine on wound contraction and granulation tissue formation in rat skin wounds.* Clin Exp Dermatol. 2010 Jun;35(4):373-9. Epub 2009 Oct 23. PubMed PMID: 19874318.